Hydrologic impacts of Landuse change in the Upper Gilgel Abay River Basin, Ethiopia; TOPMODEL Application.

Webster Gumindoga

February, 2010

Hydrologic impacts of Landuse change in the Upper Gilgel Abay River Basin, Ethiopia; TOPMODEL Application.

by

Webster Gumindoga

Thesis submitted to the International Institute for Geo-information Science and Earth Observation in partial fulfilment of the requirements for the degree of Master of Science in Geo-information Science and Earth Observation, Specialisation: Integrated Watershed Management and Modelling (Surface Hydrology)

Thesis Assessment Board

Dr. Ir. M.W. Lubczynski	(Chairman) WREM dept., ITC, Enschede
Dr. Ir. P. Reggiani	(External Examiner) Deltaris, Delft
Dr. Ir. T.H.M Rientjes	(First Supervisor) WREM dept. ITC, Enschede
Dr. A.S.M Gieske	(Second Supervisor) WREM dept. ITC, Enschede
Mr. Alemseged Tamiru Haile	(Advisor) WREM dept. ITC, Enschede

ITC

INTERNATIONAL INSTITUTE FOR GEO-INFORMATION SCIENCE AND EARTH OBSERVATION
ENSCHEDE, THE NETHERLANDS

Disclaimer

Dedications

Dedicated to my parents Mr and Mrs T.E Gumindoga.

Abstract

Landuse and landcover change affect the different hydrological components like interception, infiltration and evaporation thereby influencing runoff generation (both process and volume) and streamflow regimes. Comparatively, little is known about factors that affect runoff behaviour and their relation to landuse in a data poor catchment like the Upper Gilgel Abay basin. Remote sensing was therefore used in this study to observe catchment characteristics and to estimate the model parameters that reflect on the land surface characteristics. Firstly, the TOPMODEL approach was applied to simulate streamflow for this basin. An ASTER 30m DEM was used to compute the topographic Index, critical for the simulation of streamflow in the basin. Results of calibration gave a Nash-Sutcliffe model efficiency (NS) of 0.81 and a Relative Volume Error (RV_E) of 6.1%. Sensitivity analysis of the model showed that the parameters most critical for accurately simulating runoff were: the exponential transmissivity function (m), the soil transmissivity at saturation (T_o) and the root zone available water capacity (SR_{max}). The model was validated using a 2003 meteorological dataset and a satisfactory model performance was obtained (NS=0.75, RV_E= -4.0 %). GIS and remote sensing were further used for the quantification of vegetation indices such as SAVI and LAI. Rainfall interception as a function of LAI from different vegetation types was determined. The implementation of landuse in TOPMODEL was done by treatment of each vegetation/landuse type as a 'subcatchment' through a GIS overlay of landuse types thus creating a topographic index distribution for each landuse type. These were run separately with specific landuse parameters. The areally weighted results were summed to get a total output imitating having multiple subcatchments with different topographic index distributions. Results showed that the maximum peakflow from agricultural land increased by 51% from 1973-1986 and by 44% between 1986 and 2001. Annual runoff volume increased by 12% between 1986 and 2001 which corresponds to increases in agricultural land from 1973 to 2001. From 1973-1986 and from 1986-2001, forest and shrubland decreased in maximum peakflow by same amount (29%). The annual runoff volume also decreased by 36% from 1973-1986 and by 34% from 1986-2001. This could be attributed to decreases in forests between the years 1973, 1986 and 2001. Finally for each year, a comparison was made between the sum of all landuse simulated discharge and the observed discharge at the outlet. The following satisfactory model efficiencies were obtained: 1973 (NS=0.81, RV_E=5.82 %); 1986 (NS=0.72, RV_E=29.72 %) and 2001 (NS=0.73, RV_E= 18.50 %). These results prove that in data poor basins, a promising way to analyse hydrological impacts of land-use change is by combining remote sensing for land surface parameterization and a semi distributed rainfall-runoff model. The findings also provide useful support for land use planning and management.

Key words: Upper Gilgel Abay, Land use, Remote sensing, TOPMODEL, Nash–Sutcliffe, Streamflow.

Acknowledgements

I testify of God's grace that was sufficient for me throughout my studies at ITC.

I would also want to give special thanks to the Netherlands Fellowship Programme (NFP) for sponsoring my studies in the Netherlands.

Furthermore I would like to thank my first supervisor Dr. Ing. T. H. M. Rientjes for his guidance and advice in every stage of the project. I greatly acknowledge him for his highly stimulating discussions and comments and for imparting me his 'modelling in hydrology' skills.

I would also want to extent my great appreciation to my second supervisor Dr. A.S.M Gieske for his support, comments and assistance in programming and handling the IDL code.

The assistance of my advisor Mr. Alemseged Tamiru Haile in this project is also greatly appreciated. My fieldwork trip and stay in Ethiopia was made easier and possible by his presence. I thank him so much for sparing his time and keeping me company in Bahir dar.

The special advice of Prof. Keith Beven, the Professor of Hydrology and Fluid Dynamics at the Lancaster Environment Centre will not go unmentioned. His quick replies and the concept of 'treating each vegetation type as a "subcatchment" and creating a topographic index distribution for each vegetation type' gave me a good kick start into the issue of landuse simulations using TOPMODEL.

Finally I give special thanks to all my lecturers, who helped me with great ideas throughout the beginning of the course to the completion of the thesis and of course not forgetting the beautiful WREM 2008-2010 buddies. I am also greatly indebted to my parents, brothers and sisters in Zimbabwe for their prayers and support. To the Mupamhangas, thanks so much for the motivation and other forms of support. My friends from ITC Fellowship and the Zimbabwean community at ITC, I thank you so much for the fellowship we shared.

Table of contents

List of figures

List of tables

1. INTRODUCTION

1.1. Background

The significance of land cover as an environmental variable has made land use change an important subject in global environmental changes and sustainable development (Li, 1996; Veldkamp and Fresco, 1997). Furthermore landuse and landcover change affect the different hydrological components like interception, infiltration and evaporation thereby influencing the soil moisture content, runoff generation (both process and volume) and streamflow regimes. In this regard, the spatial variation of hydrological components and the use of spatially variable model parameters in hydrological modelling are important for successful assessment of landuse change impacts on hydrology (Niu *et al*., 2005). Remote sensing now allows for the spatial and temporal quantification of major environmental variables such as topography (Lane *et al*., 2004), landcover and landuse (Chrysoulakis *et al*., 2004). Landcover is one of the most important products of remote sensing and it is a primary input of many hydrologic models. In this regard, it is imperative to integrate the various quantification methods with the spatial data handling capabilities of Geographic Information Systems (GIS) to process data for hydrological modelling. For this modelling, the Topographic Model (TOPMODEL) developed by Beven and Kirkby (1979) is selected for assessing the hydrologic impacts of landuse change in the Upper Gilgel Abay Basin. GIS and remote sensing serve to prepare inputs to the TOPMODEL and can help to predict and quantify the impacts of landuse change on the hydrology of any catchment. This also could further help to meet the challenges of managing water related problems and sustainable development of such catchments.

TOPMODEL is a semi-distributed model which has a simple representation of basin characteristics and hydrologic processes (Beven, 1997b) as compared to fully distributed and data demanding models like MIKE SHE (Refsgaard and Storm, 1995). The semi-distributed form of TOPMODEL makes full use of topographic data, and in its application one can obtain field evidence that shows the strengths and limitations of what were, originally, a set of theoretical concepts. TOPMODEL's low number of parameters minimizes optimization problems and this makes the final optimized values more physically meaningful (Sorooshian and Gupta, 1995). The model is applied to simulate outflows from catchments and to predict spatial and temporal soil moisture dynamics and variable source areas in space and time (Ambroise *et al*., 1996). The use of TOPMODEL in hydrological

modelling nowadays allows for input of digital elevation models (DEM) of less than 30m resolution for small scale research catchments but also for larger areas.

1.2. Statement of the problem

The Upper Gilgel Abay Basin is the largest catchment in the Lake Tana basin that discharges to the lake. Comparatively, little is known about factors that affect runoff behaviour and their relation to landuse. Predicting and estimating flows from data poor catchments like the Upper Gilgel Abay basin is difficult. Remote sensing data may be used to observe catchment characteristics and to estimate the model parameters that reflect on the land surface characteristics. In hydrological models, landuse is an essential input because it largely affects the water balance mainly by the processes of evaporation, transpiration, interception and surface runoff. An analysis of the effectiveness of the different approaches to integrate land-use in hydrological models is complex because of the different principles underlying the various approaches. In data poor basins, a promising way to include land-use change is by combining remote sensing and a semi distributed rainfall-runoff model. Therefore, in this work TOPMODEL is selected since it applies a semi-distributed model domain while it only requires few parameters. It predicts the catchment responses following a series of rainfall events by solving a water balance for each model calculation time step where precipitation, actual evapotranspiration, changes in storage and runoff are considered. The model consists of a surface interception and depression storage while runoff consists of overland flow and baseflow where overland flow occurs as saturation excess from the saturated runoff source areas. The model requires a fine resolution DEM to establish the drainage pattern in the catchment.

In the studies by Beven and Kirkby (1979) and Beven (1984), simulations using TOPMODEL has not been applied using distributed data sets. In most of these studies, the topographic index, a measure of hydrologic similarity, has been derived from field surveying. Beven (1997a) has noted that grid sizes that are large in relation to the length of hillslopes cannot be used to derive meaningful topographic index distributions which are intended to physically reflect pathways. Thus the introduction of an ASTER 30m DEM acquired from remote sensing and other methodologies for land surface parameterization could improve the prediction of streamflow in the basin. Quinn *et al* (1991) has also noted that fine-scale resolution raster DEMs is crucial for distributed modelling of rainfall-runoff processes and provides an adequate description of hillslope flow pathways.

In this study the impacts and effects of land-use change are analysed. It is often noted (see Huang and Jiang, 2002; Niehoff et al., 2002) that the use of rainfall-runoff models for prediction of the hydrologic effects by changes in land cover could be made simpler when integrating remote sensing

methodologies with ground based data. Thus remote sensing has been further used in this study for the quantification of vegetation indices such as the Soil-Adjusted Vegetation Index (SAVI) and Leaf Area Index (LAI) together with the spatial data handling capabilities of GIS. Aided with the simplicity of the model code (Beven, 1997a), this allowed the TOPMODEL's structure to be changed to reflect the perceptions of the hydrological response to landuse changes in the Upper Gilgel Abay basin..

1.3. Previous TOPMODEL studies

TOPMODEL has been successfully applied in many catchments to predict long streamflow records and to make hydrological predictions in space and time for example for catchments in mid-Wales, see (Quinn *et al*., 1991). In Beven and Freer (2000), the model has been applied where the assumption of a quasi-steady state saturated zone configuration is replaced by a kinematic wave routing of subsurface flow. Such is implemented in a way that allows the simulation of dynamically variable upslope contributing areas. All this has led to significant advances in TOPMODEL simulations.

Many versions of TOPMODEL do not have an explicit parameterization of landuse, but there are many extensions, e.g. (Famiglietti and Wood, 1995; Peters-Lidard *et al*., 1997), RHESSys (Band *et al*., 1991) or the MACAQUE model for forests (Watson, 1999) which uses the TOPMODEL approach for runoff estimation but extended it with a parameterization scheme for transfers of energy between surface and atmosphere. The ITC MSc thesis work by Deginet (2008) focused on the quantification of land surface parameters by remote sensing in the Gilgel Abay catchment but the work did not include an analysis of how TOPMODEL can be used to assess the hydrologic impacts of landuse changes. In addition, the improvement of TOPMODEL to handle hydrological impacts of landuse could be a major step forward in hydrological modelling studies and to the challenges of managing water scarcity. This work also builds on the work of Kebede (2009) who in his MSc thesis work applied the HBV-96 model to evaluate the model response to the land cover changes for the years 1973, 1986 and 2001. Thus the landcover maps developed in his work have been processed further to assess the hydrological impacts of landuse on streamflow using TOPMODEL.

1.4. Objectives of the study

The main objective of this study is to assess the hydrologic impacts of landuse change in the Gilgel Abay catchment. Further it was assessed whether the integration of remote sensing methodologies with ground based data could improve TOPMODEL simulation results.

The specific objectives of this study are:

- To assess whether land surface parameterization of TOPMODEL can be achieved by use of remote sensing.
- To evaluate how streamflow contributions from TOPMODEL can be used to initialize the model.
- To identify a suitable structure of TOPMODEL that allows for analyzing hydrologic impacts of landuse change.
- To evaluate the streamflow contributions from different landuse classes.
- To assess the hydrological impact of landuse changes on streamflow.
- To assess sensitivity of model parameters in simulating streamflow.

The research questions are:

- Can land surface parameterization of TOPMODEL be achieved by the use of remote sensing?
- How well can TOPMODEL simulate streamflow in the catchment?
- How should the TOPMODEL structure be modified so that it can account for hydrologic impacts of landuse change?
- What are the streamflow contributions from the different landuse classes?
- How does landuse change affect the peakflow, baseflow and runoff volume in the basin?
- How does the sum of discharge from different landuse classes compare to the observed discharge at the outlet?

The hypotheses that follow are therefore:

- Land surface parameterization of TOPMODEL can be achieved through remote sensing.
- The model's performance in simulating streamflow is expected to be greater than 0.7 in terms of the Nash-Sutcliffe model's performance.
- There is a difference in stream flow contributions from the different landuse classes.
- Landuse change has an effect on the peakflow, base flow and runoff volume.

1.5. Thesis outline

This thesis has six chapters**.** In the first chapter a brief background to the study is preceded by a review of various quantification methods of landuse change on hydrologic processes with the spatial data handling capabilities of GIS. In the same chapter the problem statement, research objectives, research questions, research hypothesis and previous studies in the Gilgel Abay Basin are addressed. The second chapter describes the location, topography, climate and land cover of the study area and also discusses the various literatures this study is based on. In the third chapter, there is a discussion of fieldwork activities, an outline of the methodology used in this study and how the TOPMODEL

structure can be modified to include the impacts of landuse change. Remote sensing and field data used in this study area are described in the fourth chapter as well as the preparation of the various input data for TOPMODEL. The chapter also explains the various analyses of the landuse data and other related inputs to allow for application of TOPMODEL in a semi distributed fashion. Then the fifth chapter firstly describes the results obtained and that is followed by a discussion of these results. Chapter six contains the conclusion of this study, and finally recommendations for future studies are made.

2. STUDY AREA AND LITERATURE REVIEW

2.1. Background to the study area

This section gives a description of the study area and its geographic location and other relevant information pertaining to the study area such as climate.

2.1.1. Geographic location

The Upper Gilgel Abay Basin is located in north western Ethiopia as shown by figure 2.1. Geographical coordinates of the area are 10º56' to 11º51'N latitude and 36º44' to 37º23' E longitudes. The Upper Gilgel Abay Basin is one of the main subbasins of the Lake Tana basin. Runoff from the Gilgel Abay contributes about 60% of the flow to the Lake Tana basin (Wale *et al*., 2009). Based on field visits in the study area in September 2009, this river originates from a small spring at Gish Abay Mountain near Sekela town at elevation of 2900 m.

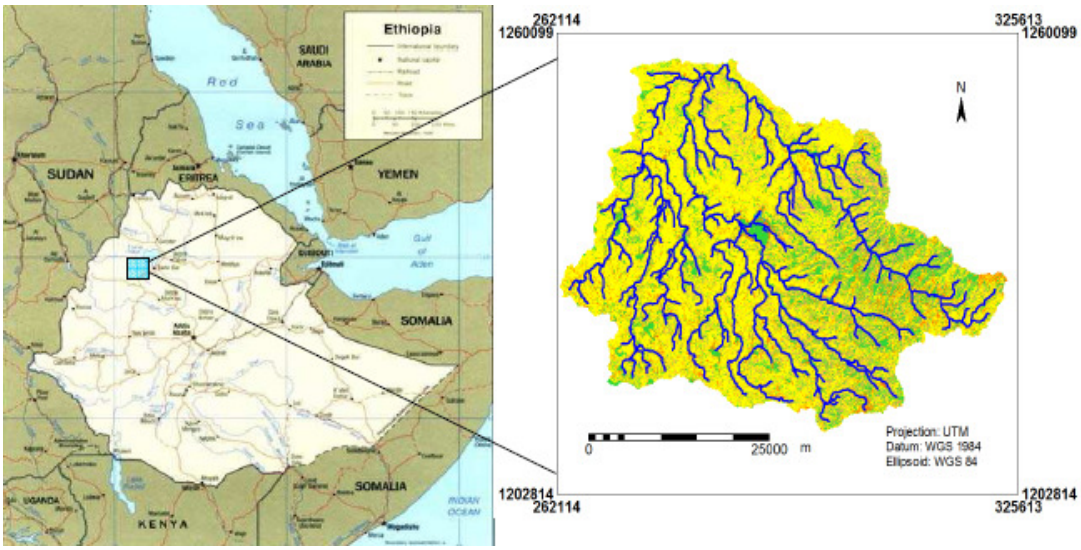

Figure 2-1: Location of the Upper Gilgel Abay Basin: Ethiopia.

2.1.2. Topography

Rugged mountainous topography characterizes most part of the catchment especially in the southern part but there is some low land within the basin as well. Elevation ranges from 1805m above mean sea level (a.m.s.l) to 2811m a.m.s.l. Around 80% of the catchment area falls in the slope range of (0-6%), 15% of the area falls in the slope range of (7-14%) and the remaining 5% is steeper than (14%) (Ashenafi, 2007).

2.1.3. Climate

Ethiopia's climate is generally affected by the Inter-Tropical Convergence Zone (ITCZ). The ITCZ passes over Ethiopia twice a year and this migration alternatively causes the onset and withdrawals of winds from north and south (SMEC, 2007). The Upper Gilgel Abay Basin falls within the cool semi-humid zone with mean annual temperature of 17-20°C. The dry season occurs between October and May while the wet season occurs mostly between June and September when the ITCZ is to the north of the country. The climate is generally temperate at higher elevations and tropical at the lower elevation. The long term mean annual rainfall (1992-2003) at Bahir Dar station (1828m a.m.s.l) south of the Lake Tana is estimated to be 1416 mm. According to Wale *et al.,* (2009), the mean annual humidity (1994-2004) at Bahir Dar station is estimated to be 58%.

2.1.4. Soil

There are seven types of soil groups observed in this area, Alisols, Fluvisols, Leptosols, Luvisols, Nitisols, Regosols, Vertisols (BCEOM, 1998) in combination with four diagnostic horizon modifiers: chromic, eutric, haplic, and lithic. According to the work of BCEOM (1998), the whole Gilgel Abay catchment is mostly covered by Haplic Luvisols with an areal coverage of around 2583 km^2. The cultivated areas mostly lie on this type of soil throughout the study area. In low lying areas particularly north of the Gilgel Abay basin, soils have been developed on alluvial sediments (SMEC, 2007).

2.1.5. Land use and Land cover

Most of the Gilgel Abay catchment area is characterised by cropland with scarce woodlands and forested highlands. The main croplands as observed during a field visit consist of maize, turf and potato. Besides the cultivated lands, the main landcover types are grassland, marshland, and forest with frequent patches of shrubs, eucalyptus woods and trees. According to a landcover classification of 2001 done by Kebede (2009), the major land cover types include 62%, agriculture, 17% forests, 11.6% shrub land, 9% grassland, and 0.4% water and marshy lands. Agricultural production is very low because of the shortage of skilled manpower, backward technology, poor infrastructure in rural Ethiopia, recurrent drought, and land degradation. Land degradation is perhaps the most significant factor (Tessema, 2006).

2.2. Literature review: Topmodel approach

This section describes the dominant runoff processes occurring at the hillslope, the concept of TOPMODEL, the governing equations and how TOPMODEL solves the water balance for a catchment.

2.2.1. Dominant flow processes at the hillslope

There are many processes that contribute to catchment runoff at the catchment outlet point. Figure 2-2 shows a schematic representation of flow processes which may contribute to the catchment runoff.

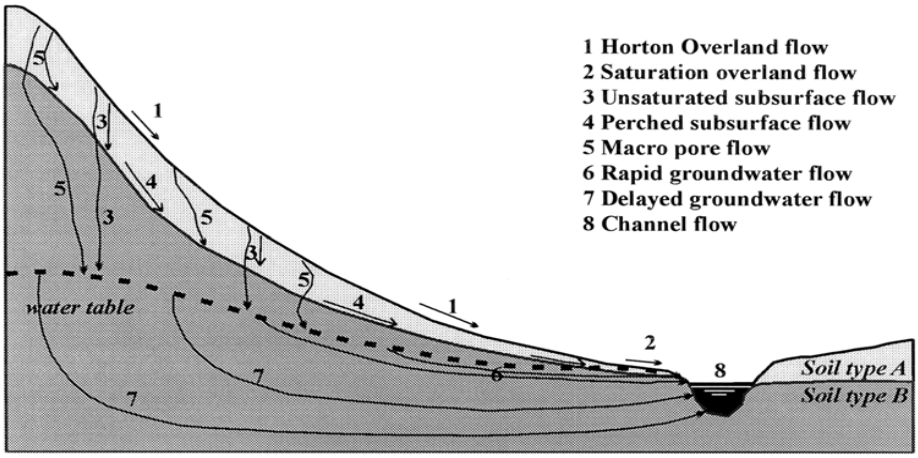

Figure 2-2: Cross-sectional schematization of runoff process in a sloping area at the catchment scale. (After Rientjes, 2007).

Hortonian overland flow (infiltration excess overland flow) occurs when rainfall intensity exceeds the infiltration capacity of the soil. This may occur at any location in a catchment and is common in arid climates and in low permeable areas e.g. urbanized areas. In contrast, saturation overland flow occurs when the soil is saturated due to a rise of the phreatic groundwater level. This process is much less aggressive compared to Hortonian overland flow and is common in lower parts of the catchment. On top of these saturated zones, overland flow is generated by exfiltration of subsurface water and by rainfall. These zones are termed the 'saturation overland flow source areas' and are shown in figure 2-3. Unsaturated subsurface flow is the flow of water in a matrix flow system where the movement of water is due to suction head gradients. Infiltration of rainfall in the subsurface can be in the form of matrix flow or macro pore flow (or small natural pipes). A matrix flow system is often discontinuous due to macro pores as caused by (drought) cracks, wormholes or rooting of vegetation. Perched subsurface flow is generated when the saturated hydraulic conductivity of a given subsurface layer is significantly lower than the overlaying soil layer. Groundwater flow is the flow of water in the saturated zone. The groundwater system acts as a storage reservoir for base flow generation. Groundwater flow contributions can be 'rapid' and

‘delayed’. When water reaches the natural or artificial catchment drainage system, water is transported through the main channels. Finally in the channel system, runoff contributions from the various runoff processes is collected and routed downstream to the catchment outlet.

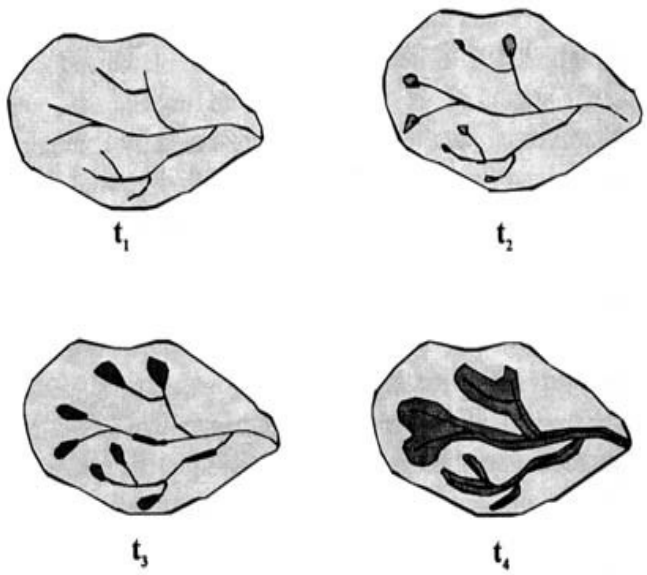

Figure 2-3: Expansion of saturated overland flow source areas during a storm event, (Rientjes (2007), modified after Dunne (1978)).

2.2.2. The Topographic index

TOPMODEL is based on the use of the topographic index (*ln(a/tanβ)*) which predict local variations in water table (Kirkby, 1975). In this case *a* is the area draining through a point from upslope and *tanβ* is the local slope angle. The *ln(a/tanβ)* is considered a measure of hydrological similarity because areas of the same catchment with approximately equal values of the topographic index are assumed to behave in a hydrologically similar manner. High topographic index values will tend to saturate first and will therefore indicate potential subsurface or surface contributing areas (Beven, 1997a). The calculated values of both *a* and *tanβ* will depend on the analysis of flow pathways from the DEM data and the grid resolution used (Qin *et al*., 2007). Figure 2-4 shows the distribution of *a, tanβ*, and topographic index across a hillslope. Surface and subsurface water is directly delivered to the stream but routing of water on hillslopes is not explicitly simulated. However routing of water in the stream is simulated using a very simplified scheme described in section 2.8.

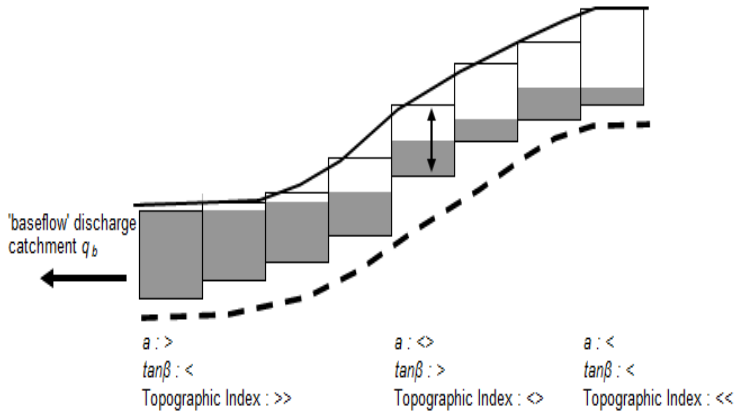

Figure 2-4: Distribution of a, $\tan\beta$ and topographic index across a hill slope: (modified after (Rientjes, 2007)).

2.2.3. Progression in simulations using TOPMODEL concept

A long number of developments are reported and variations on the basic principles of the original TOPMODEL have been made allowing it to be described from the two sources of runoff. These are outflow from subsurface saturated zones including return flow and overland flow caused by precipitation on saturated areas (Seibert *et al*., 1997). In early applications of TOPMODEL, the major role of subsurface flow was to determine the extent of saturated overland flow, and subsurface flow itself was only a minor contributor to runoff (Beven and Kirkby, 1979). The structure of the model with regard to interception and root zone storage compartments is variable thus allowing for much flexibility in simulating different systems (Quinn and Beven, 1993). The limitation of the topographic index approaches in the original version is the assumption that there is always downslope flow from upslope contributing area that is constant from any point in the catchment. A dynamic TOPMODEL can be derived by an explicit redistribution of downslope fluxes from one group of hydrologically similar points to another, where the definition of hydrologically similar can be based on more flexible criteria than the original topographic index. Grouping of similar pixels results in computational efficiency that might be advantageous in applications to large catchments or where large numbers of model runs are required to assess predictive uncertainty. This is the basis for a new, more dynamic, version of TOPMODEL (Beven and Freer, 2000).

To allow for landuse simulations, the model version in this work does include infiltration excess calculations and parameters based on the exponential conductivity Green-Ampt model (Green and Ampt, 1911) in Beven (1984). However if infiltration excess does occur it does so over the whole area of a subcatchment. Spatial variability in conductivities have been handled by specifying

different saturated hydraulic conductivity (K_s) parameter values for different subcatchments, even if they have the same $ln(a/tan\beta)$ and routing parameters, i.e. to represent different fractions of the same catchment area.

2.2.4. Assumptions of TOPMODEL

In summary, TOPMODEL is based on the assumption that local soil moisture dynamics strongly depends on the size of the upslope area (a) that drains through an observed catchment point, the local surface topographic slope ($tan\ \beta$) that represents the hydraulic gradient for saturated water flow, and the downslope soil transmissivity (T_o).

The four underlying assumptions are:

(i) Dynamics of the saturated zone can be approximated by successive steady state representations

(ii) Hydraulic gradient of the saturated zone can be approximated by the local surface topographic slope

(iii) Transmissivity with depth is an exponential function of the storage deficit or the depth to the water table.

(iv) Saturation of the soil column occurs from below and as such runoff generated by the saturation excess overland flow mechanism.

2.2.5. Description of the model and governing equations

For this study a code of the model approach has been developed using the IDL programming language. Equations and algorithms of the code are by Beven (1997) and Beven (2001). The lecture notes by Rientjes (2007) and the MSc thesis by Pilot (2002) have also been used for explanation of these equations. The essential concepts of TOPMODEL are primarily concerned with a simplified model of the saturated zone and its control of surface and subsurface contributing areas. However, to complete a continuous simulation model it is necessary to introduce further components to deal with interception, infiltration, evapotranspiration, the unsaturated zone and flow routing (Beven, 1997a).

2.2.6. What happens in the saturated zone?

The TOPMODEL approach is based on the storage principle and applies a Darcy type flow equation to allow water transport between subsurface storage elements. This equation is not solved numerically where hydraulic heads are updated per calculations time step but topographic gradients serve as fixed hydraulic gradients to simulate mass transfer (Rientjes, 2007). One of the parameters in the Darcy equation is Transmissivity that is equal to the depth of the flow domain as multiplied by the hydraulic conductivity. Since groundwater flow only is possible in the saturated zone,

transmissivity must be calculated for that part of the subsurface that is fully saturated and any cross sectional flow area for groundwater flow is a function of the depth of the saturated zone (Pilot, 2002).

$$T = T_o e^{-fz} \quad \text{or} \quad T = \int_0^{\infty} k_o e^{-fz} dz = \frac{k_o}{f} \qquad \textbf{[1]}$$

Where:

T_o = the transmissivity at the surface (lateral transmissivity), [L^2T^{-1}]

z = local water table depth, [L]

f = a scaling parameter [L^{-1}]

The distribution of transmissivity in downslope direction can be simulated by an exponential function of the local storage deficit. This deficit refers to the amount of water to reach full saturation of the soil column Similarly, the decline of local transmissivity with decreasing storage in the soil profile has been approximated by an exponential function (Quinn *et al.*, 1995).

$$T = T_o e^{-s_i/m} \qquad \textbf{[2]}$$

Where:

S_i = current local saturated zone storage deficit,

m = parameter controlling the shape of the function.

If the soil saturation reaches its maximum (i.e. deficit becomes zero), the lateral discharge becomes maximum. The saturated zone is recharged by rainwater although important processes such as infiltration and unsaturated flow zone are ignored.

Subsurface flow

If S represents the storage deficit, the maximum discharge in the subsurface is observed when the entire soil profile becomes saturated and discharge is equal to:

$$q_{\max} = TS \qquad \textbf{[3]}$$

The actual groundwater discharge is a function of the upstream area '*a*' as multiplied by the recharge rate '*R*'

$$q_{act} = Ra \qquad \textbf{[4]}$$

Where:

q_{act} = actual lateral discharge [m/hr] [L^2T^{-1}]

R = recharge rate or proportionality constant [LT^{-1}]

a = specific catchment area [L]

The proportionality constant in TOPMODEL approach may be interpreted as "steady state" recharge rate, or "steady state" per unit area contribution to base flow (Rientjes, 2007). When comparing the actual discharge to the maximum discharge an indication is obtained towards the "relative wetness" '*w*' or saturation degree of the subsurface grid cell that represents the real world soil column (Dunne, 1978). The relative wetness describes the ratio of actual discharge and maximum discharge and may be interpreted as available storage depth to reach full saturation in the saturated subsurface:

$$w = \frac{q_{act}}{q_{\max}} = \frac{Ra}{TS_i} \qquad \textbf{[5]}$$

Full saturation occurs when the wetness becomes larger than 1 or when following equation **[5]:**

$$\frac{a}{T \tan B} > \frac{1}{R} \qquad \textbf{[6]}$$

Figure 2-5 (left) shows the principle of comparing an inflow and outflow discharge by means of a linear reservoir approach. Given that T is a function of S_i, the actual discharge may be expressed by:

$$q_{act} = T_{s_i} \tan \beta \qquad \textbf{[7]}$$

In the TOPMODEL-concept, the subsurface of a grid cell i can be schematised as a store with a continuity equation of mass and momentum. The local soil moisture deficit S_i is subject to the equilibrium between these two equations. Figure 2-5 (right) shows the lateral saturated subsurface flow q through a soil column. On top the saturated subsurface is bounded by the water table and at the bottom by an impermeable layer. D = the thickness of the saturated subsurface; d = the depth to the water table; d_{max} = the maximum depth to the water table.

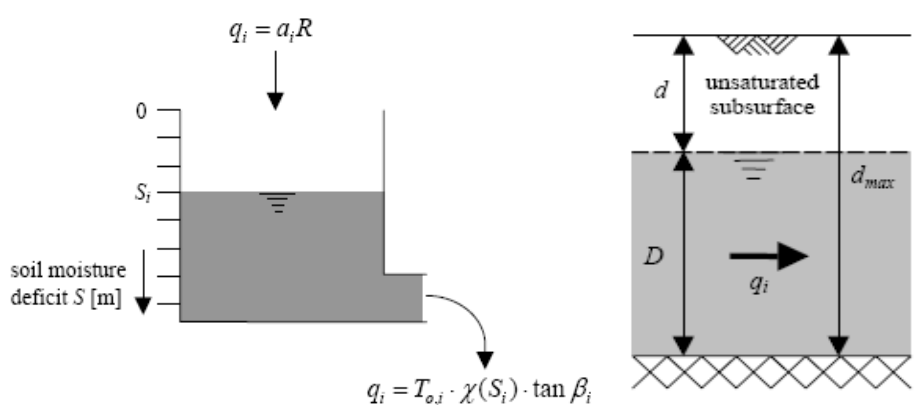

Figure 2-5: A subsurface element as a linear storage reservoir and lateral saturated subsurface flow q through a soil column.

In equation **[7]** the topographic gradient term is often interpreted as a wetness index and in Dunne (1978) it determines the locations of saturation from below and consequently a soil moisture deficit

may occur. When T is assumed to be fixed property because K is uniformly distributed and D is finite, then:

$$\frac{a}{T\tan\beta} = \frac{a}{\tan\beta} \qquad \text{or} \qquad \ln\left(\frac{a}{\tan\beta}\right) \qquad \textbf{[8]}$$

The relative wetness becomes:

$$w = \frac{Ra}{\tan\beta} \qquad \textbf{[9]}$$

If the hydraulic conductivity is uniformly distributed and assuming that the depth of the soil column is finite:

$$w = \frac{Ra}{T\tan\beta} = \bar{w}\frac{a/\tan\beta}{\frac{1}{A}\int\left(a/\tan\beta\right)da} \qquad \textbf{[10]}$$

If the 'unsaturated zone" thickness is simulated it becomes:

$$z = D(1-w) \qquad \textbf{[11]}$$

When the exponential K assumption that describes the saturated hydraulic conductivity is introduced then the transmissivity reduces exponentially (equation [**11**]), and:

$$aR = T_o \tan\beta e^{-fz_i} \qquad \textbf{[12]}$$

With the same logic of equation [s], the local soil deficit can be expressed by:

$$z_i = -\frac{1}{f}\ln\left(\frac{Ra}{T\tan\beta}\right) = \bar{z} - \frac{1}{f}\left(\ln\frac{a}{\tan\beta} - \lambda\right) \qquad \textbf{[13]}$$

When the local deficit over the entire catchment is integrated to give a mean depth $\bar{z}$ to the water table gives:

$$\bar{z} = \frac{1}{A}\int_A z_i dA = \frac{1}{fA}\int_A\left\{-\ln\left(\frac{a}{\tan\beta}\right) - \ln R\right\}dA \qquad \textbf{[14]}$$

Now equation [**11**] is assumed to hold for water table rising above the soil surface. When rewriting equation [**12**] and when substituting this for R in equation [**14**], R is eliminated and $\bar{z}$ becomes a function of topographic and physiographic properties only:

$$\bar{z} = \frac{1}{f}\left\{-\frac{1}{A}\int_A \ln\left(\frac{a}{T_o\tan\beta}\right)dA + fz_i + \ln\left(\frac{a}{T_o\tan\beta}\right)\right\} \qquad \textbf{[15]}$$

or

$$f(\bar{z} - z_i) = \left\{ \ln\left(\frac{a}{\tan\beta}\right) - \lambda \right\} - \{\ln T_o - \ln T_a\} \qquad \textbf{[16]}$$

Where:

$$\lambda = \frac{1}{A}\int \ln\left(\frac{a}{\tan\beta}\right) dA$$

$$\ln T_A = \frac{1}{A}\int \ln T\, dA$$

The equation expresses the deviation of the local depth of the water table scaled to parameter '*f*' in terms of the deviation in the logarithm of transmissivity away from the integral value *Ln* T_A and a deviation in the local topographic index away from its integral value λ, the catchment topographic constant as described (Beven and Kirkby, 1979).

Rewriting equation **[15]** for z_i gives:

$$z_i = \bar{z} \frac{1}{f}\left(\ln\frac{a}{\tan\beta} - \lambda \right)$$

Where:

$$\bar{z} = -\frac{1}{f}\left(\lambda + \ln\frac{R}{T} \right)$$

2.2.7. What happens in the unsaturated zone and root zone reservoir?

Figure 2-6 shows a schematic structure of the root zone storage and unsaturated zone. The vertical drainage from the unsaturated zone to the saturated zone as suggested by Beven and Wood (1983) is given by the following equation:

$$q_v = \frac{S_{uz}}{S_i t_d} \qquad \textbf{[17]}$$

Where:

q_v	=	the vertical (gravity) drainage from the unsaturated zone	[LT^{-1}]
S_{uz}	=	the unsaturated zone storage	[L]
S_i	=	local saturated zone deficit	[L]
t_d	=	time delay constant of the unsaturated zone	[T]

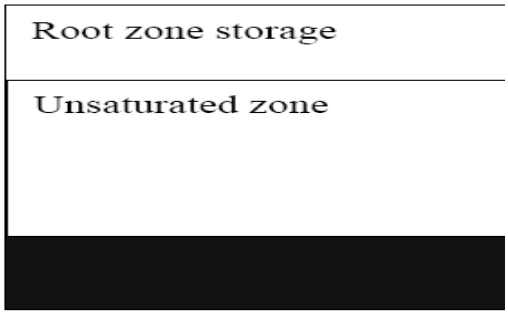

Figure 2-6: The root zone and unsaturated zone stores (Kim and Delleur, 1997).

The water balance of the root zone and the unsaturated zone stores is maintained for each of these stores. The root zone allows for some of the precipitation to be lost to evapotranspiration and allows an intermediate storage so that precipitation input is not added to the unsaturated zone store. Potential ET (E_p) is provided as an input. Actual evapotranspiration is calculated as a function of potential evapotranspiration and maximum root zone moisture storage deficit. This storage represents water available for evapotranspiration from the root, system interception storage and for microtopographic depression storage (Gunter et *al*., 1999). In the TOPMODEL description of Beven (1991), evaporation is allowed at the full potential rate for water draining freely in the saturated zone and for predicted areas of surface saturation. A reduction from the potential evapotranspiration value occurs depending on the moisture status of the root zone.

$$E_a = E_p (1 - SRZ / SR_{\max}) \qquad \textbf{[18]}$$

Where:

E_a	=	actual evapotranspiration	[L]
E_p	=	the potential evapotranspiration	[L]
SRZ	=	the root zone storage	[L]
SR_{max}	=	maximum root zone storage deficit	[L]

Any remaining water based on the relative values of the unsaturated zone storage and local storage deficit is allowed to evaporate with the maximum limit of SR_{max}. A value for the single parameter SR_{max} is specified for calibration. The SR_{max} represents the field storage capacity, i.e. the maximum amount of matrix water that can be held against gravity. This value has to be exceeded in order to initiate soil water percolation and water table recharge. According to Molicová (1997), the SR_{max} value is conceptualized in current TOPMODEL theories as a root zone reservoir and does not only responds to the evapotranspiration demand but also determines the rate of deep leakage loss from the soil.

2.2.8. Overland flow and channel network routing

Runoff generated in large catchments reaches the outlet at different time instants since flow paths are of different time and nature. To simulate flow travel time, TOPMODEL uses a very simple scheme that is essentially a delay approach as illustrated in figure 2-7. Fractional area and its distance from the outlet are required as well as channel velocity which has a fixed value across the catchment. The model computes the time span it will take for a water particle to travel from each fractional area to contribute to the catchment outlet. Then for each area contributions are defined and accumulated for the calculation time steps (Beven and Kirkby, 1979). The time taken to reach the basin outlet (td_j) from any point is assumed to be given by

$$td_j = \sum_{i=1}^{N} \frac{x_i}{CHV tan\beta_i} \qquad [19]$$

Where:

x_i = the plan flowpath length [L]

$tan\beta_i$ = slope of the ith segment of a flow path comprising N segments between point j and the catchment outlet.

CHV = velocity parameter (main channel routing velocity) [LT^{-1}]

If this velocity parameter is assumed constant then this equation allows a unique time delay histogram to be derived on the basis of basin topography for any runoff contributing area. The routing procedure lumps overland and channel flow together and uses *CHV* parameter to route this surface runoff to the outlet.

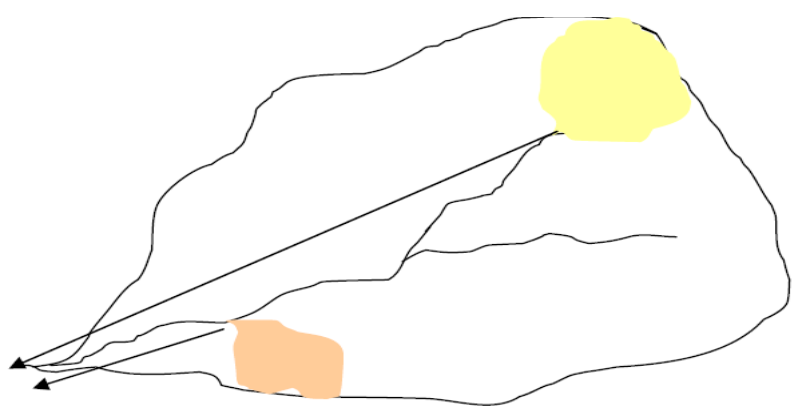

Figure 2-7: Illustration of the routing concept (Fedak, 1999).

2.2.9. Choice of transmissivity profile.

The shape of recession curves tells something about the catchment hydrological behaviour. A master

recession curve is an artificial curve but is made of a collection of measured single recession curves (Pilot, 2002). It describes the depletion of the catchment area in time from the highest measured peak discharge to the smallest measured amount of outflow. With the master recession curve, the parameters of the TOPMODEL-concept can be derived. To start with a relative local soil moisture deficit, δi is defined:

Exponential	*Parabolic*	*Linear*	
$S_i/m = \delta_i$	$S_i/m = \delta_i$	$S_i/m = \delta_i$	**[20]**

Where:

S_i	=	local soil moisture deficit	[m]
S_m	=	maximum soil moisture deficit	[m]
m	=	rate of exponential decrease of T_i with S_i	[m]
δ_i	=	relative local storage deficit	[-]

The momentum equations are given as:

Exponential	*Parabolic*	*Linear*	
$q_i = T_{o,i} e^{-\delta_i} tan\beta_i$	$q_i = T_{o,i}(1-\delta_i)^2 tan\beta_i$	$q_i = T_{o,i}(1-\delta_i) tan\beta_i$	**[21]**

Within this newly obtained equation the soil moisture deficit is the hydrologic state variable:

Exponential	*Parabolic*	*Linear*	
$q_i = T_{o,i} e^{-\delta_i} tan\beta_i$	$a_i R = T_{o,i}(1-\delta_i)^2 tan\beta_i$	$a_i R = T_{o,i}(1-\delta_i) tan\beta_i$	**[22]**

Representation of the recession curve within the TOPMODEL-concept

For the situation of a base flow recession period (a period of drainage without recharge), Ambroise *et al.,*(1996) proposed a procedure on how to determine the transmissivity profile that is corresponding to the involved catchment. If Q_b is the discharge at the catchment outlet [m^3/d] and Q_o is the discharge of the base flow in case $\delta = 0$ [m^3/d] then the relation between Qb and δ can be written for Q_b as a function of time. In case the mean relative storage deficit $\delta = 0$ and thus $Qb = Q_o$, the corresponding stored volume of groundwater, V_o, in the catchment is:

Exponential	*Parabolic*	*Linear*	
$Vo = \infty$	$Vo = AS_m$	$Vo = AS_m$	**[23]**

It is assumed that there is no lower limit in the exponential transmissivity profile. In the period of drainage without recharge, the conservation equation reads:

$$Q_b = AS_m \frac{d\delta}{dt} \qquad \textbf{[24]}$$

The general differential equation that describes the decrease of the outflow with time in the base flow recession curve is:

$$\frac{dQ_b}{dt} = \frac{Q_b}{AS_m}\frac{dQ_b}{d\delta} \qquad \textbf{[25]}$$

with $S_m = m$ in case of the exponential transmissivity profile.

The base flow recession curve can be written for Q_b at $t = ts + \tau$. with any specified discharge Q_s at $t = ts$:

Exponential	*Parabolic*	*Linear*	
$Q_b = \dfrac{Q_s}{1 + Q_s \dfrac{1}{Am}\tau}$	$Q_b = \dfrac{Q_s}{\left(1 + \sqrt{Q_s}\dfrac{\sqrt{Q_o}}{AS_m}\tau\right)^2}$	$Q_b = Q_s e\left(-\dfrac{Q_o}{AS_m}\tau\right)$	**[26]**
first order	hyperbolic second order	hyperbolic exponential	

Equation [**26**] gives the expressions for the base flow recession curve for each of the three defined transmissivity profiles. For the exponential transmissivity profile, this results in a first order hyperbolic recession curve, for the parabolic profile in a second order hyperbolic curve and assuming a linear transmissivity profile results in an exponential base flow recession curve.

2.2.10. TOPMODEL parameters

The version of TOPMODEL used in this study has 8 parameters that are described in Table 2-1.

Table 2-1: TOPMODEL parameter values

Parameter	Meaning/definition	Where parameter is used
m [m]	Parameter of the exponential transmissivity function or recession curve. Controls rate of decline of T_o. Derived from an analysis of catchment recession curves. A plot on vertical axes (1/discharge) and on horizontal axes (time in hours) graph (Beven *et al*., 1995). Lower limit 0.005.	Use in the equation of decline of local transmissivity with decreasing storage in the soil profile. (Quinn *et al*., 1995). $T = T_o e^{-s_i/m}$ Equation **[2]**
T_o [m^2/h]	Average transmissivity of the soil when the profile is just saturated. A homogeneous soil throughout the catchment is assumed. Published values include 35 for a 60 m grid cell &42 for 20m grid cell size (Saulnier *et al*.1997).	$T = T_o e^{-s_i/m}$ Equation [**2**]

t_d [h]	Time delay constant for routing unsaturated flow (> 0.0). Values used for the dynamic TOPMODEL 0.1–120 (Peters *et al.*, 2003).	Used as time delay per unit of deficit $q_v = \frac{S_{uz}}{S_i t_d}$ Equation [**17**]
CHV [m/h]	The main channel routing velocity.	Is the velocity used in overland flow and channel routing. $td_j = \sum_{i=1}^{N} \frac{x_i}{CHV \tan \beta_i}$ Equation [**19**]
RV [m/h]	The internal subcatchment routing velocity.	
SR_{max} [m]	The root zone available water capacity. Is also the soil profile storage available for transpiration.	$E_a = E_p (1 - SRZ / SR_{\max})$ Equation [**18**]
Q_o [m/h]	Initial stream discharge, where by default Q_0 is set to the first observed discharge but may be changed by user, The first streamflow input is assumed to represent only the subsurface flow contribution of the watershed.	Used as Q_b in the decrease of the outflow with time in the base flow recession curve is: $\frac{dQ_b}{dt} = \frac{Q_b}{AS_m} \frac{dQ_b}{d\delta}$ Equation **[25]**
SR0 [m]	Initial value of root zone deficit. also called *SRinit* For the dynamic TOPMODEL 0.1 – 120 (Peters *et al.*, 2003).	

Table 2-2: Parameter values used in different TOPMODEL studies (Beven, 1997b)

Catchment	**Area (Km^2)**	**DEM (m)**	**λ=catchment average of *ln (a/tanβ)***	***m* (m)**	**T_0 (m^2/h)**	**Reference**	**Comment**
Gardsjon,G1, Sweden	0.0063	5	5.1		1.8		f=13m^{-1},variable Δθ (f is the equivalent of *m*).
Saeternbekken Minifelt, Norway	0.0075	2	5	0.0053	1.31	Lamb, (1996)	
Ecerex B, French Guiana	0.015	2.5	5.62	0.0035	7	Molicová *et al.,* (1997).	
Ringelbach, France	0.34	5	5.94	0.041	2.75	Ambroise *et al.*, (1996).	Parameters for exponential transmissivity version
Slapton wood, UK	1	10	7.87	0.004-0.25	0.01-30	Fisher and Beven, (1996).	Parameter ranges used in Monte Carlo experiments

White Oak Run,VA USA	5	30-90	6.04-6.08	0.027	0.0007-0.0012	Wolock and McCabe, (1995).	Different parameters derived from different DEM grid sizes and analysis algorithms
Maurets ,France	8.4	20-120	6.40-6.96	0.025	1.05-1.5	Saulinier *et al.*, 1997 (1997).	For different DEM grid sizes after excluding river pixels from ln(a/tanβ) distribution
Wye,UK	10.5	10-100	5-9.8	0.0093	9.223-27.11	Quinn *et al*, (1995)	Different parameters derived from different DEM grid sizes
North fork Rivanna,VA	456		7.64	0.0092	11.75	Beven and wood, (1983)	

2.3. Literature review: Landuse change

This subsection describes the capabilities of remote sensing to acquire information on landuse and landcover that is relevant in hydrological simulations. It further looks at how vegetation and soils plays a dominant role in hillslope hydrology and finally how different model approaches are designed to handle landuse change impact studies.

2.3.1. Remote sensing application on landuse and landcover analysis

Remote sensing has the capability to acquire spectral signatures instantaneously over large areas information. The spectral signatures allows for the extraction of information pertaining to land cover, vegetation cover, emissivity, albedo, surface temperature and energy flux (Lucas *et al.*, 2002). Land cover and land use changes can be analysed over a period of time using Landsat Multispectral Scanner (MSS) data and Landsat Thematic Mapper (TM) data by image classification techniques. Using independent validation data, error matrix also known as a confusion matrix is calculated to determine the accuracy of the classification and to identify where misclassification occurs. In addition, the use of spectral vegetation indices, namely SAVI and LAI is applied to detect areas where vegetation covers decrease.

2.3.2. Vegetation and soil as controlling factors in hillslope hydrology.

Vegetation cover is directly related to the maintenance of infiltration capacity and the conditioning effect of organic material on soil structure, bulk density, and porosity. Land-use, while highly interrelated with vegetation cover, may have effects independent of cover (Whipkey and Kirkby, 1978). Adverse land-use practices such as overgrazing by sheep and cattle, repeated burning of litter and humus layers on the forest floor, and topsoil loss by accelerated erosional processes commonly have the greatest effect on infiltration. Table 2-3 gives a sample of some final constant infiltration rates in order to indicate the range of this parameter in agricultural, grasslands, rangelands and forests.

The physical properties and depth of the soil as controlled by vegetation and landuse change are probably the most important controls on subsurface production at a site. If the texture is coarse, vertical flow usually dominates and when this soil is deep, subsurface flow response may be delayed if the texture is fine, resistance to vertical flow results and lateral or shallow subsurface flow sometimes occurs quickly. Soil structure is also extremely important. Fissures, cracks, or channels are less likely to occur or to be of importance in coarse-textured soils. In fine-textured or layered soils, cracks, fissures and/or channels are more likely to occur providing possible routes for flow, and largely replacing textural voids as the main avenues for unsaturated and saturated flow (Whipkey and Kirkby, 1978).

Table 2-3: Constant infiltration rates measured with a sprinkling infiltrometer or under rainfall. (modified after (Dunne, 1978)).

Landcover	Soil type	Final Infiltration rate (cm/hr)	Location	Source
Hardwood forest	Sandy loam and silt loam	>7.6	Ohio, USA	Whipkey (1969)
Agriculture (corn)	Silt loams	0.2-0.46	Midwestern USA	Musgrave and Holtan (1964)
Agriculture (hay)	Silt loam	1.5	Midwestern USA	Musgrave and Holtan (1964)
Bare (crusted)	Silt loams	0.68	Midwestern USA	Musgrave and Holtan (1964)
Rangeland (grazed range)	Soils developed on Shales	Dry 1.6-2.2 Wet 1.4-2.1	W. Colorado, USA	(Lusby *et al.*, 1963)
Rangelands (brush and grass)	Gravelly sands and gravelly loams	1.3-4.3	Arizona/New Mexico	(Kincaid *et al.*, 1966)

2.3.3. Parameterization of landuse change in different hydrological models

Table 2-4 gives a comparative approach on 3 different models that handle the issue of landuse changes. The models are Soil and Water Assessment Tool (SWAT), TOPMODEL-based Land Atmosphere Transfer Scheme (TOPLATS) and Variable Infiltration Capacity (VIC). The 3 models have all been used for scenario studies focusing on the impacts of land use changes. This review summarizes the different approaches to integrate land-use in different hydrologic models and simulation results will provide useful insight on TOPMODEL studies.

Table 2-4: Summary table on the model approaches that are designed for landuse change impact studies.

	SWAT	TOPLATS	VIC
Background and structure	A semi-distributed hydrological catchment model that contains both conceptual and physical based approaches (Neitsch et al., 2002). It predicts impact of land management practices on water, sediment and agricultural chemical yields in large complex watersheds of varying soils and land use.	Uses the TOPMODEL method for runoff and extended it with a parameterization of transfer between surface & atmosphere (Famiglietti and Wood, 1995; Peters-Lidard et al., 1997). Model developed originally to simulate the surface water and energy balance for warm seasons.	A macroscale hydrologic model that solves full water and energy balances (Liang *et al.*, 1994) Land surface is modelled as a grid of large (>1km), flat, uniform cells Water can only enter a grid cell via the atmosphere.
Parameters for landuse change	Land use scenarios considering soil property changes Averaging the transmissivity coefficients of all grid cells characterizes the catchment-wide saturated permeability of the soils Land-use components are modelled by a raster-based model which produces land-use maps for the SWAT model.	Land cover parameters are taken from literature (Peters-Lidard et al., 1997), while values for the Leaf Area Index (LAI) can be taken from field observations. Analyze changes in soil hydraulic properties due to land use change (K_s, residual water content, saturated water content, pore size distribution index, bubbling pressure)	Vegetation library file: This routine reads in a library of vegetation parameters for all vegetation classes used in the model. Vegetation parameter file: This routine reads in vegetation parameters (e.g. LAI, root fraction) for the current grid cell and relates each vegetation class in the cell to appropriate parameters in the vegetation library.
Technical & programming approaches to include landuse.	Public domain software program (FRAGSTATS) designed to compute a wide variety of landscape metrics with emphasis on spatial distribution of map patterns. The technical integration of land-use changes is done by external programs or manual input,. The hydrological response units (HRU) attribution is internally defined by overlaying the input soil map and land use map with a sub-catchment map.	Combines the local-scale and process oriented soil-vegetation-atmosphere-transfer scheme approach (SVAT) to represent local-scale vertical water fluxes of single grid cells with the catchment scale. GIS used as an interface to spatial data like land-use and as a general user-interface and handles not only maps but also links to time series and static parameters. The technical solutions of how to include land-use is a component based approach where every modelling task is handled by a single and separate component.	Versions 4.1.0 and later include a lake/wetland cover type For a given tile, *jarvis-style* vegetation stomatal response used in computing transpiration Version 4.1.0 and later can consider canopy energy balance separately from ground surface geographic locations When configurations of land cover types are not considered; VIC lumps all patches of same cover type into 1 tile.
Data format structure to incorporate landuse changes.	The catchment is partitioned into a number of sub-basins based on DEM and river channel delimitation. Divided into HRU based on land cover and soil maps Each HRU contains a number of water storage volumes for canopy. Soil map aggregated to new class soil map.	A grid-based spatially distributed model, which combines the physically based simulation of spatially distributed, single SVAT schemes with lateral TOPMODEL concept. Aggregation of DEM, soil map and land use classification for the calculation of regional water balances.	Can subdivide each grid cell's land cover into arbitrary number of "tiles", each corresponding to the fraction of the cell covered by that particular land cover

REFERENCES

- Neitsch, S.L., Arnold, J.G., Kiniry, J.R., Williams, J.R. and King, K.W., 2002. Soil Water Assessment Tool Theoretical Documentation.
- Famiglietti, J.S. and Wood, E.F., 1995. Multiscale modelling of spatially variable water and energy balance processes. Water Resour. Res., 30.
- Peters-Lidard, C.D., Zion, M.S. and Wood, E.F., 1997. A soil-vegetation-atmosphere transfer scheme for modelling spatially variable water and energy balance processes. J. Geophys. Res., 102.
- Liang, X., Lettenmaier, D.P., Wood, E. and Burges, S., 1994. A simple hydrological based model of land surface water and energy fluxes for general circulation models. . Journal of Geophysical Research, 99(D7): 14 415-14 428.

3. METHODOLOGY

3.1. Sequence of the research process and methodology.

Parameterization of TOPMODEL and assessment of hydrologic impacts of landuse change were performed based on the spatial data sets available and other data sets obtained by remote sensing and field observations. The methodology and research process can be summarized by figure 3.1.

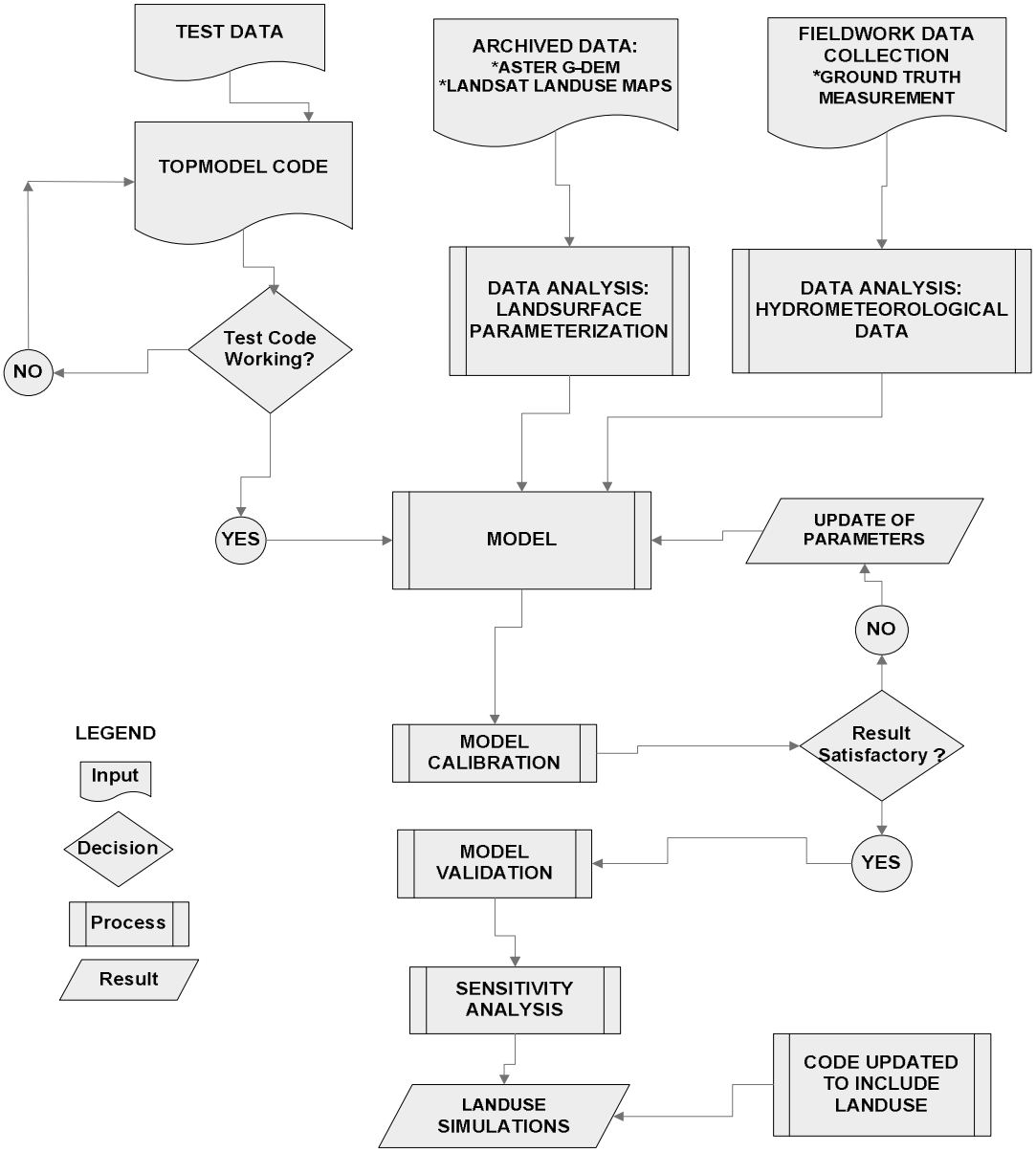

Figure 3-1: Flow chart showing sequence of the research process and methodology.

3.1.1. Data availability and fieldwork activities

Available data for this research include time series of landuse/cover change in the Gilgel Abay catchment for the years 1973, 1986 and 2001 from the work of Kebede (2009) who performed a supervised land cover classification with the use of Landsat ETM images. There is also discharge data from a gauge station of Wetet Abay from 2001 to 2003. The total gauged area is 1656.2km^2. The meteorological data include rainfall and potential evapotranspiration time series from 2001 to 2003 as provided by the National Meteorological Agency of Ethiopia (NMAE). The meteorological data are from Adet, Enjibara, Dangila Kidamaja, Sekela and Wetet Abay stations.

Table 3-1: Fieldwork Activities.

Activity	Equipment used	Purpose/use of the data
Collecting ground truth data.	GPS, Topomaps	Validation of georeferenced satellite images and classified landsat imagery.
Insitu measurement of soil moisture.	Soil moisture (theta) probe. Theta probe designed to take moisture to a soil depth of 0.06 m	To gain an insight into soil moisture distribution among the different landuse classes, terrain in the basin. Comparing Topographic index derived saturation potential against actual wetness in the catchment
Collection of soil samples and laboratory experiments.	Soil sample rings & polythene bags. The top 5-10 cm of soil collected with soil moisture rings of diameter=55 mm (mass ~100 g).	For validation of the soil moisture measured by the theta probe.

3.1.2. Computation of missing values by the simple linear regression method.

To fill in the missing data the method used is the simple linear regression method by (Salas, 1993) from the Handbook of Hydrology. The filling in of the missing records was done separately considering the wet and dry seasons. The correlation coefficients of 6 rainfall stations (all seasons) were calculated to see the strength of the relationship between the stations' measured rainfall data. Stations that have the highest correlation coefficients were used for filling in the missing data. Salas (1993) highlights that this method is most commonly applied to transfer hydrological information between two stations. The relation is established based on the concurrent records of the two rainfall stations. This is applicable in this study where there is l long or complete rainfall records for example of Dangila station but missed records for example in the case of Adet station**.** The simple regression model computes a regression between Dangila and the other recording stations. The formula is given by:

$$y_t = a + bx_t + a\theta(1-\rho)^{1/2}\sigma_y\varepsilon_t \qquad \textbf{[27]}$$

Where:

y_t = dependant variable (rainfall from dependent station) [L]

x_t = independent variable (rainfall from independent station) [L]

a, b = population parameters for the regression [-]

σ_y = population standard deviation [-]

ρ = cross correlation of two time series [-]

ε_t = normal uncorrelated variable with mean 0 and variance 1 which is uncorrelated with x_t [-]

The estimation of parameters of *a* and *b* are given by

$$a = \bar{y}_t - b\bar{x} \quad \textbf{[28]}$$

$$b = rS_1(y)/S_1(x) \quad \textbf{[29]}$$

When just few records are missing, equation **[27]** without noise may be used for filling in missing data i.e. ε_t (θ=0). In this situation only few records were missing, so this formula is used. If *r* is the sample cross correlation coefficient, then it reads as:

$$r = \frac{\sum (x_i - \bar{x})(y_i - \bar{y})}{\sqrt{\sum (x_i - \bar{x})^2 \sum (y_i - \bar{y})^2}} \quad \textbf{[30]}$$

Where:

x_i and y_i = rainfall records of the independent and the dependent stations [L]

$\bar{y}$ and $\bar{x}$ = the estimated mean of the variable y_t and x_t

$S_i(y)$ and $S_i(x)$ = corresponding estimated standard deviation of y_t and x_t,

Using this formula the linear equations were developed for calculating missing rainfall records. To have a better or more accurate fit, the wet season and the dry season were considered separately.

3.1.3. Validation of the method of filling in missing data

To evaluate the effectiveness of the simple linear regression method, a simple validation method is by comparing estimates to observed values. The observed values are considered unknowns and the completed values for the stations were compared with the original values. The Root Mean square error (RMSE) was used to assess the efficiency and accuracy of this method. The RMSE is one of the many ways to indicate the deviation between the true value and the estimated ones. It is a quantitative measure that can determine the quality of the method of filling in the missing values.

The formula for calculating RMSE reads:

$$RMSE = \sqrt{\frac{\sum (Q_{obs} - Q_{sim})^2}{N}} \quad \textbf{[31]}$$

Where:

Q_{obs} = the observation

Q_{sim} = estimated counterparts

N = number of sample.

3.1.4. Evaluation of the rainfall distribution using GIS

Accurate estimation of distribution of rainfall is critical to the successful modeling of hydrologic processes. After filling in the missing data, areal rainfall in this study was estimated by the Thiessen polygon method. The Thiessen polygons are used to model or approximate the zones of influence around points. Panigrahy (2009) has noted that rainfall distributions are accurately estimated by assuming a spatial geometry tied to point rain gage observations using the Thiessen polygons. Therefore in this study meteorological stations were used. Thiessen weights for each station were calculated by dividing the area of influence of each station by the total area of the catchment and this is used as a weighting factor for the station.

$$\overline{P} = \frac{1}{A}\sum_{s=1}^{s=n}\left(A_s P_s\right) \qquad \textbf{[32]}$$

Where:

$\overline{P}$ = average rainfall

P_s = rainfall measured at each station.

n = number of meteorological stations

A = total subbasin area

A_s = area of each polygon inside the basin

3.1.5. Evaporation calculation.

For daily estimate of evaporation the Penman-Monteith method was used. The FAO (Food and Agricultural Organization) Penman-Monteith method for calculating potential evapotranspiration reads: (after Allen *et al.*, 1998).

$$ET_o = \frac{0.408\Delta\left(R_n - G\right) + \gamma\frac{900}{\left(T+273\right)}u\left(e_s - e_a\right)}{\Delta + \gamma(1+0.34u)} \qquad \textbf{[33]}$$

Where:

ET_0 = daily reference crop evapotranspiration [mm day^{-1}]

R_n = net radiation flux [MJ m^{-2} day^{-1}]

G = heat flux density into the soil, it is very small and can be neglected, [MJ m^{-2} day^{-1}]

T = mean daily air temperature [^{o}C]

γ	=	psychometric constant	[kPa $^{o}C^{-1}$]
U	=	wind speed measured at 2m height	[ms^{-1}]
e_s	=	saturation vapour pressure, $e_s = 0.611\exp\left(\frac{17.27T}{T+273.3}\right)$	[kPa]
e_a	=	actual vapour pressure $e_a = e_s \times \frac{RH}{100}$	[kPa]
RH	=	relative humidity	[%]
$e_s - e_a$	=	saturation vapour pressure deficit	[kPa]
Δ	=	slope of saturation vapour pressure curve	[kPa °C^{-1}]

3.1.6. Choice of transmissivity profile.

TOPMODEL assumes an exponential profile of soil transmissivity, a form that is frequently observed in the soil upper layers and that is easy to handle analytically (Beven, 1984). To test which of the transmissivity profiles applies best to the catchment, equation [**26**] is transformed into the linear functions of time:

Exponential	*Parabolic*	*Linear*	
$\frac{1}{Q_t} - \frac{1}{Q_s} = \alpha\tau$	$\sqrt{\frac{1}{Q_r}} - \frac{1}{\sqrt{Q_s}} = \alpha\tau$	$\ln Q_b - \ln Q_s = -\alpha\tau$	[**34**]

Where:

$\alpha = \frac{1}{Am}$	$\alpha = \frac{\sqrt{Q_o}}{AS_m}$	$\alpha = \frac{Q_o}{AS_m}$

In the related transformed *Q-t* graphs, these linear functions plot as a straight line with gradient α. The transformed *Q-t* graph are for the exponential transmissivity profiles as a 1/*Q* - *t* graph, for the parabolic profile a *Q* - *t* graph, and for the linear transmissivity profile a ln *Q* - *t* graph. Ambroise *et al.,* (1996) states that the master recession curve of a catchment should plot as a straight line in the transformed *Q-t* graph of the assumed transmissivity profile. Figure 3-2 shows an example of this method. Beven (1997b) states that not all recession curves show such an explicit result. Therefore some care needs to be taken as similar shapes of recession curves can be obtained under different sets of assumptions (Pilot, 2002).

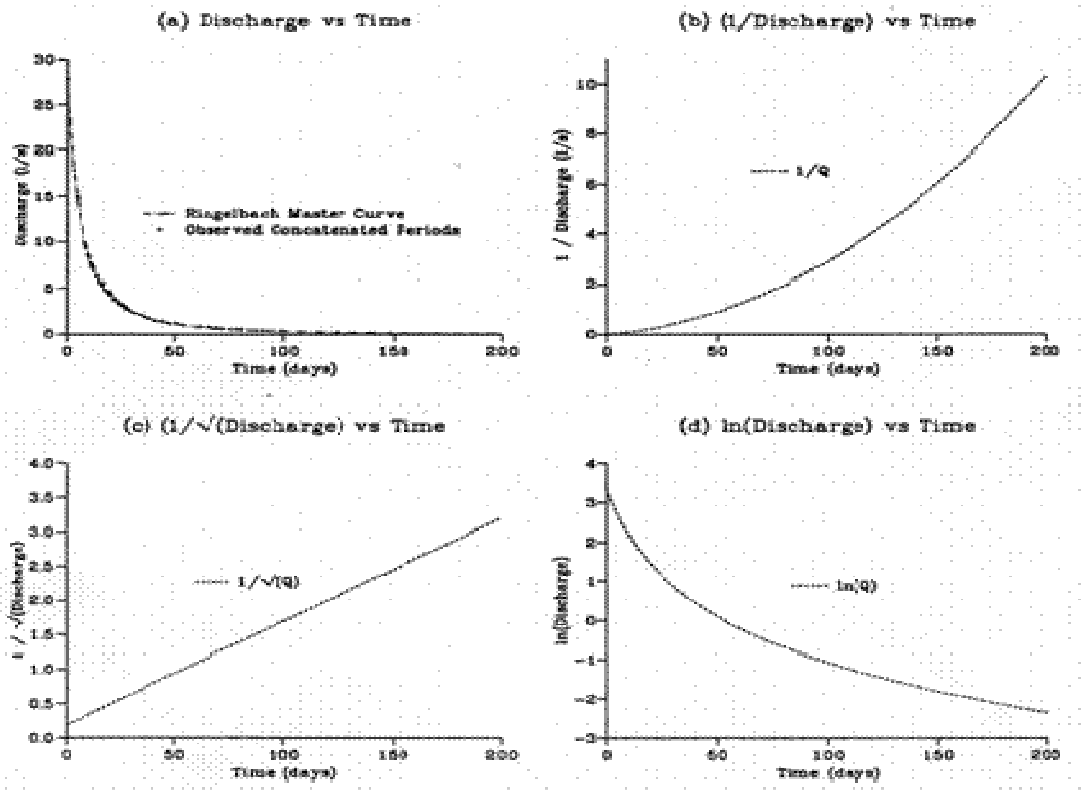

Figure 3-2: Derivation of an estimate for the TOPMODEL *m* perimeter using recession curve analysis: modified after Beven (2001).

3.1.8. Code modification and version of TOPMODEL applied

The IDL TOPMODEL code was modified to allow application in a semi distributed fashion. Once operational the code was applied to the Gilgel Abay Basin. The code is a conversion of Keith Beven's (1979) FORTRAN (viz. FORmula TRANslator) version of TOPMODEL where an infiltration excess overland flow component is considered to allow for landuse simulations. The IDL code was chosen because it can handle relatively large sizes of the topographic index histogram. The infiltration excess flow is calculated using the Green- Ampt infiltration model whereby water infiltrates as a piston like sharp wetting front (Green and Ampt, 1911). However in the initial run the concept of Green and Ampt is ignored. A concept that has been implemented without the infiltration excess overland flow is from Quinn and Beven (1993). This is because in reality, there is often not a sharp wetting front and/or the soil above the wetting front may not saturate. In the Quinn and Beven (1993) concept the difference between precipitation and evaporation is directly added to the water table. Finally comparisons have been made for simulations with and without the Green and Ampt model.

3.1.9. Sensitivity analysis, calibration and validation for TOPMODEL

Sensitivity analysis is a useful tool to assess the effect of parameter changes on model output. An initial run of the model is made for the period 2001-2002 with some parameters values obtained from literature.

Values for each chosen parameter is varied across the range provided from literature as described by Beven and Kirkby (1979) while keeping the values of the other parameters fixed. Having gained a knowledge of which parameters are most sensitive, 3 parameters were chosen to further evaluate model sensitivity. These are the soil hydraulic conductivity decay parameter (m), the soil transmissivity at saturation (T_o) and the root zone available water capacity (SR_{max}).

Calibration for the period 2001-2002 was done manually by 'trial and error' where the TOPMODEL parameters are manually changed to optimize model performance. For each model run, parameter values in the text file containing parameters are changed. Calibration was to optimize the model efficiency by first fitting the baseflow recession. After calibration of the baseflow the peak flows were fitted. For example m, SR_{max}, and T_O parameters were adjusted until the recession tail matched, then the peak flow and finally the runoff volume of the simulated hydrograph best matched the observed hydrograph. These parameters were also adjusted until the rising limb of the simulated hydrograph and timing of the peak flow closely matched the observed hydrograph. By optimizing the SR_{max} parameter, the timing of the peak flow could be improved since a higher value of SR_{max} results in a model response that cause better fit of rising limb.

Model validation has been carried out to test whether the model, using the same parameter set obtained by optimisation (2001-2002 period), but with independent data sets, can produce outputs with reasonable accuracy. The model has been validated using the 2003 data set. The parameters found by calibration were used for validation of the model. The parameter values were initially set based on expected ranges and also based on best fits of outputs. As such the simulated streamflow is compared to observed streamflow. This is done graphically (visual comparison) or numerically (comparison of observed and predicted values) using performance measures. The performance measures used in this study are the Nash-Sutcliffe Efficiency (NS) and Relative Volume Error (RV_E).

Nash-Sutcliffe efficiency

The Nash-Sutcliffe efficiency measure goes to 1 as the fit improves. A value between 0.6 and 0.8 indicates that the model performs reasonably. Values between 0.8 and 0.9 indicate that the model performs very well and values between 0.90 and 1.0 indicate that the model performs extremely well (Nash and Sutcliffe, 1970). The formula for Nash-Sutcliffe (NS) reads:

$$R^2 = 1 - \frac{\sum_{i=1}^{N} (Q_{obs} - Q_{sim})^2}{\sum_{i=1}^{N} (Q_{obs} - \overline{Q}_{obs})^2} \qquad \textbf{[35]}$$

Where:

Q_{obs} = the observed discharge [L^3T^{-1}]

Q_{sim} = predicted observed discharge [L^3T^{-1}]

$\overline{Q}_{obs}$ = the observed mean. [L^3T^{-1}]

N = the total number of time steps [-]

Relative Volume Error (RV_E)

The second performance measure, the RV_E is used for quantifying the volume errors. This RV_E can vary between ∞ and - ∞ but performs best when a value of 0 is generated since no difference between simulated and observed discharge occurs (Janssen and Heuberger, 1995). A relative volume error less than +5% or -5% indicates that a model performs well while relative volume errors between +5% and +10% and -5% and -10% indicate a model with reasonable performance.

$$RV_E = \left[\frac{\sum (Q_{sim} - Q_{obs})}{\sum Q_{obs}} \right] * 100\% \quad \textbf{[36]}$$

3.2. Parameterization of land-use in TOPMODEL.

Landuse change in any catchment affect many processes like evapotranspiration, resistance to surface runoff, interception, and shading from solar radiation among others. A description of how these processes are implemented in TOPMODEL is done.

3.2.1. Soil Adjusted Vegetation Index (SAVI)

SAVI is the Soil Adjusted Vegetation Index, which was introduced by Huete (1988). The initial construction of this index was based on measurements of cotton and range grass canopies with dark and light soil backgrounds. The SAVI reads:

$$SAVI = \frac{(1+L)(NIR - R)}{NIR + R + L} \quad \textbf{[37]}$$

Where:

NIR = near-infrared reflection

R = red reflection

L = soil adjustment factor, most often defined as 0.5.

The adjustment factor 'L' was found by trial and error until a factor that gave equal vegetation index results for the dark and light soils was found (Huete, 1988). The standard value of L typically used in most applications is 0.5, which is for intermediate vegetation densities. Negative SAVI indicates presence of water.

3.2.2. Leaf Area Index (LAI)

The LAI is defined as the ratio of the total area of all leaves on a plant to the ground area covered by the plant. If a plant has only one layer of leaves and these would cover the ground exactly, then the LAI would be 1, because the leaf area would equal the ground area covered (figure 3-3). For crops such as maize the LAI goes up during the growing season to values ranging between 2 and 5. The LAI is then computed from the SAVI map. In this study a combination of the SAVI values obtained from the 1973, 1986 band 2001 landsat imagery were compared to the literature values shown in table 3-2.

Figure 3-3: Illustration of concept of LAI after (after Parodi, 2002).

$$LAI = \frac{SAVI - C_1}{C_2} \qquad [38]$$

Where:

C_1, C_2 = empirical constants

Table 3-2: Literature values for SAVI constants and maximum LAI

Crop	Country	C_1	C_2	Max.LAI	Source
Cotton	USA	0.82	0.78	3.5	Huete, Jackson, and Post (1985)
Maize	Italy	1.27	1.1	3.3	Durso and Santini (1996)
Maize	USA	0.68	0.5	6	Dauntry *et al*. (1992)
Soyabean	USA	0.72	0.61	6	Dauntry *et al*.(1992)
Wheat	USA	0.73	0.67	5	Choudhury *et al* (1994)
Fruit trees	Italy	1.34	2.7	2.6	Durso and Santini (1996)
Winter vegetables	Italy	1.31	2.75	4.2	Durso and Santini (1996)
Bush and grassland	Niger	0.14	0.3	1.2	van Leeuwen *et al* (1997)
Grassland	Niger	0.13	0.35	1.3	van Leeuwen *et al* (1997)
Millet	Niger	0.13	0.47	0.8	van Leeuwen *et al* (1997)
Degraded bush	Niger	0.11	0.28	1	van Leeuwen *et al* (1997)
All crops		0.69	0.59	6	

3.2.3. Interception module.

For the estimation of interception of rainfall methods have been used for agricultural crops and for trees and forests. These methods have been described in the agro hydrological model Soil-Water- Atmosphere and Plant (SWAP) (see Kroes and van Dam, 2003). Interception is assumed not to contribute to infiltration or runoff and therefore an interception depth is subtracted from the rainfall before infiltration and runoff are estimated.

Agricultural crops and grasslands

The interception of precipitation can be highly variable in space and time, particularly in catchments with mixed land use, so an interception module (figure 3-4) based on Dam (2000) was used:

$$P_i = aLAI\left[1 - \frac{1}{1 + \frac{bP_{gross}}{aLAI}}\right] \qquad \textbf{[39]}$$

Where:

P_i	=	intercepted precipitation	[cm]
LAI	=	leaf area index	[m^2 m^{-2}]
P_{gross}	=	gross precipitation	[cm]
a	=	empirical coefficient	[cm]
b	=	the soil cover fraction (=LAI/3.0)	[-]

The method is an assumption that the amount of interception storage asymptotically reaches a maximum value that is factored in the *a LAI* part of equation [**39**] (Braden, 1985). Therefore the *aLAI* term is called the saturation amount. In principle *a* must be determined experimentally but in this work all parameters were obtained from the literature and from landuse maps. In agricultural crops a value of *a* = 0.25 was assumed following Dam (2000). This interception model has been applied in such as the Soil-Water-Atmosphere-Plant (SWAP) model.

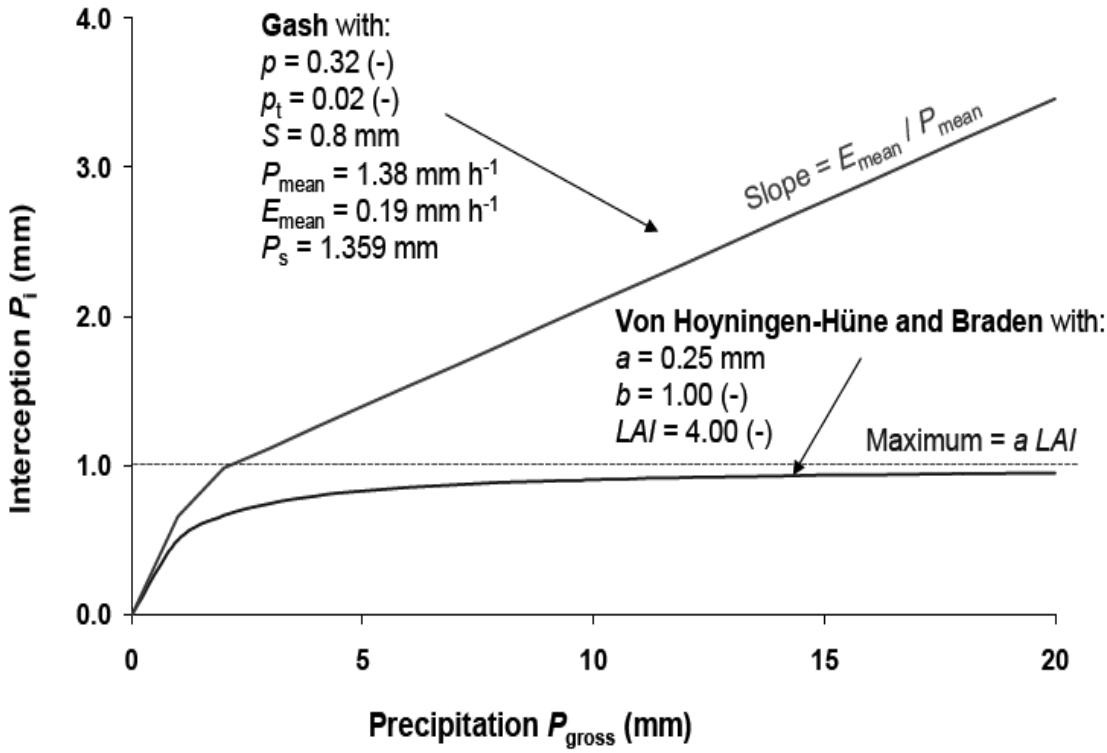

Figure 3-4: Interception for agricultural crops (Von Hoyningen-Hüne, 1983; Braden, 1985) and forests (Gash, 1979; Gash *et al*., 1995).

Forests

An important drawback of equation [**39**] is that the effect of rain duration and evaporation during the rain event is not explicitly taken into account. In case of interception by trees the effect of evaporation during rainfall cannot be neglected. Gash (1979, 1985) formulated a physically based and widely used interception formula for forests. Rainfall is considered to occur as a series of discrete events, each comprising a period of wetting up, a period of saturation and a period of drying after rainfall ceases. The canopy is assumed to have sufficient time to dry out between storms. During wetting, the increase of intercepted amount is described by:

$$\frac{\Delta Pi}{\Delta t} = (1 - p - p_t)P_{mean} - \frac{P_i}{S}E_{mean} \qquad \textbf{[40]}$$

Where:

p	=	a free throughfall coefficient	[-]
p_t	=	the proportion of rainfall diverted to stemflow	[-]
P_{mean}	=	the mean rainfall rate	[mmh^{-1}]
E_{mean}	=	the mean evaporation rate of intercepted water when the canopy is saturated	[mmh^{-1}]
S	=	the maximum storage of intercepted water in the canopy	[mm]

Integration of equation **[40]** yields the amount of rainfall, P_s [mm] which saturates the canopy:

$$P_s = \frac{P_{mean}}{E_{mean}} S \ln\left(1 - \frac{E_{mean}}{P_{mean}(1-p-p_t)}\right) \quad \text{with} \quad 1 - \frac{E_{mean}}{P_{mean}(1-p-p_t)} \geq 0 \qquad \textbf{[41]}$$

For small storms $(P_{gross} < P_s)$ the interception can be calculated from:

$$P_i = (1-p-p_t)P_{gross} \qquad \textbf{[42]}$$

For large storms ($P_{gross} > P_s$) the interception according to Gash (1979) follows from:

$$P_i = (1-p-p_t)P_s + \frac{E_{mean}}{P_{mean}}(P_{gross} - P_s) \qquad \textbf{[43]}$$

Figure 3-4 shows the relation of Gash for typical values of a pine forest as a function of rainfall amounts. The slope $\frac{\Delta Pi}{\Delta P_{gross}}$ before saturation of the canopy equals (1-p-p_t), while after saturation this slope equals E_{mean}/P_{mean}. This analytical model has been used with considerable success to predict interception in a wide range of environments including the Tai forest of Ivory Coast by Hutjes (1990).

3.2.4. Evapotranspiration calculated using the crop coefficient approach

Evapotranspiration from each specific vegetation type or crop evapotranspiration (ET_c) is calculated using the crop coefficient approach (K_c) from the FAO Irrigation and Drainage Paper No. 56 (Allen *et al.*, 1998). In the crop coefficient approach, crop evapotranspiration is calculated by multiplying the reference evapotranspiration (ET_o) by K_c as follows:

$$ET_c = K_c ET_o \qquad \textbf{[44]}$$

Where:

ET_c	= crop evapotranspiration	[mm d^{-1}]
K_c	= crop coefficient	[mm d^{-1}]
ET_o	= reference crop evapotranspiration	[mm d^{-1}]

The crop evapotranspiration differs distinctly from the reference evapotranspiration as the ground cover, canopy properties and aerodynamic resistance of the crop are different from grass. The effects of characteristics that differentiate different vegetation types from grass are integrated into the single crop coefficient (K_c). The K_c varies predominately with the specific crop characteristics while climatic settings only have marginal effects. This enables the transfer of standard values for K_c between locations and between climates. The reference ET_o is defined and calculated using the FAO Penman-Monteith as in Equation [**33**]. The crop coefficient, K_c is basically the ratio of the crop ET_c to the reference ET_o, and it represents an integration of the effects of four primary characteristics that

distinguish the crop from reference grass. These characteristics are crop height, albedo (reflectance) of the crop-soil surface, canopy resistance and evaporation from soil. In this study literature values were used that differentiates all the crop growth stages as also shown in figure 3-5.

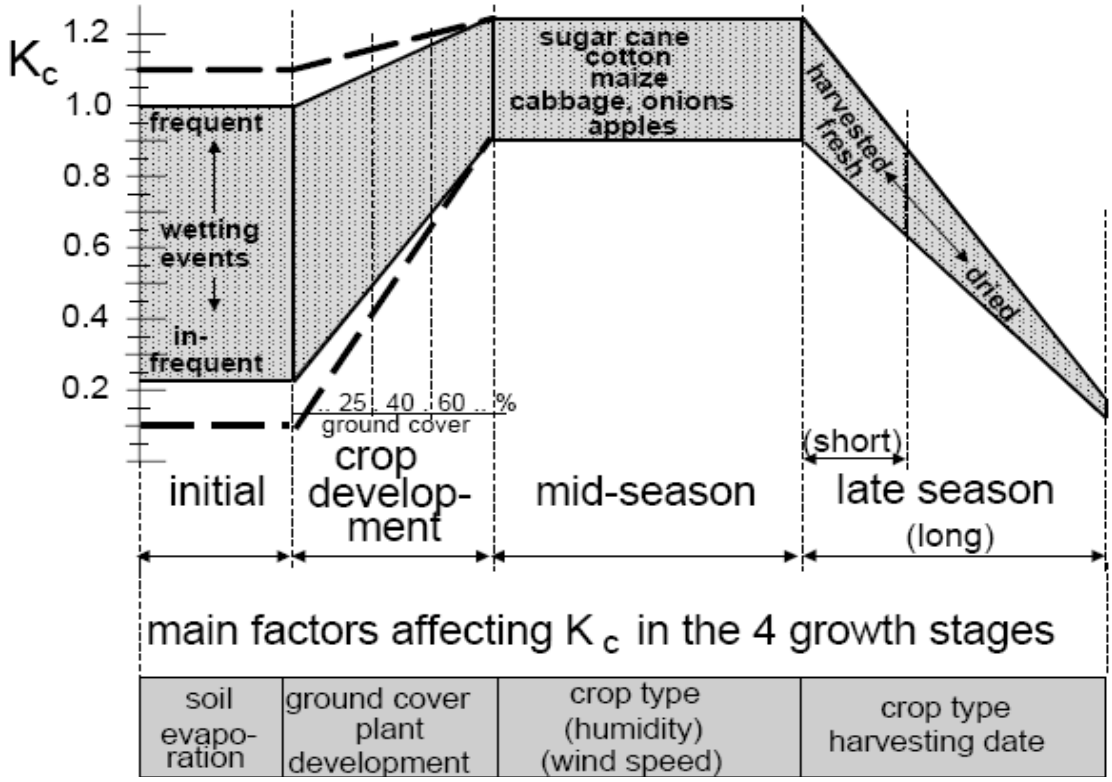

Figure 3-5: Typical ranges expected in K_c for the four growth stages, (Allen *et al.*, 1998).

3.2.5. Green and Ampt model for landuse analysis

In this study the saturated hydraulic conductivity of soils of different land uses in the Upper Gilgel Abay basin were obtained from literature by considering the main soil texture in those landuse classes. TOPMODEL uses the exponential Green-Ampt infiltration equations to compute runoff according to the infiltration excess mechanism. The original Green and Ampt method is used for modelling infiltration of water as a function of time (Green and Ampt, 1911). Green and Ampt uses physically based equations and describes how infiltration rates decrease from an initial maximum to final minimum rate. The modified Green-Ampt model assumes piston flow with a sharp wetting front between the infiltration zone and soil at the initial water content (Beven, 1984). In this model, however, the hydraulic conductivity is assumed to be an exponential function of depth, z. The effective hydraulic conductivity behind the wetting front is given in terms of the hydraulic conductivity at the surface, k_0 as:

$$k(z) = k_0 \, e^{fZ} \qquad [45]$$

Where:

$k_0 =$ the hydraulic conductivity at the surface [LT^{-1}]

z = depth below soil surface [L]

f = constant

If the wetting front has reached a depth z, the infiltration rate, i is given by the generalization of the relationship for layered soils (Childs and Bybordi, 1969)

$$i = \frac{dI}{dt} = \frac{\Delta\psi + z}{\int_{z=0}^{z=Z} [dz / k(z)]} \qquad [46]$$

Where I is the cumulative infiltration [L]

In the approach it is assumed that at the time of ponding t_p, the wetting front is at a depth Z_p which is given by the infiltration rate I_p divided by the change in moisture content $\Delta\theta$

$$z_p = I_p / \Delta\theta \qquad [47]$$

The cumulative infiltration at the time of ponding is given by:

$$I_p = rt_p \qquad [48]$$

Where:

$r =$ the rain rate

At the onset of ponding the rain rate r is assumed to be equal to the infiltration rate i and the infiltration rate is given by

$$r = \frac{k_0 f(\Delta\psi + I_p / \Delta\theta)}{1 - e^{-fI_P / \Delta\theta}} \qquad [49]$$

At any time after ponding has started, the cumulative infiltration is I and the infiltration rate is given by:

$$\frac{dI}{dt} = \frac{k_0 \times f(\Delta\psi + I / \Delta\theta)}{1 - e^{-fI / \Delta\theta}} \qquad [50]$$

The time required for the surface to reach saturation is the time to ponding. Ponding will only occur when the rain rate is greater than or equal to the hydraulic conductivity at the surface. The time to ponding, t_p, is calculated as:

$$t - t_p = \frac{1}{f^* k_0}\left[\ln(I + c\right] - \frac{1}{e^{f*c}}\ln\left(I + C\right) + \sum_{m=1}^{\infty}\frac{\left\{f*(I_p + C)\ \right\}^m}{m!m} - \lambda] \qquad [51]$$

Where:

C = $\Delta\psi\Delta\theta$ is the storage suction factor and

$f\ *$ = $-\ f\ /\ \Delta\theta$

λ = constant given by:

$$\lambda = \ln(I_p + c) - \frac{1}{e^{f*c}}\left[\ln(I_p + c) + \sum_{m=1}^{\infty}\frac{\left\{f*(I_p + C)\ \right\}^m}{m!m}\right]$$

Equation [**51**] is used in Newton-Raphson iterative procedure to calculate the time to ponding. By comparing the infiltration rate with the rain rate the excess rainfall and hence the infiltration excess overland flow is calculated

Table 3-3: A summary of the additional parameters needed for landuse analysis.

Parameter	Meaning/definition
INFEX [-]	An infiltration flag set to 1 to include infiltration excess calculations, otherwise 0. Infiltration excess runoff is calculated using Beven's version of the Green-Ampt model where saturated hydraulic conductivity decreases as an exponential function of depth and the (see Beven, 1984).
K_o [m/hr]	Surface value of the saturated hydraulic conductivity (*Ks*) K_s declines exponentially with depth
Ψ_f [m]	Effective suction head for the calculation of infiltration excess flow
θ [-]	Water content change across the wetting front.(Beven, 1984).

3.2.6. Calibration and sensitivity analysis on landuse analysis.

For comparison of streamflow for the years 1973, 1986 and 2001, m, SR_{max} and K_s were not changed but were only varied for the different landuse types. For initial estimates of the parameters, a guess based on published values was made. Furthermore by applying a trial-and-error method, expert knowledge has been used to identify parameter values and physically meaningful ranges for those parameters were determined.

Sensitivity analysis was carried out to evaluate and quantify the effect of the parameter variations on model output. In this study agricultural land has been selected to evaluate model sensitivity. This was done for the 3 parameters (i.e. m, SR_{max} and K_s). In this study sensitivity analysis was done on a combination of these 3 parameters varying them across their range, keeping the values of the other parameters constant. The sensitivity analysis is carried out for the years 1973, 1986 and 2001

separately but the results plotted in once graph for comparison. The range of all the parameter values was constrained by selected ranges from literature.

It was however difficult to assess whether the streamflow contributions from each landuse are accurate because the model is run separately for each landuse. Furthermore, on the actual ground, a landuse class is not a hydrological subcatchment. The most approximate way was through accumulating the simulated streamflow for the different land uses and by comparing with the observed outflow for the whole catchment. The NS and RV_E performance measures were performed to evaluate the TOPMODEL's efficiency in simulating streamflow for each year.

3.2.7. How to use TOPMODEL for the different landuse classes?

The 1973, 1983 and 2001 landuse maps classified by Kebede (2009) were used in this study. In order to calculate streamflow from the different landuse, the approximate way of doing so is by treating each vegetation/landuse type as a "subcatchment" through a GIS overlay of landuse type. As such also a topographic index distribution has been created for each landuse type. Each 'subcatchment' is run separately with specific vegetation/landuse parameters. The areally weighted results are summed to get a total output in a similar way to having multiple subcatchments with different topographic index distributions. An Area Distance file for overland flow and channel routing is obtained for each landuse type. In order to implement the subsurface storage, each landuse type is allowed to have a specific S_i (mean catchment deficit) calculation since landuse types in the Gilgel Abay basin do not cover the whole subcatchment. In this case it is the recharge rate from each landuse type that needs to be areally weighted and summed before updating S_i at each time step. To implement the impacts of landuse change in TOPMODEL, few additional parameter values are required for example for the Green and Ampt infiltration excess model. These parameters are fixed at each run. The rainfall as an input into the model is considered as uniform depth after subtracting the interception storages. Finally stream flow for historical land cover (1973, 1986 and 2001) is simulated for each. The sensitivity analysis is done by changing the parameters as if they are correct values. Table 3-4 gives a summary of the implementation of landuse analysis in the TOPMODEL approach.

Table 3-4: Summary of how landuse/landcover is implemented in TOPMODEL and terms of the water balance

Process	Agricultural land	Grassland	Forest &Shrub	Water & marshy	Implementation in TOPMODEL
Interception	Increased canopy interception due to higher LAI	Average canopy interception due to intermediate to low LAI	Increased canopy interception due to higher LAI	Assumed no canopy interception	Storage approach: storage capacity proportional LAI. For agricultural crops (Von Hoyningen-Hüne, 1983; Braden, 1985) and forests (Gash, 1979; Gash et al., 1995).
Actual Evapotranspiration (ETa)	Increased ETa from crop surfaces	Intermediate levels of ETa	Increased ETa from canopy	ETa from water bodies	Grass reference ET (ET_o) is multiplied by crop coefficient factor (K_c) to get ET specific for each landcover [ET_c]. ETa computed by the model as a function of ET_c & maximum root zone storage deficit.
Change in soil properties and infiltration	Subsurface stormflow resulting from 'plough-pans' created by repeated ploughing compaction (Minshall and Jamison, 1965). Crop residue below depth of mechanical disturbance however improves soil structure and macro-porosity, increasing inherent permeability of deeper zones. Due to root action and tillage an increase in hydraulic conductivity.	In undisturbed soils, dead and decaying grass root material contributes to development of macro-porosity in the depths at which root penetration occurs. Some crusting of the soil means average to less infiltration capacity and intermediate hydraulic conductivity.	Dead and decaying root systems (at depth>2m) create important fissures or channels for free water conduction, mainly in vertical direction (Champerlin, 1972). Due to root action increase in hydraulic conductivity.	No change in soil properties, no infiltration and no hydraulic conductivity.	Application of Green and Ampt parameters (Green and Ampt, 1911): K_s Ψ_f and θ These parameters are obtained from literature and linked to soil texture in the study area.
Runoff generation and routing	Saturation overland flow	Fast sub-surface storm flow	Delayed interflow	Deep percolation and large porous groundwater	Contributing areas derived from topographic index of each landuse type. Travel time procedure used.
Hydrograph shape	Rises slower, lower peak discharge, higher baseflow (recession limb)	Rises relatively faster, Intermediate peak discharge and baseflow (recession limb)	Rises slower, lower peak discharge, higher baseflow (recession limb)	Rises faster, higher peak discharge , lower baseflow (recession limb)	Recession function

4. DATA ANALYSIS AND PREPARATION

4.1. Measurement of soil moisture in the field

One of the applications of TOPMODEL is to predict the spatial and temporal soil moisture dynamics in space and time (Ambroise *et al*., 1996). In this research, in situ soil moisture observed through theta probe and gravimetric measurements. Some 414 soil moisture measurements were taken at various locations in the Upper Gilgel Abay Basin using a theta probe at depth of measurements of 0-6 cm of depth. Validation of the theta probe measurements was through gravimetric measurements using soil sample rings that were analyzed in a soil mechanics laboratory. The sites selected represent different soil types, vegetation cover and terrain variables.

4.1.1. Vertical profile of soil moisture

TOPMODEL can be extended to handle the spatial variability of soil transmissivity with depth (Saulnier *et al*., 1997). Thus in this research soil moisture measurements were made at depth of (0cm, 20cm, 40cm, 60cm and 80cm as shown by figure 4-1. Measurements were taken at 8 rivers banks and 2 trenches in the Upper Gilgel Abay Basin. In all sites, the soil moisture increases with increase in soil depth up to 90cm. Below this depth, soils saturate and curves become vertical in gradient. However for Tekagadle River and Addis Kidan stream, the soil moisture levels off at 60cm of depth. Generally the entire at the 10 sites is consistent with the exponential decrease of transmissivity with depth which is one of TOPMODEL's assumptions.

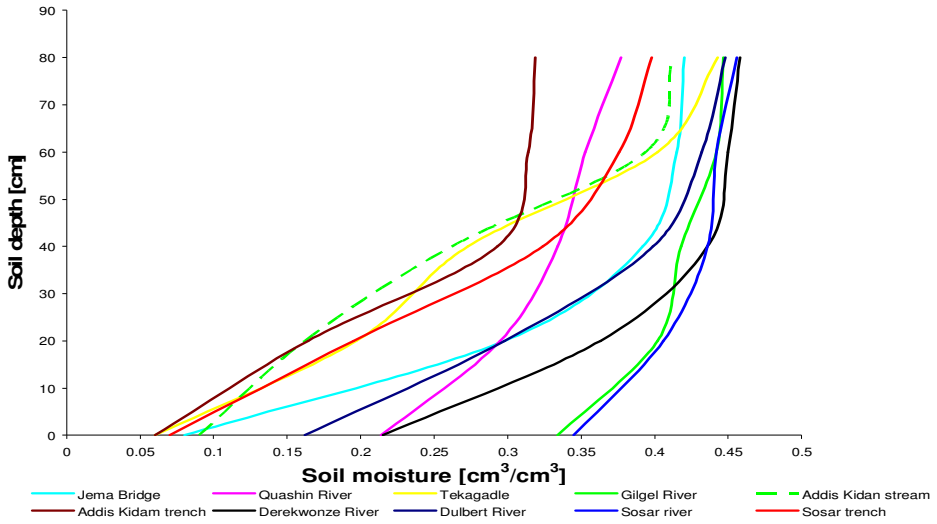

Figure 4-1: Vertical soil moisture profile at different places.

4.1.2. Validation of volumetric soil moisture measurements

Soil moisture laboratory experiments (gravimetric measurements) were evaluated since measurements serve to validate the insitu based soil moisture measurements using the theta probe. Evaluation was by performing a two-sample z-test for means with known variances. The test uses the null hypothesis that says that there is no significant difference between the two sample means of the soil moisture recordings from theta probe measurement and the soil sample rings measurements against either one-sided or two-sided alternative hypotheses. Table 4-1 first shows the frequency distribution of the data measurements from the soil sample rings and the theta probe recordings. The means of the 2 data sets are almost equal but the standard deviation for the soil sample rings is higher (0.151) than for the theta probe measurements (0.079). It is noted that the number of samples of the theta probe recordings is by far larger (414) than the measurements from the soil sample rings (20) and will have an effect on the standard deviation.

Table 4-1: Frequency statistics for the soil moisture data

	Soil Sample rings (gravimetric measurements)	Theta probe (volumetric)
N	20	413
Mean	0.33640	0.35165
Std. Error of Mean	0.033741	0.003869
Median	0.31850	0.36600
Mode	0.097	0.362
Std. Deviation	0.150894	0.078637
Variance	0.023	0.006
Range	0.660	0.417
Minimum	0.097	0.113
Maximum	0.757	0.530

The significance (2 tailed) for the accepted and rejected cases when equal variances are not assumed is greater than (0.05) and this is summarized in table 4-2. In this case we fail to reject the null hypothesis that stated that there is no significant difference between the two population means of the volumetric and gravitational measurements. Therefore the conclusion is that there is no significant difference between the two population means at 95% confidence interval. In this case the volumetric soil moisture recordings relate well to the gravitational measurements in the Upper Gilgel Abay Basin.

Table 4-2: Independent T-samples test for soil moisture

	t-test for Equality of Means					**95% Confidence Interval of the Difference**	
	t	df	Sig. (2-tailed)	Mean Difference	Std. Error Difference	Lower	Upper
Equal variances not assumed	-0.449	19.53	0.658	-0.01525	0.03396	-0.08621	0.05571

4.2. DEM Hydro processing

An ASTER DEM covering the study area has been retrieved free of charge from the website of the Global Aster Gdem, http://www.gdem.aster.ersdac.or.jp/. Figure 4-2 shows maps for the original DEM, filled DEM and the sink map.

4.2.1. Removal/filling of sinks

The fill sinks operation removes local depressions. With this procedure this can be done both for single and multiple pixels. The height value of a single pixel depression is raised to the smallest value of the 8 neighbours of a single-pixel depression and height values of a local depression consisting of multiple pixels are raised to the lowest value of a pixel that is adjacent to the outlet for the depression and that would discharge into the initial depression (Hengl *et al.*, 2007). This will ensure that flow direction will be found for every pixel in the map.

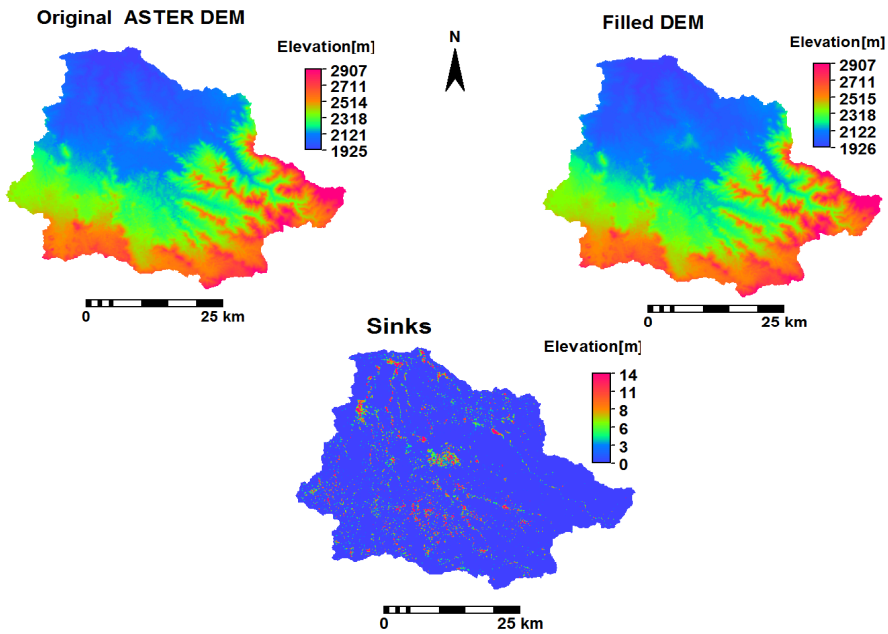

Figure 4-2: DEM hydroprocessing: the original DEM, the filled DEM and sink map.

4.2.2. Flow determination for computing the Topographic Index

The D8 algorithm computes a new attribute of flow direction which can take eight different directional values which can be expressed as degrees or as numeric codes. The D8 method was chosen in the calculations of upslope contributing area because it is more applicable to delineation of the drainage network for drainage areas with well-developed channels (Garbrecht and Martz, 1999). Furthermore, the flow accumulation layer adds up all the upstream water available for runoff using the flow direction information layer along the steepest slope. Thus for each pixel in the basin the number of upstream pixels

weighted with their water available for runoff is added to get a flow accumulation layer. One of the main TOPMODEL input files created from the products of DEM pre-processing is the topographic index file (*TI=Ln(a/tanβ)*) as described in section 2.2.2. The upslope contributing area is *a* and in this case *a*=Flow accumulation map × pixel size (30m). The flow direction, flow accumulation, slope and *TanB* maps are shown in figure 4-3.

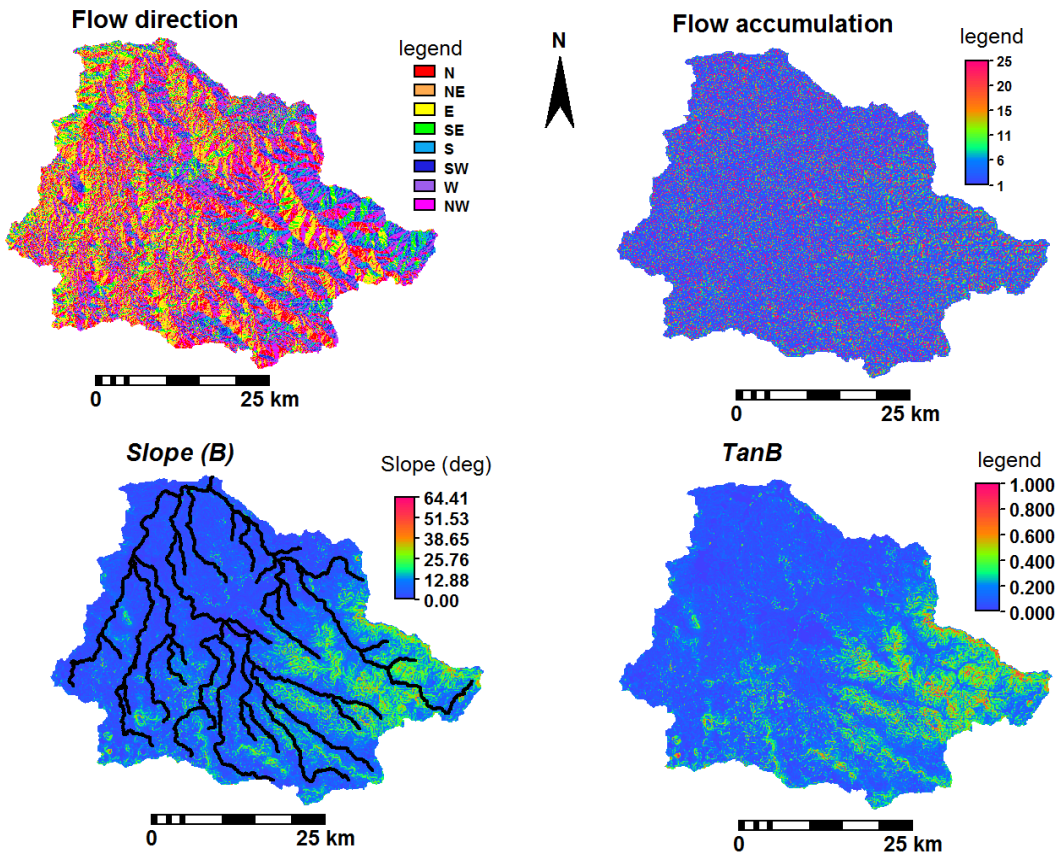

Figure 4-3: Flow direction, Flow accumulation, Slope (β) and *Tanβ* maps.

4.3. The Topographic Index file

The topographic index map of the Upper Gilgel basin is shown in figure 4-4. Higher topographic indices are found in the central and northern part of the basin especially in and around the streams. Lower *Tanβ* values indicate lower hydraulic gradient and more accumulation of water. The areas with higher *ln(a/tanβ)* imply a higher degree of wetness thus more soil moisture contents by higher upslope contributing areas. This is consistent with TOPMODEL's demonstrated principles of hillslope hydrology in which locations with large upslope contributing areas and low surface gradients maintain higher soil moisture levels than locations that are steep or have a small upslope contributing areas (Band *et al*., 1991). The histogram for the topographic index, *Ln(a/tanβ)* derived from ASTER DEM is shown in figure 4-4. The highest number of pixels is found in the topographic index of 7.

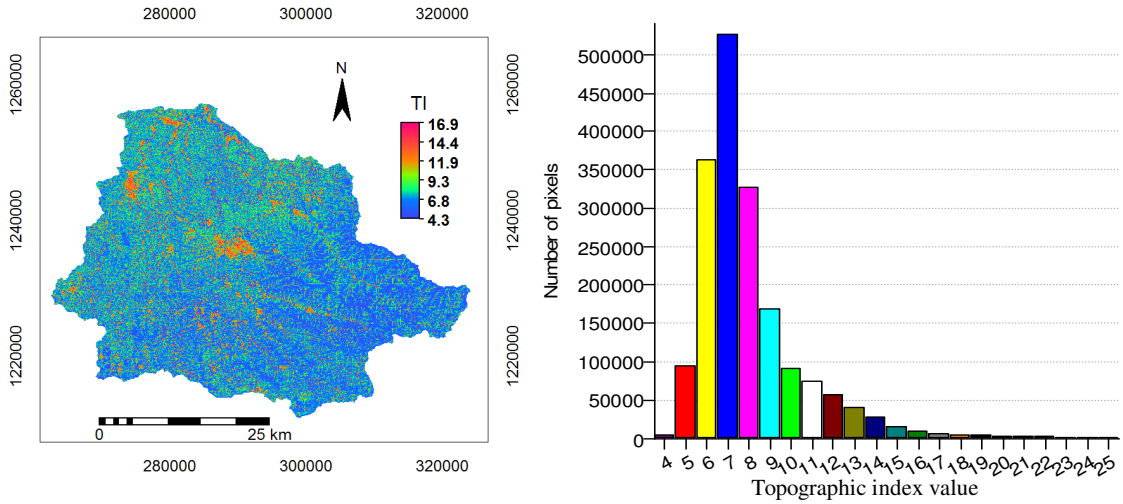

Figure 4-4: The Topographic Index map (left) and frequency distribution of the Topographic index value

4.4. Area Distance file for channel routing

Figure 4-5 shows the area distance map computed from GIS for routing of overland flow by the use of a distance-related delay. Using a point outlet map, a distance calculation was produced and to each pixel the shortest distance to the catchment outlet is shown. However the distance map is sliced into segments for simplicity for the routing of surface flows to the outlet.

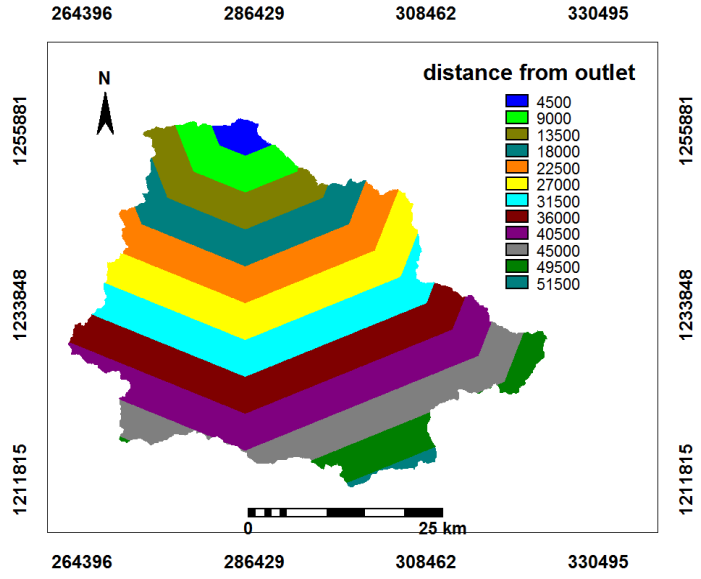

Figure 4-5: Channel routing scheme for the Gilgel Abay basin

4.5. Variation of RMSE: filling in of missing rainfall data

A correlation coefficient table as shown in Appendix 3 of the 6 rainfall recording stations for the wet and dry season was first performed inorder to see the strength of the relationship that exists in the stations' measured rainfall. Table 4-3 shows the results of RMSE values used for the validation method

of filling in missing data by the simple linear regression method. The RMSE values in the dry season are lower as compared to the wet season. This shows that the simple linear regression method is a fairly good method that can be used in terms of the way it estimates missing rainfall as compared to the original rainfall (true value) in terms of precision of the method especially in the dry season.

Table 4-3: RMSE values to validate the simple linear regression method.

	Simple linear regression method	
	Dry Season	Wet Season
Enjibara	1.67	19.32
Wotet Abay	1.33	9.39
Adet	2.49	16.18
Kidamaja	5.50	25.77
Sekela	3.06	22.86

4.5. Evaluation of the rainfall distribution using GIS

The approximate zones of influence of each rainfall recording station are shown in figure 4-6. It can be observed in the table that Adet station which is outside the catchment area and the furthest of all the stations would have a thiessen weight of 0.013. A station such as Sekela inside the station would have more influence and thus have a weight of 0.382.

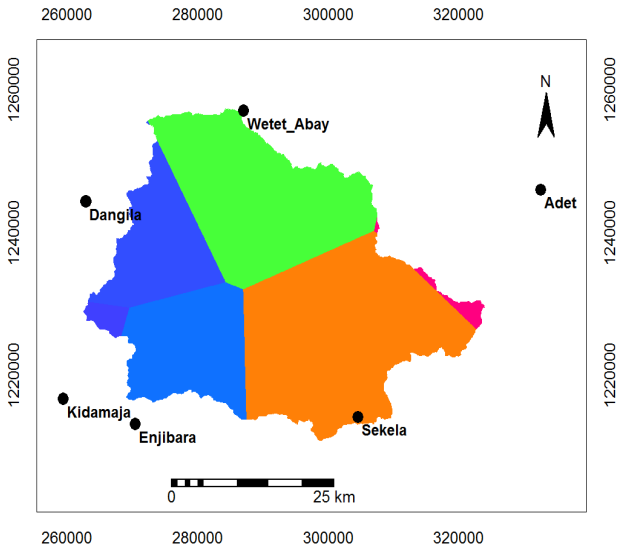

Station	Thiessen weight
Adet	0.013
Enjibara	0.136
Dangila	0.161
Kidamaja	0.297
Sekela	0.382
Wetet Abay	0.010
Total	1

Figure 4-6: Approximate zones of influence around stations by Thiessen Polygons and the Thiessen weights.

The daily areal rainfall of the Upper Gilgel Abay basin is estimated for 2001 to 2003 using the Thiessen Polygon by applying the weights of these meteorological stations. To validate this method, the daily rainfall obtained from the Thiessen polygons method is compared to the average daily areal rainfall

recorded for all the stations. The results are plotted in figure 4-7. Estimates of the Thiessen Polygon method show higher peaks of daily rainfall than the average daily rainfall.

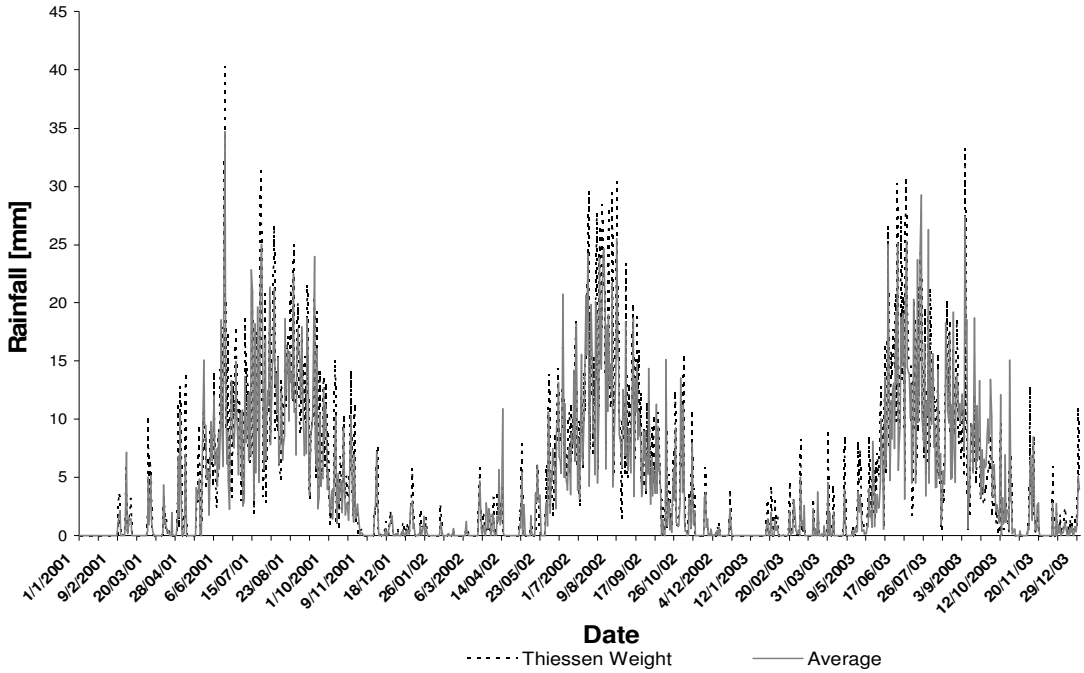

Figure 4-7: Comparison of the daily rainfall: Thiessen polygon method versus the daily average rainfall.

4.6. Comparison of classification results with field based ground control points

Landsat image classification results as shown in figure 4-8 are made by Kebede (2009) for the year 2001 and have been validated by ground survey during a field visit of September 2009. In this case ground control points were taken from different landuse and landcover classes such as grassland, eucalyptus, maize, potatoes, millet and turf fields. The error matrix was used to quantify the level of error from the correct or actual measurements on the ground. The confusion matrix as derived from the image map and field data was generated for accuracy assessment. As shown in table 4-4, accuracy, and reliability are above 60% which shows that the classification result done by Kebede (2009) is satisfactorily. Agricultural land (AG) was the most difficult landcover to classify as shown by only 38% of the agricultural land pixels in the classified image actually representing agricultural land on the ground and the remaining 62% being confused to other landcover types such as Grassland (G) and Forest (F). Secondly the classification accuracy could be due to actual landuse changes. It is noted that the image was acquired in 2001 while the field survey was conducted in 2009.

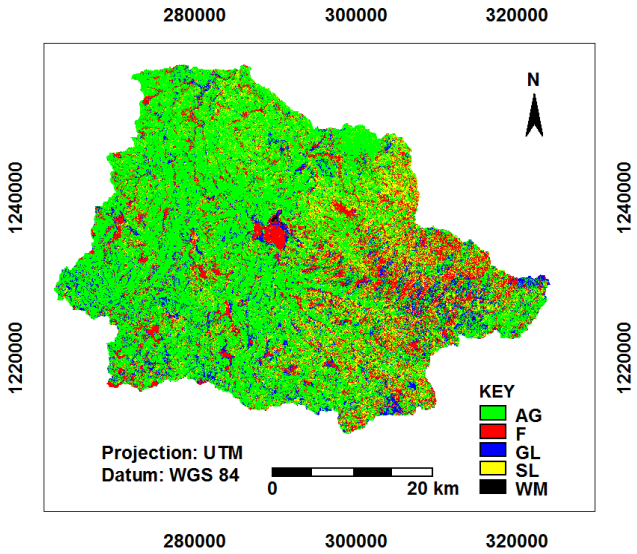

Figure 4-8: Classified landuse map of 2001 for the Upper Gilgel Abay Basin (Kebede, 2009)

Table 4-4: Confusion matrix for validation of land cover map of 2001: classification by Kebede (2009).

	AG	F	GL	SL	WM	PRODUCER'S ACCURACY
Agricultural land (AG)	43	0	0	3	0	93
Forest (F)	26	63	18	12	0	53
Grassland(GL)	28	4	43	9	0	51
Shrubland (SL)	17	0	0	28	0	62
Water & marshy Land (WM)	0	2	1	0	36	92
USER ACCURACY (%)	38	91	69	54	100	

Average Accuracy = 70.43 %, Average Reliability = 70.44 %, Overall Accuracy = 63.96 %.

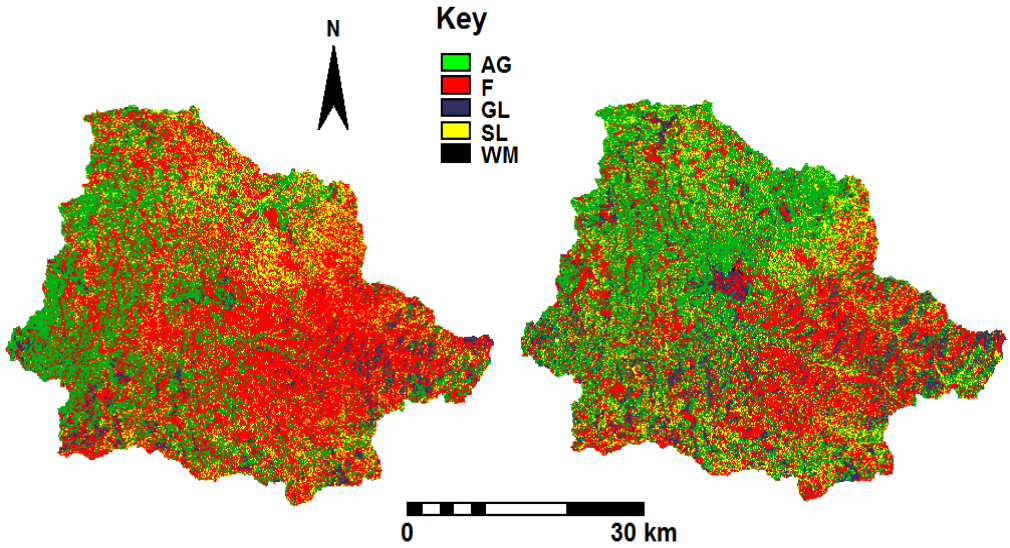

Figure 4-9: The classified landuse maps for 1973 and 1986 (Kebede, 2009)

The 1973 and 1986 landsat image classification results done by Kebede (2009) are shown in figure 4-9 . Figure 4-10 shows the actual percentages occupied by these different landcover types in the years 1973, 1986 and 2001. There have been significant landuse changes where agricultural land covered 30% of the catchment in 1973, 40% in 1986 and 62% in 2001. This could be attributed to the increase in population that has increased the demand for agricultural land. Farmers in this area commonly remove forests to create land for agriculture. The resulting effect was the decrease in forest land from 52% in 1973, 33% in 1986 and to 17% in 2001. However the area occupied by shrubs (shrubland) remained constant. There has been a small percentage of area (less than 1%) occupied by water and marshy area in all of the years.

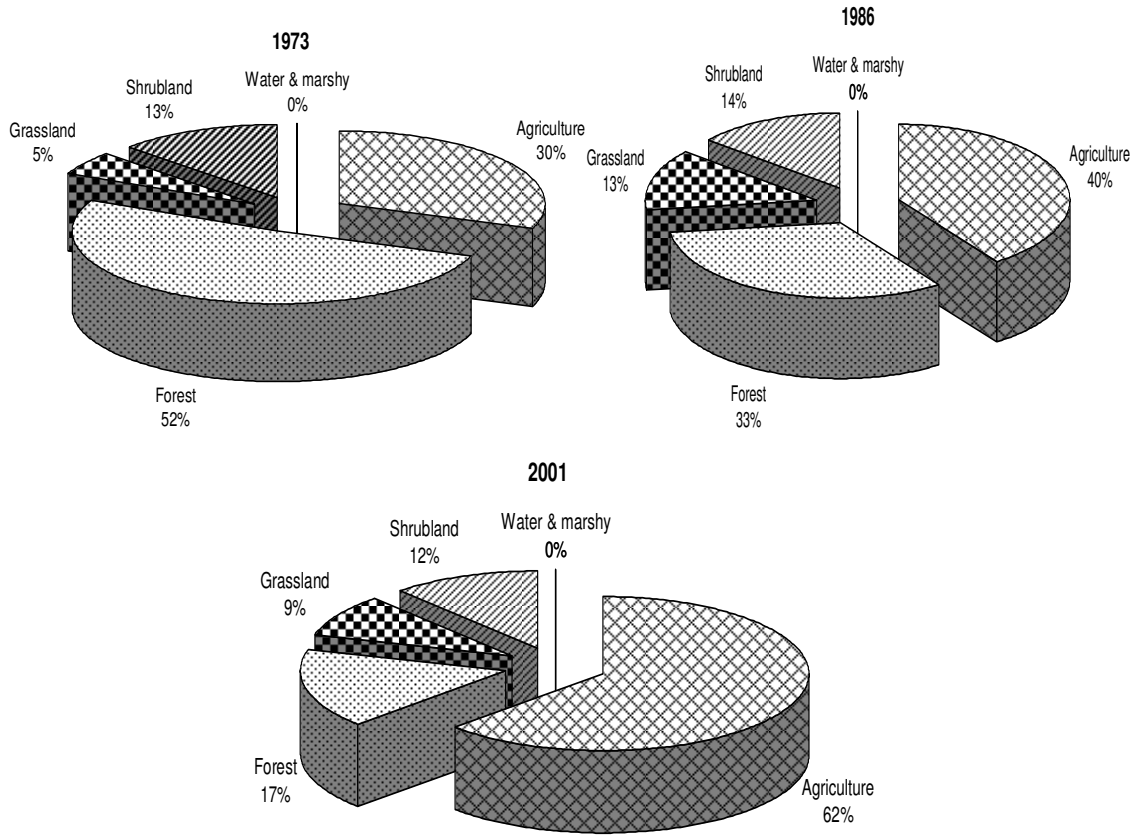

Figure 4-10: Landcover types in the Upper Gilgel Abay Basin: classification by Kebede (2009).

4.7. Distribution of Topographic Index with landuse.

Histograms of the Topographic index distribution for the Upper Gilgel Abay basin for the 30m ASTER DEM are shown in figure 4-11. The highest fractional area of the topographic index is around 0.3 and this is occupied by the topographic index of 7. Agricultural land and forests are contributing to the highest fractional area occupied by this topographic index.

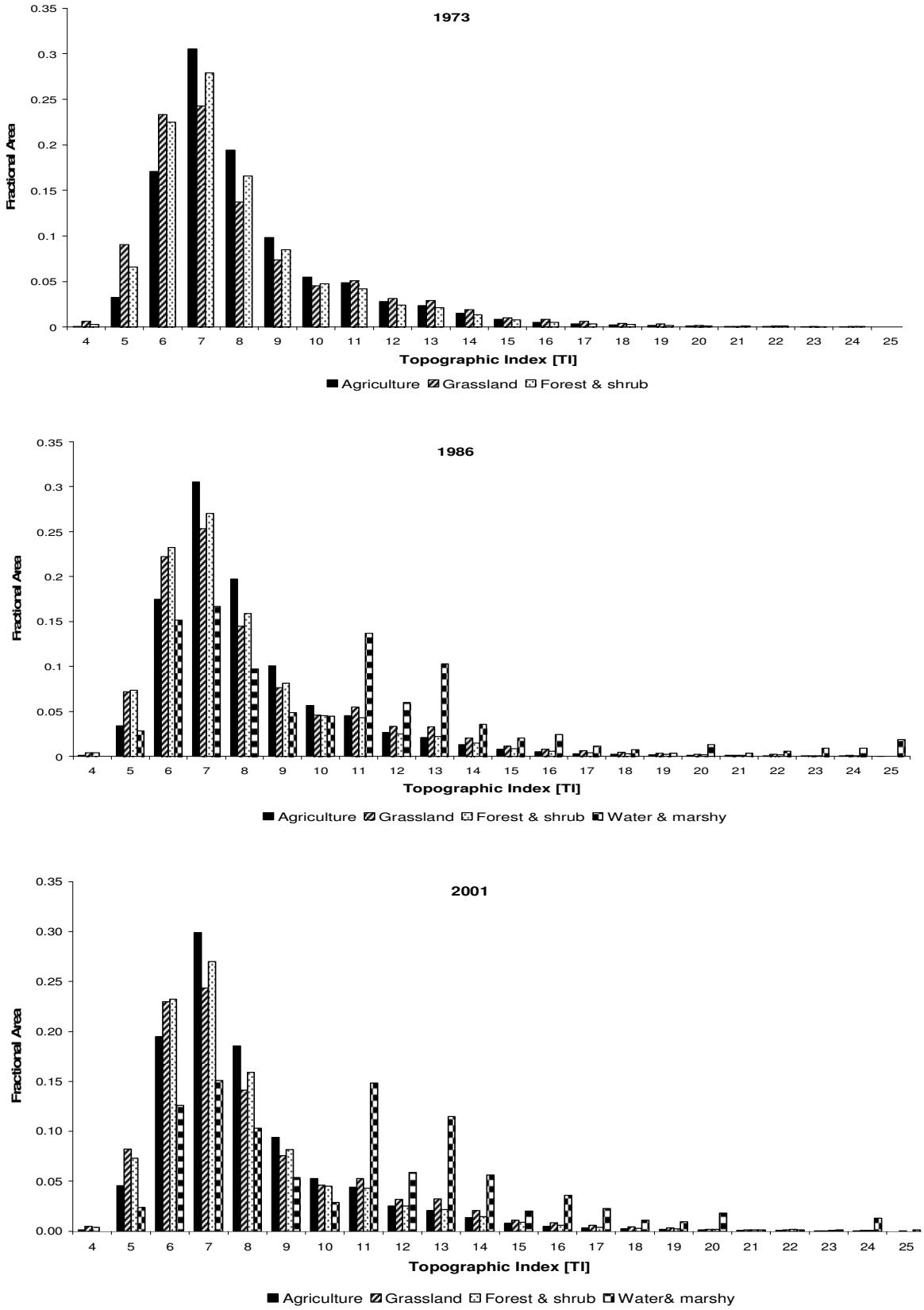

Figure 4-11: Fractional Distribution of Topographic index with Landuse.

5. RESULTS AND DISCUSSION

This chapter is divided into two sections. The first section is on general simulation results for TOPMODEL and the topographic index. The second section is on modelling landuse change impacts landuse simulation results using TOPMODEL.

5.1. Hydrograph simulation and the Topographic Index

Figure 5-1 shows streamflow simulation results for the Upper Gilgel Abay catchment. TOPMODEL was able to reproduce the peaks and the baseflow in a satisfactory way except for the end of 2001. Rising limbs of hydrographs of the years 2001 and 2002 however do not match well. The Nash Sutcliffe model efficiency obtained was 0.788 indicating a high ability of the model to simulate streamflow. Furthermore the Relative Volume Error (RV_E) used for quantifying the volume errors was 10 % and suggests a reasonable performance. Table 5-1 shows the parameter values used in this simulation.

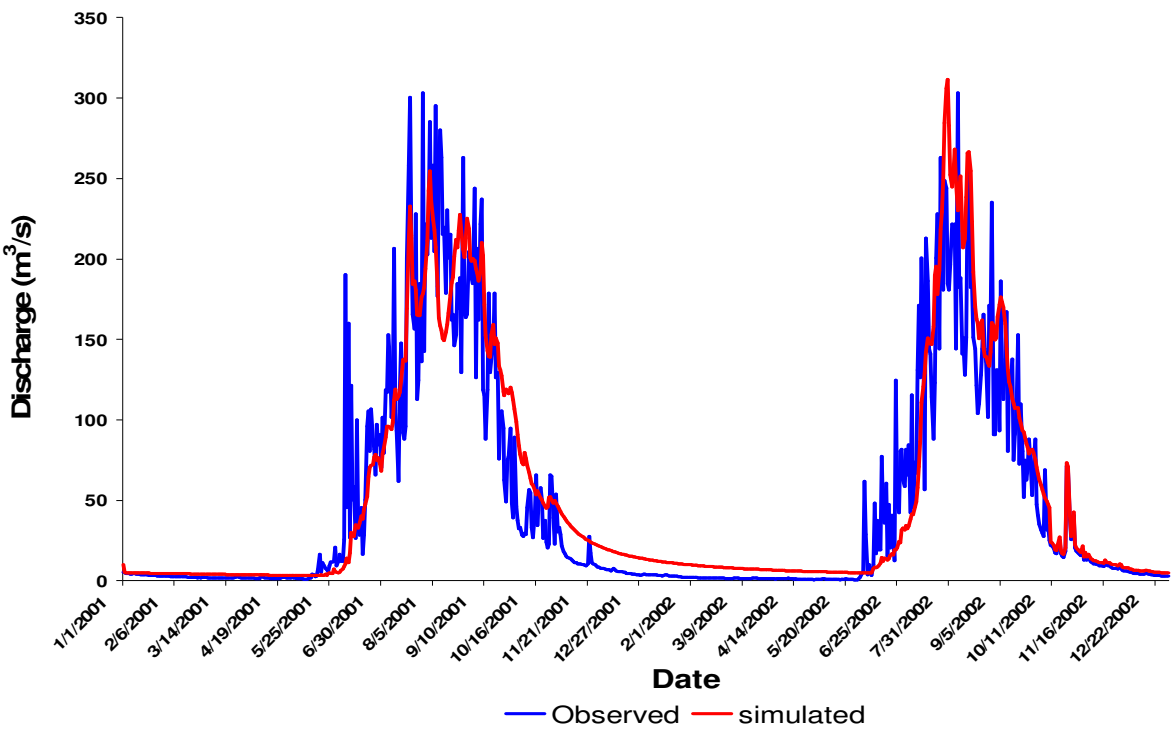

Figure 5-1: Simulation results for the Upper Gilgel Abay Basin..

Table 5-1: Parameter values used in the model.

Parameter	m [m]	T_o [m^2/h]	Td [h]	CHV [m/h]	RV [m/h]	SRMAX [m]	Q0 [m/timestep]	SR0 [m]	INFEX [-]	XKO [m/hr]	HF [m]	DTH [-]
value	0.05	5	22	3900	1900	0.05	0.000286	0.002	0	3	0.135	0.36

5.1.1. Sensitivity analysis: effects of the *m* parameter

Figure 5-2 shows the sensitivity of TOPMODEL to changes in the *m* parameter. As the *m* parameter was being varied, the other parameter values in table 5-1 were fixed at the values indicated. Both the shape of the hydrograph and the peak flow change quite dramatically when the *m* parameter is changed from 0.075 to 0.015. For lower values of *m* (i.e. 0.015 and 0.025 m), the peak flow is much larger than for higher values of *m* (i.e. 0.042 and 0.05). For example in July 2001, with *m* set at 0.015, the peak flow rises to approximately 600 m^3/s but for a higher value of *m* like 0.065 the peak flow becomes as low as near 230 m^3/s. This is the same case for the selected months of 2002 as shown in figure 5-2. For larger values of *m*, the proportion of rainfall that reaches the outlet via a surface route decreases. This is because large values of *m* like 0.05 and 0.075 indicate a deeper effective soil that allows for more rainfall to infiltrate and vice versa (Fedak, 1999). The subsurface portion of the runoff is also influenced significantly by the *m* parameter. For lower values of *m*, the amount of subsurface flow decreases and water travels quicker arriving at the outlet almost coincident with the surface flow (Fedak, 1999). This results in high peakflows and very little contribution to baseflow after the rainfall has ended. All this helps to explain the variation in the Nash Sutcliffe model efficiency (NS) values as *m* changes (table 5-2). The model efficiency tends to decrease as *m* decreases and vice versa. There is a dramatic decrease in the model efficiency to about 0.409 when the *m* parameter is set to 0.015. The RV_E also increases with smaller values of *m* and this suggests larger water balance errors.

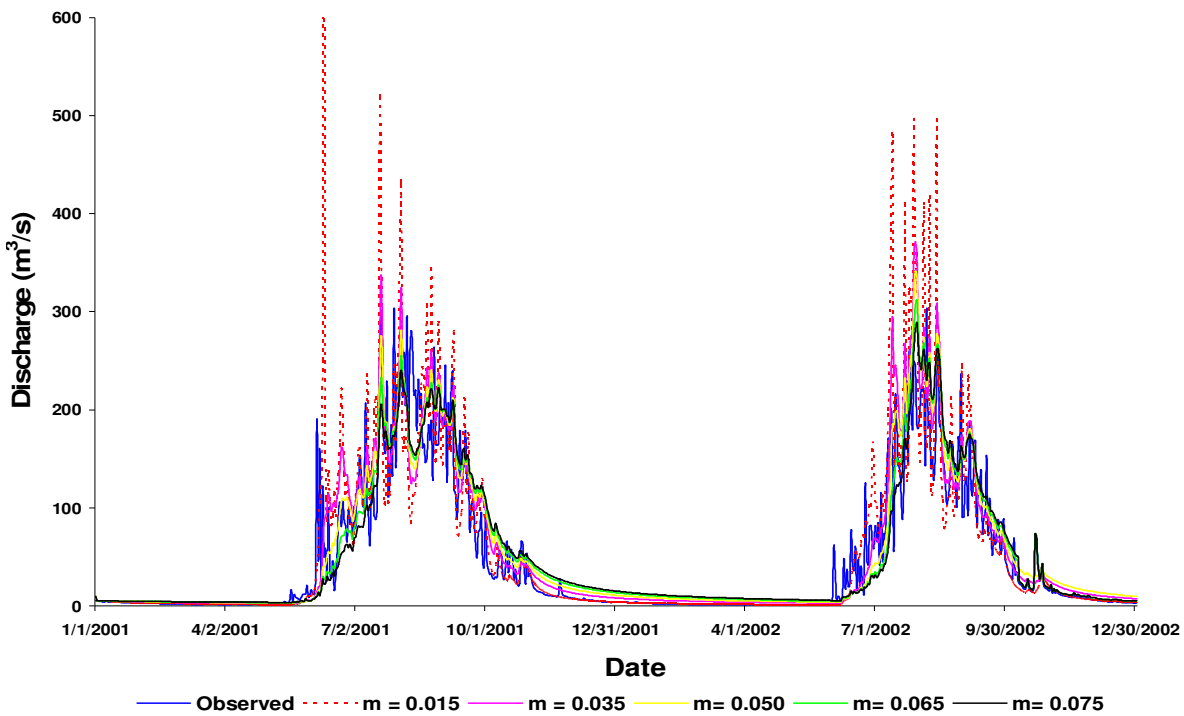

Figure 5-2: Sensitivity of the model to changes in *m*.

Table 5-2: Effects of the *m* parameter on model efficiency.

Run	*m* (m)	Nash Sutcliffe (NS)	Relative Volume Error (RV_E (%))
1	0.075	0.777	7.399
2	0.065	0.754	8.828
3	0.050	0.788	9.99
4	0.035	0.754	12.834
5	0.015	0.409	15.07

5.1.2. Sensitivity analysis: effects of the T_O parameter

All parameter values in table 5-1 were fixed as the T_O parameter values were changed from 1-35. Figures 5-3 shows that both the shape of the hydrograph and the peak flow slightly change with a change in the T_O parameter. The surface and subsurface components of a hydrograph have been examined to better understand the effect of the T_O parameter. The T_O parameter does not seem to significantly impact the recession tail of the hydrograph or baseflow which is dominated by subsurface flow. The simulated and observed recession tails almost overlay. The T_O parameter however does have a large impact on the surface portion of the runoff. The magnitude of the peak flow seems to have little impact on the recession tail of the hydrograph or the baseflow after the rainfall event and in some cases the simulated patterns fail to match the observed flow. This situation can be been observed in figure 5-3. Table 5-3 shows the change in NS efficiency values as T_O changes. The model efficiency becomes poor as T_O decreases. The NS is only ranging between 0.751-0.772 and as shown by the output in figure 5-3 the graphs of the variation of T_0 are almost identical. The RV_E is ranges from 12.9 % for lower values of T_0 to 10.5 % for higher values of T_O.

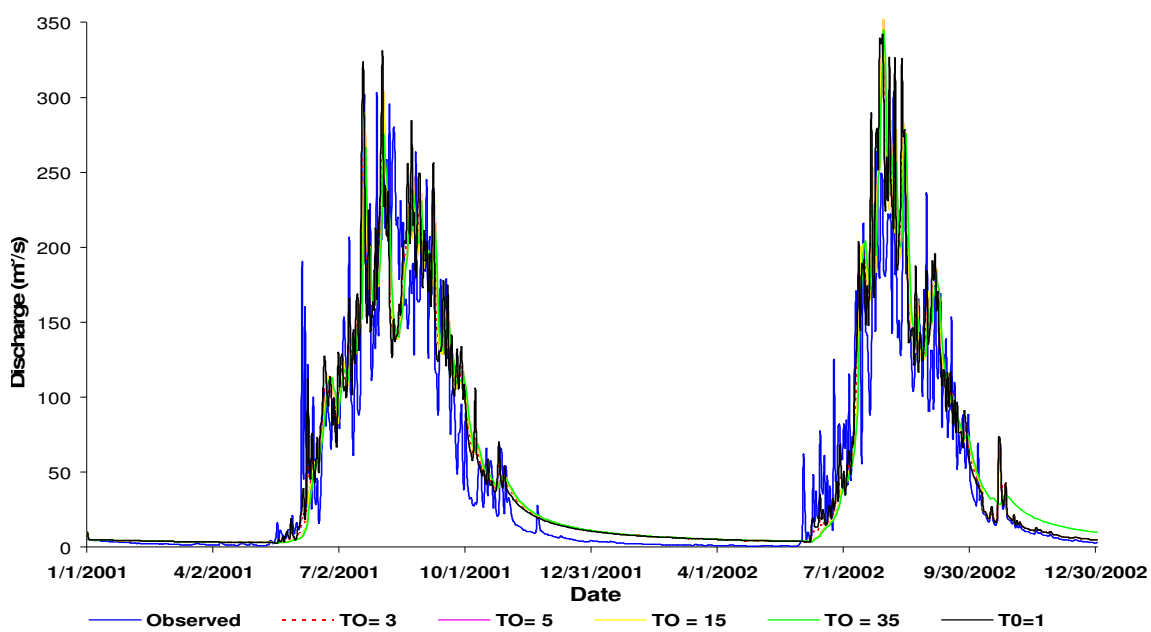

Figure 5-3: Sensitivity of model to changes in T_O

Table 5-3: Effects of the T_O parameter on model efficiency.

Run	T_O (m^2/s)	Nash Sutcliffe (NS)	Relative Volume Error RV_E (%)
1	1	0.751	12.862
2	3	0.789	11.436
3	5	0.788	9.99
4	15	0.776	10.616
5	35	0.772	10.546

5.1.3. Sensitivity analysis: effects of SR_{max} parameter

Figure 5-4 shows that the model has the capability of reproducing the overall pattern with the SR_{max} parameter set between 0.005-0.25. All the other parameter values given in table 5-1 were fixed as the SR_{max} parameter vales were changed. Smaller values of SR_{max} result in amplified simulated peak flows from May to July but the flows remain identical from August onwards. The model efficiency shows some small change from 0.788 when SR_{max} is set at 0.05 to only 0.783 when SR_{max} is 0.01 (table 5-4). Unlike the m parameter where NS has been changing drastically, the model is not very sensitive to the SR_{max} parameter. The SR_{max} parameter has much effect on the RV_E as it is changing from 17% for lower values of SR_{max} to a very good value of -0.67 for higher values of SR_{max} (table 5-4). According to Molicová (1997), the SR_{max} value is conceptualized in current TOPMODEL theories as a root zone reservoir and does not only respond to the evapotranspiration demand but also determines the rate of deep leakage loss from the soil. However increasing and decreasing SR_{max} during sensitivity analysis proved that it only affects the magnitude of the volume errors and not necessarily the simulated peaks.

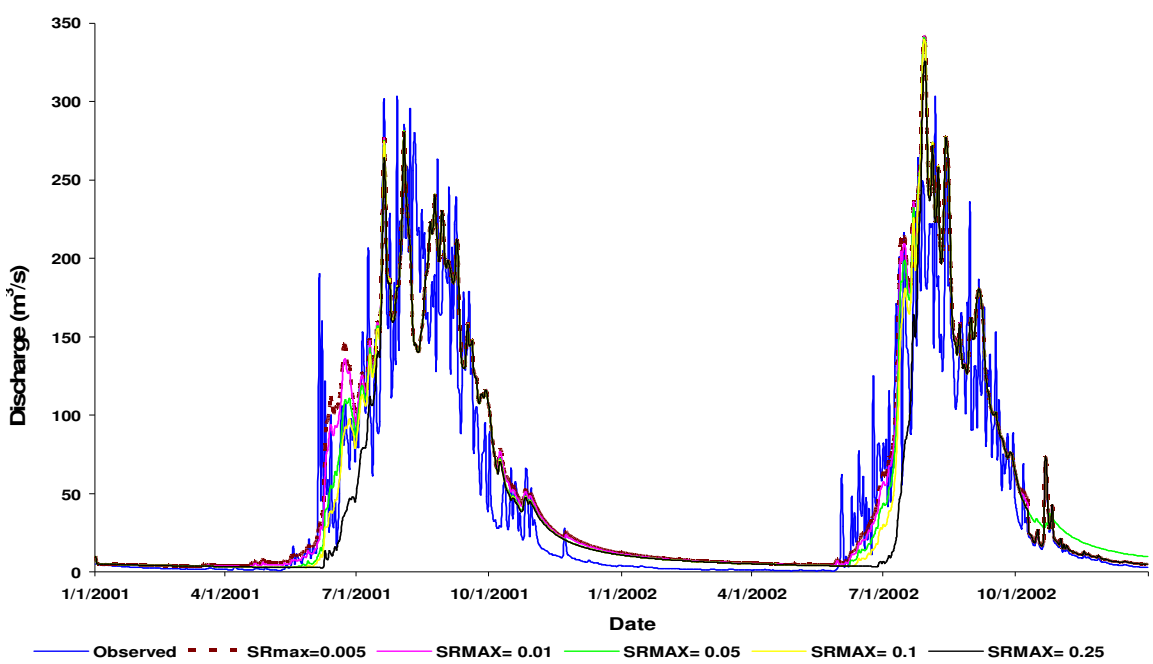

Figure 5-4: Sensitivity of model to changes in SR_{max}

Table 5-4: Effects of the SR_{max} parameter on model efficiency.

Run	SR_{max}[-]	Nash Sutcliffe (NS)	Relative Volume Error (RV_E (%))
1	0.005	0.779	17.701
2	0.01	0.783	15.308
3	0.05	0.788	9.99
4	0.10	0.784	8.095
5	0.25	0.744	-0.674

5.1.4. Calibration of the model.

Figure 5-5 shows the result of a trial and error calibration process. Table 5-5 lists the accepted best parameter values and the model performance. The parameter values that resulted in good performance using sensitivity analysis were the ones that were used for calibration. Calibrated parameter values are m=0.04, T_o=5 and SR_{max}=0.10 that yielded good overall fit of the model output to the measured hydrograph over the entire simulation period of 2001 and 2002 (Figure 5-5). As compared to the first simulation in figure 5-1, the simulated baseflow is more or less identical to observed counterparts. The peak flow pattern and the seasonal recession part of the hydrograph also improved as evidenced by an improved Nash Sutcliffe and RV_E as indicated in table 5-5. However the model does not perform satisfactorily in the timing of the rising limbs of both years.

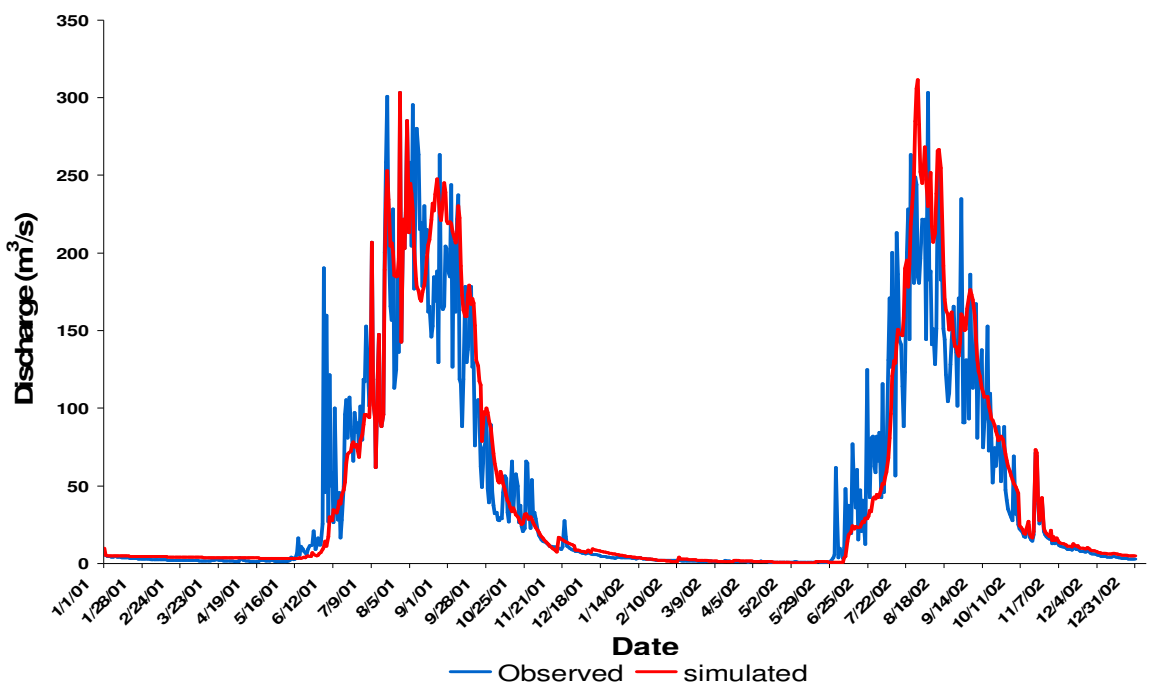

Figure 5-5: Calibration results for the Upper Gilgel Abay basin

Table 5-5: The accepted best parameter values and model efficiency after calibration.

m [m]	T_O [m^2/s]	SR_{max}[-]	Nash Sutcliffe (NS)	Relative Volume Error (RV_E (%))
0.04	5	0.10	0.805	6.1

5.1.5. Validation of the model.

The optimized parameter set used to calibrate the low flows and peak flows was applied to a different hydrometeorological data set (2003) to validate the model. Figure 5-6 shows results of the validation process. From January until May 2003, the simulated hydrograph matches well with the observed hydrograph but from June when the rainy season begins, the simulated hydrograph rises sharply and somewhat earlier than the observed discharge. The recession limb of the simulated hydrograph falls faster than the observed discharge. The under- and overestimation of the peaks and rising limbs are not entirely due to the modelling errors but also subject to data errors and the spatial distribution of rainfall. This is because 4 of the 6 stations used in the Thiessen polygon rainfall estimation method were outside the study area thus having an impact in the simulated discharge. However even though the Nash Sutcliffe model efficiency of 0.75 is lower compared to the 0.805 obtained during calibration, it still shows satisfactory performance of the model. This is also supported by a good RV_E of -4.0 %.

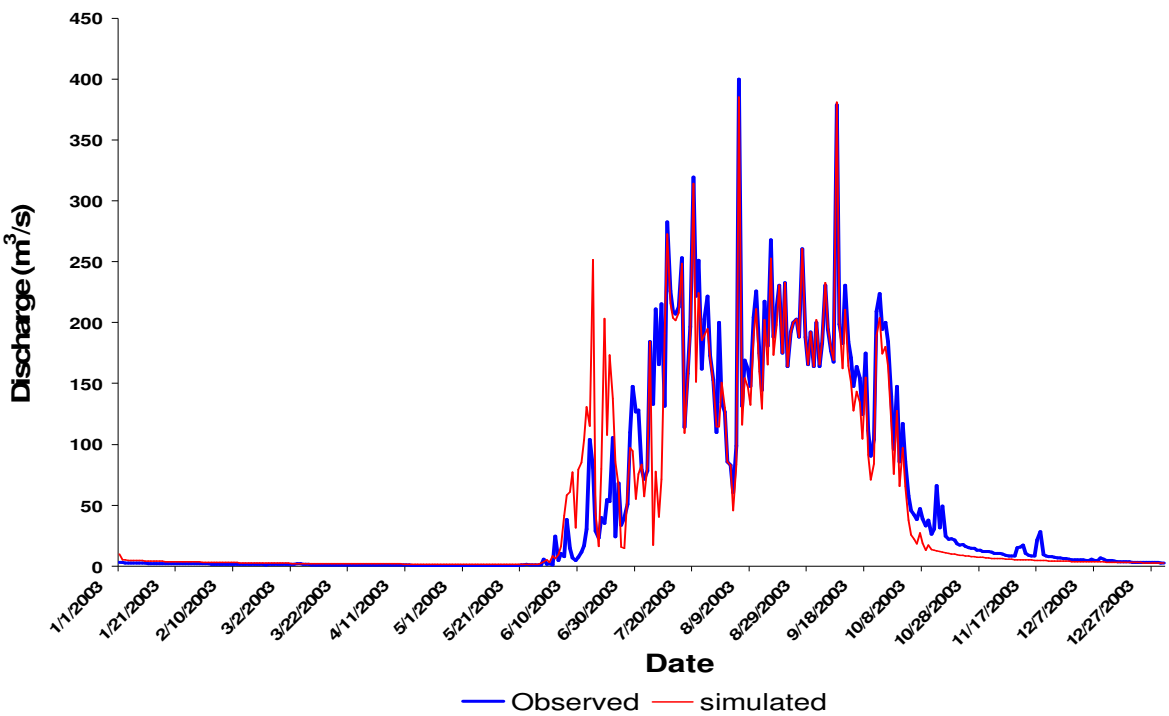

Figure 5-6: Validation results for the Upper Gilgel Abay basin in 2003.

5.2. Hydrologic impacts of Landuse changes

This subsection discusses results from different landuse class simulations of 2001, 1986 and 1973. The most important parameters influencing landuse simulations using TOPMODEL were determined by calibration and they are shown in table 5-6. The main focus during calibration was on the 3 parameters: i.e. m, SR_{max} and K_s. For comparison of streamflow for the years 1973, 1986 and 2001 these parameters were not varied but their different values were only used for the different landuse types.

Table 5-6: Parameter values obtained through calibration.

Parameter	Unit	Agriculture	Forest & shrub	Grassland	Water & marshy
m	m	0.035	0.05	0.015	0.01
T_o	m^2/h	3	5	1	10
t_d	h	22	22	22	22
CHV	m/h	1900	1900	1900	1900
RV	m/h	900	900	900	900
SR_{max}	m	0.07	0.1	0.05	0.23
Q_o	m/h	0.000285618	0.00028562	0.000285618	0.000285618
$SR0$	m	0.002	0.002	0.002	0.002
$INFEX$	-	1	1	1	0
K_s	m/hr	3	2.5	1	0.5
Ψ_f	m	0.13	0.14	0.159	0.160
Θ	-	0.355	0.360	0.365	0.365

5.2.1. Simulation results for 1973 landuse classes

Figure 5-7 shows the stream flow contributions from different landuse classes simulated for the year 1973. From the beginning of 1973 up to mid May (dry season), all 3 hydrograph simulations show a similar pattern. However from the onset of the rainy season in June, the streamflow from agriculture peaks faster than the streamflow from grassland and forest and shrubland. The reason why grassland contributes far less streamflow outflow than any of the other landuse is mainly because grassland contributes only 5% of the total catchment area compared to agriculture (30%) and forest and shrubland (65%). Therefore in this case, each particular catchment area becomes a scaling factor in determining the total runoff from each landuse type. At the end of the rain season in October, the streamflow becomes almost identical again in pattern and this time it is mainly the contribution of baseflow from each landuse type. As observed in figure 5-7, there is higher baseflow contribution from forest and shrubland, followed by agriculture and lastly grassland. This is because forests allow higher infiltration of water down into the soil because of higher porosity. This water is released slowly to the stream and results in higher baseflow. The baseflow from forest and shrubs is approximately 11m^3/s, 4 m^3/s from agriculture and 0.4 m^3/s from grasslands.

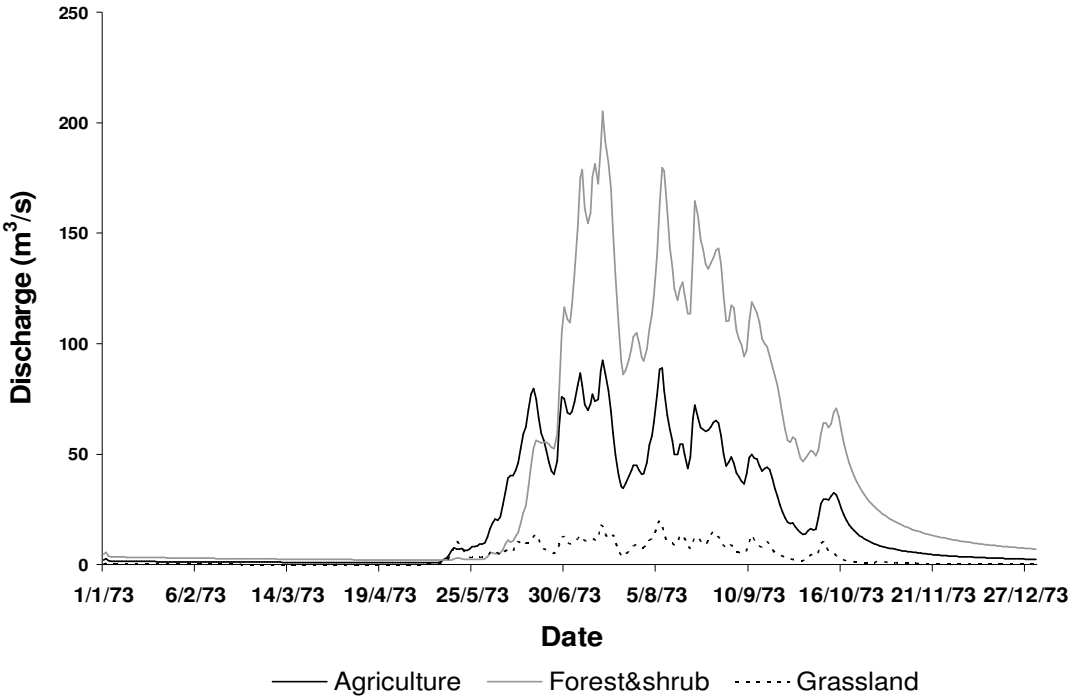

Figure 5-7: Simulation results for different landuse classes: 1973

Figure 5-8 shows cumulative infiltration in 1973 for the different landuse classes. The cumulative infiltration curves are almost identical in the dry season (January-mid May) but at the onset of the rainy season cumulative infiltration from agriculture rises slightly above all the other landuse types. At the end of the rainy season in October all the plots for the landuse levels off at 150m. The cumulative infiltration and the effect on streamflow is attributed to how different landcover and landuse classes affect the parameters of the Green and Ampt infiltration excess model whereby K_s decrease as an exponential function. For example due to deep root system of forests, dead and decaying root systems (at depth greater than 2m) can create important fissures or channels for free water conduction, mainly in vertical direction (Champerlin, 1972). As for agricultural land there can be subsurface storm flow resulting from 'plough-pans' created by repeated ploughing compaction (Minshall and Jamison, 1965). However the crop residue below depth of mechanical disturbance (roots and incorporated plant materials) improves soil structure and macro-porosity that increases inherent permeability. Overally, due to the root system and tillage, there is high infiltration capacity and increase in hydraulic conductivity. In undisturbed soils, dead and decaying grass root material contributes to the development of macro-porosity in the depths at which root penetration occurs. However in the Gilgel Abay basin, most of the grasslands have been turned into grazing lands (SMEC, 2007). Due to overgrazing on these grasslands this has resulted in some crusting of the soil and resulted in reduced infiltration capacity and lower hydraulic conductivity.

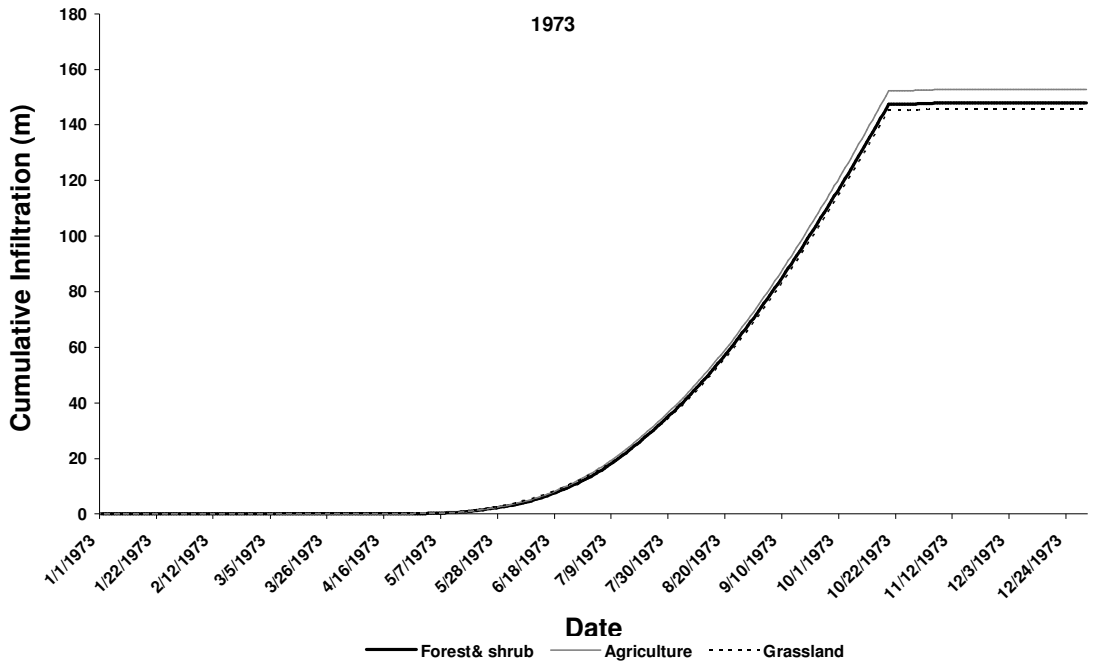

Figure 5-8: Simulated cumulative infiltration for 1973.

Figure 5-9 shows the simulated discharge of the different landuse classes in 2001 obtained by summing up the simulated discharge from the grassland, forest and shrubland and agriculture. This is plotted with the observed discharge for the Upper Gilgel Abay catchment in 1973. The simulated discharge is almost identical to the observed discharge throughout the year except in some parts if the rain season. In general the baseflow is captured reasonably well by the model over the entire simulation period. The NS is 0.805 and RV_E is 5.82 % which suggests that the model performs well. This demonstrates that the TOPMODEL approach is a satisfactory method of quantifying streamflow from the different landuse types in 1973 by producing a pattern that is almost identical to the observed hydrograph. The peak discharges are systematically overestimated. This could be a result of so many factors amongst them the fact that the computation of crop canopy interception was only considered to be controlled by the canopy density (LAI) only. However there are other factors that were not taken in to consideration such as and rainfall intensity and duration (Kozak *et al.*, 2007).

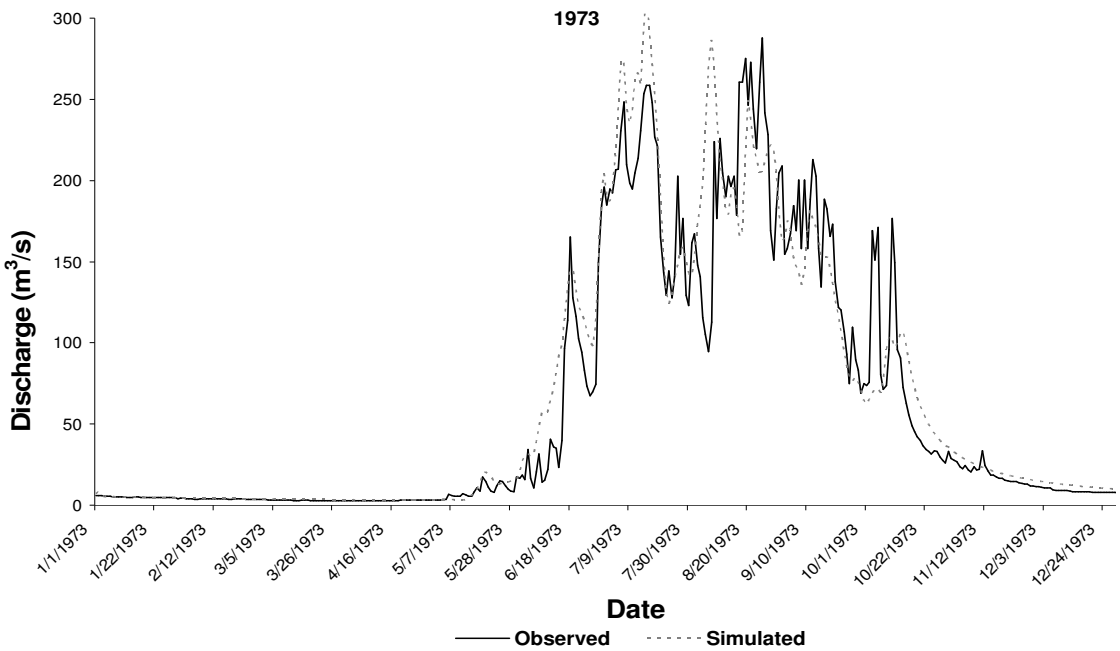

Figure 5-9: Comparison of observed and total simulated discharge.

5.2.2. Simulation results for 1986 landuse classes

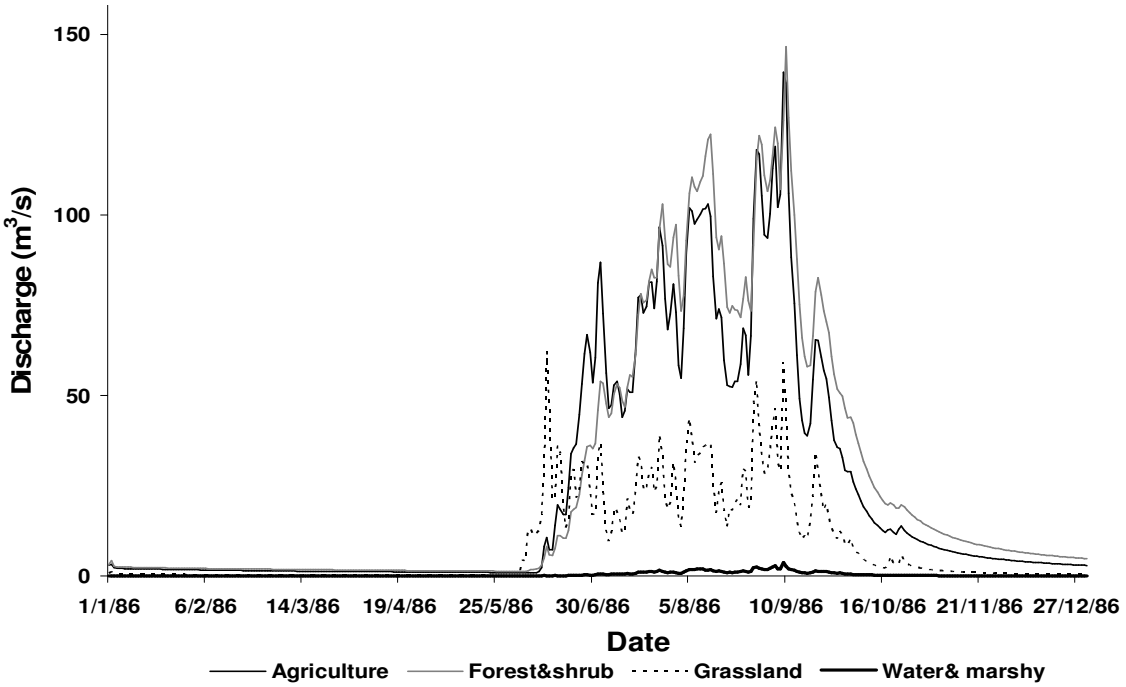

Figure 5-10: Simulation results for different landuse classes: 1986.

The simulations in 1986 also consists of water and marshy area which have been observed in the landcover classification results. As shown on figure 5-10, from the onset of the rainy season in June, the streamflow from grassland peaks faster than the streamflow from agriculture and forest and shrubland.

This is because in most grassland areas, there is less infiltration due to increased compaction caused by overgrazing. However it is agriculture and forest land that has higher peak flows (nearly 150 m^3/s). Very low streamflow (nearly 3.9 m^3/s) has been simulated from water and marshy areas. Therefore the area occupied by each landuse type act as scaling factor in influencing the peak flow and total streamflow from the respective landuse types. An example is that water and marshy areas occupy about 0.3% of the total catchment area and as a result there is relatively less runoff that will be simulated from this landuse type. As also observed in 1973, forest and shrubland have higher baseflow due to higher porosity and the slower release of water to the catchment outlet.

In 1986 the Nash Sutcliffe model efficiency is 0.716 and RV_E is 29.72 %. This shows a satisfactory ability of TOPMODEL to simulate stream flow in this catchment from the different landuse types in this year. However there were still some systematic overestimations of the peakflow throughout the simulation period by the model.

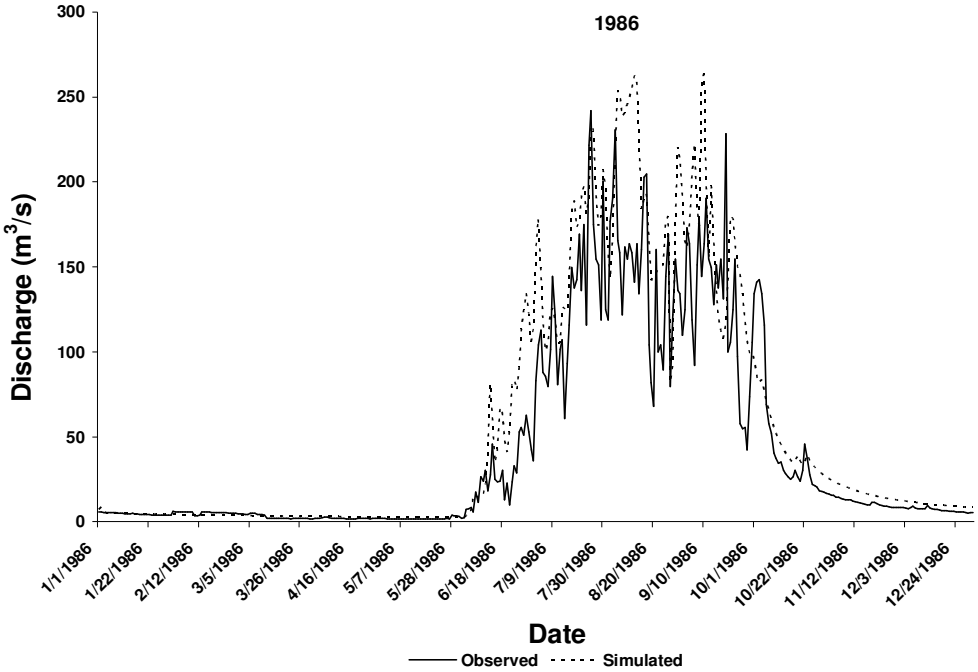

Figure 5-11: Comparison of observed and total simulated discharge.

5.2.3. Simulation results for 2001 landuse classes

For the 2001 simulations, figure 5-12 shows that there is higher maximum peakflow from agriculture than any other landuse and these differences are observed in the rainy season (June to October). In 2001 there has been an increase in agricultural land to occupy 62 % of the total catchment area. Water and marshy area occupy about 0.4 % of the total catchment area and in this case there is very low streamflow and a peakflow of only 2 m^3/s. Unlike in 1973 and 1986, agricultural land cause higher base

flow than forest land and other landuse types. This is because agricultural activities cause increased infiltration due to loosening of the soil. This infiltrated water is later released to the outlet slowly thus causing a higher baseflow. The Nash Sutcliffe Model Efficiency obtained in 2001 is 0.733 and the RV_E is 18.5 %. This shows that TOPMODEL has satisfactory ability to simulate the streamflow from the different landuses.

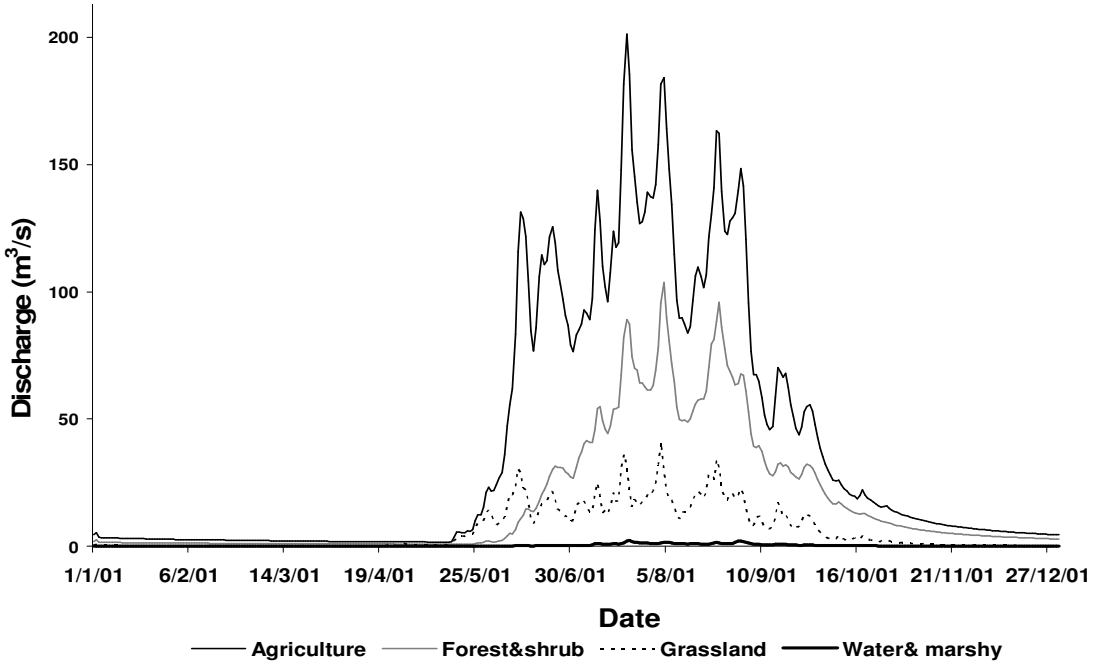

Figure 5-12: Streamflow contributions from all landuse in 2001.

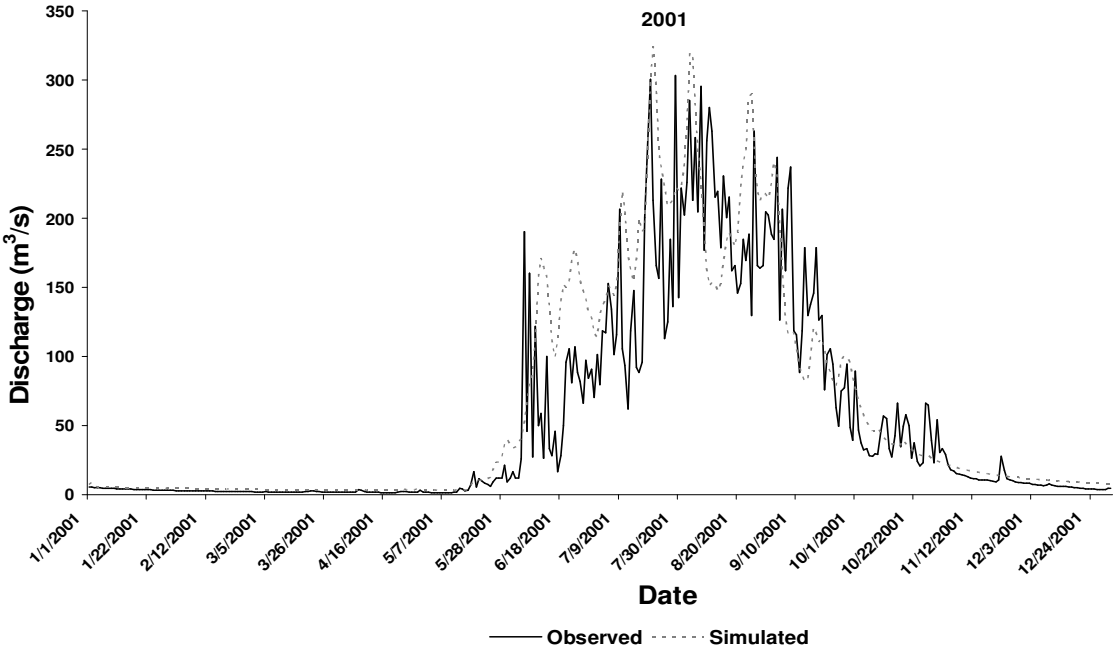

Figure 5-13: Comparison of observed and total simulated discharge.

5.2.4. A comparison of total streamflow from landuse classes

Table 5-7: A comparison of peak flow discharges and annual runoff volumes for different landuse.

Landuse	Year	Maximum peakflow (m^3/s)	Annual Runoff volume (Mm^3/yr)	% change in peakflow	% change in Annual Runoff volume
Agriculture	1973	92.5	649.2		
	1986	139.4	725.7	51	12
	2001	201.2	1209.3	44	67
Forest & shrub	1973	205.1	1286.6		
	1986	146.5	828.5	-29	-36
	2001	103.5	549.7	-29	-34
Grassland	1973	19.9	117.6		
	1986	62.1	277.6	212	136
	2001	40.9	204.4	-34	-26
Water & marshy	1973				
	1986	3.8	12.4		
	2001	2.4	10.4	-38	-16

Table 5-7 shows a summary of the total stream flow contributions from different landuse. Figure 5-14 shows the hydrographs for the different landuses. The results show that agricultural land causes an increased peakflow by 51% between 1973 and 1986 and 44% between 2001 and 1986. Annual runoff volume increased by 12% between 1986 and 2001. This increase also matches with increases in agricultural land area coverage between the years 1973, 1986 and 2001 (area coverage of 30.5%, 40.2 % and 62.8% respectively). Between 1973 and 1986 and between 1986 and 2001 there were decreases in maximum peakflow, all by 29%. The annual runoff volume also decreased by 36% between 1973 and 1986 and by 34% between 1986 and 2001. These changes could be attributed to decreases in forest and shrubland area coverage that have occurred in the Upper Gilgel Abay basin between the years 1973, 1986 and 2001 (area coverage of 64%, 46.8% and 28.4% respectively). Clearing of forest means that there is less infiltration because of decrease in porosity and less interception of water. For grassland there is a large increase in maximum peakflow by 212% between 1973 and 1986 but followed by a decrease of 34 % between 1986 and 2001. Annual runoff volume increased by 136 % between 1973 and 1986 but decreased by 26% between 1986 and 2001. This could also be a result of an increase in grassland from 5% of the total catchment area in 1973 to 13% of the total catchment area in 1986 and to a decrease of 9% in 2001. Thus this increase of grassland allows less infiltration of water due to crusting of the soil which causes both higher peak flows (figure 5-14) and an increase in total values of discharge in a year. Besides, rainfall patterns are different and this may affect water storages and runoff processes. The water and marshy area stream flow contribution in 1986 is higher than in 2001 even though there has been a slight increase in area occupied by water and marshy from 1986 to 2001 according to a landcover classification done by Kebede (2009). Figure 5-15 shows a histogram with peakflow and runoff volumes for the different landuse.

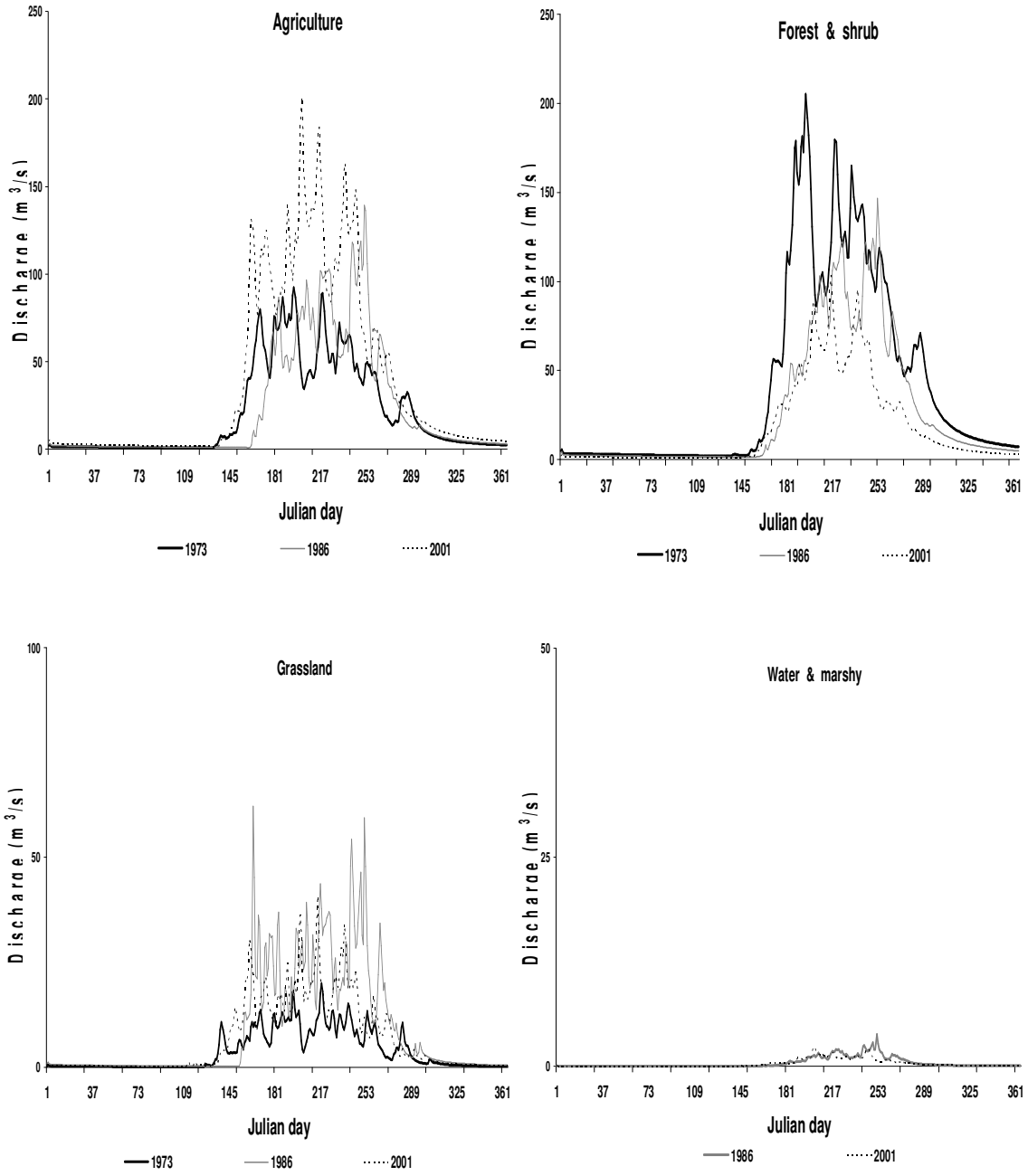

Figure 5-14: Discharge from different landuse types.

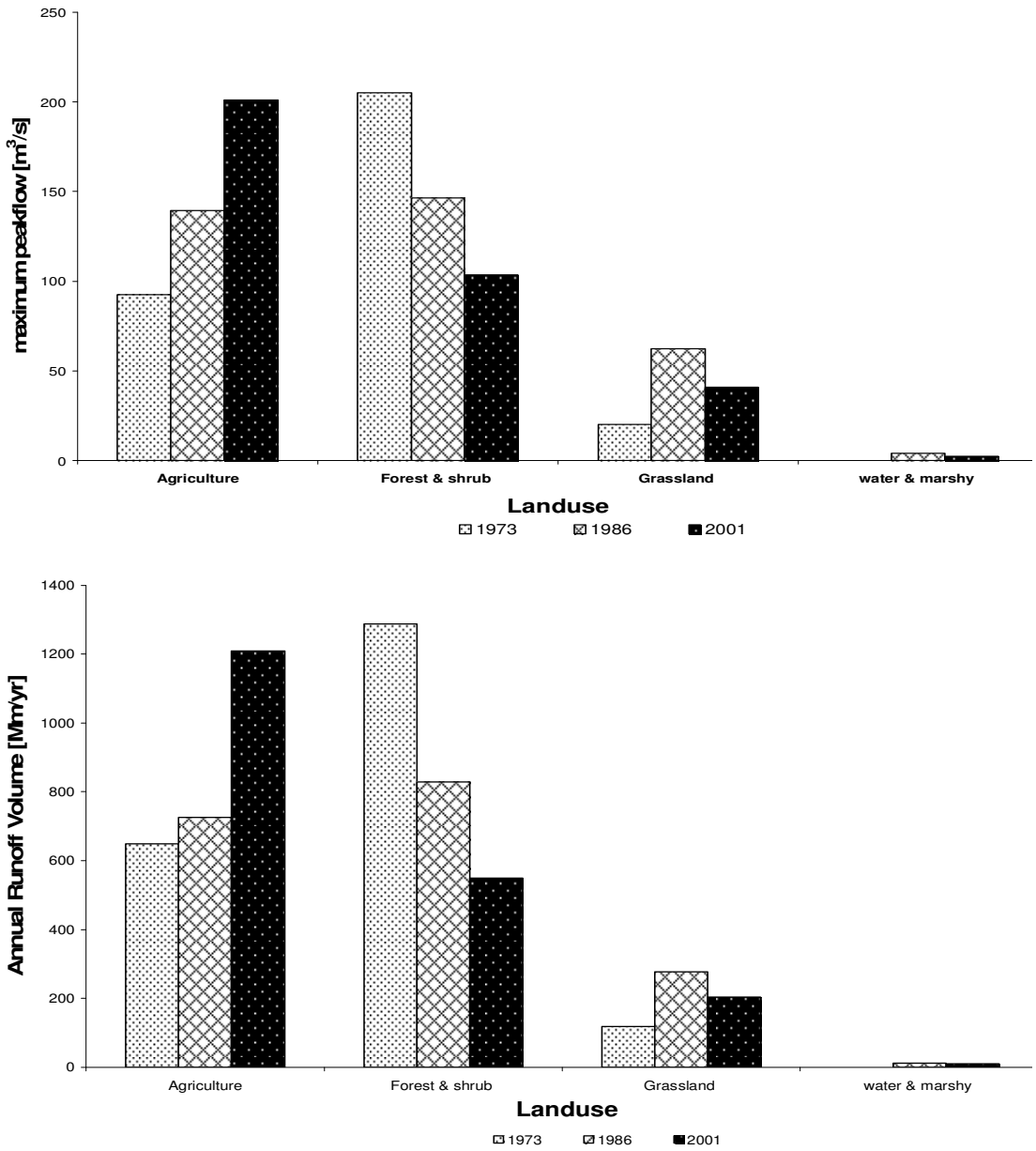

Figure 5-15: Maximum peakflow and annual runoff volume from different landuse types.

Even though the area coverage of each landuse type acts as a scaling factor in the runoff contributions, there could be other factors contributing to the above described patterns. Examples of other factors are the values of the LAI computed from remote sensing imagery that have an impact on the amount of intercepted water and the potential evapotranspiration calculations (specific for each landcover type). Of importance also is the topographic index value for each landuse type that quantifies the runoff from each landuse type. The configuration of rain gauges that were used to estimate the rainfall for each landuse by the Thiessen Polygon method also differed for 1973, 1986 and 2001 by availability of the rainfall data.

5.2.5. Sensitivity analysis on landuse simulations

Figure 5-16 shows results from sensitivity analysis that was carried out to evaluate and quantify the effect of the parameter of the exponential transmissivity function (*m*), the root zone available water capacity (SR_{max}) and saturated hydraulic conductivity (K_s) on model output. In this case agricultural land was selected for the sensitivity analysis for 1973, 1986 and 2001. Table 5-8 shows the parameter values used. The sensitivity analysis was carried out separately on each individual landuse and for each year the results are shown in figure 5-16. An increase in the value of *m* implies more infiltration of water into the soil that consequently results in lower peak flow. At the same time higher values of SR_{max} implies lower peak flow. Thus a combination of higher *m,* higher *SRmax* with higher K_s results in increased infiltration and less water released to the outlet as shown in figure 5-16.

Table 5-8: Parameter values used for sensitivity analysis on agricultural land

Run	*m* (m)	SR_{max} (m)	K_s (m/h)
1	0.015	0.025	1
2	0.035	0.07	3
3	0.05	0.1	5

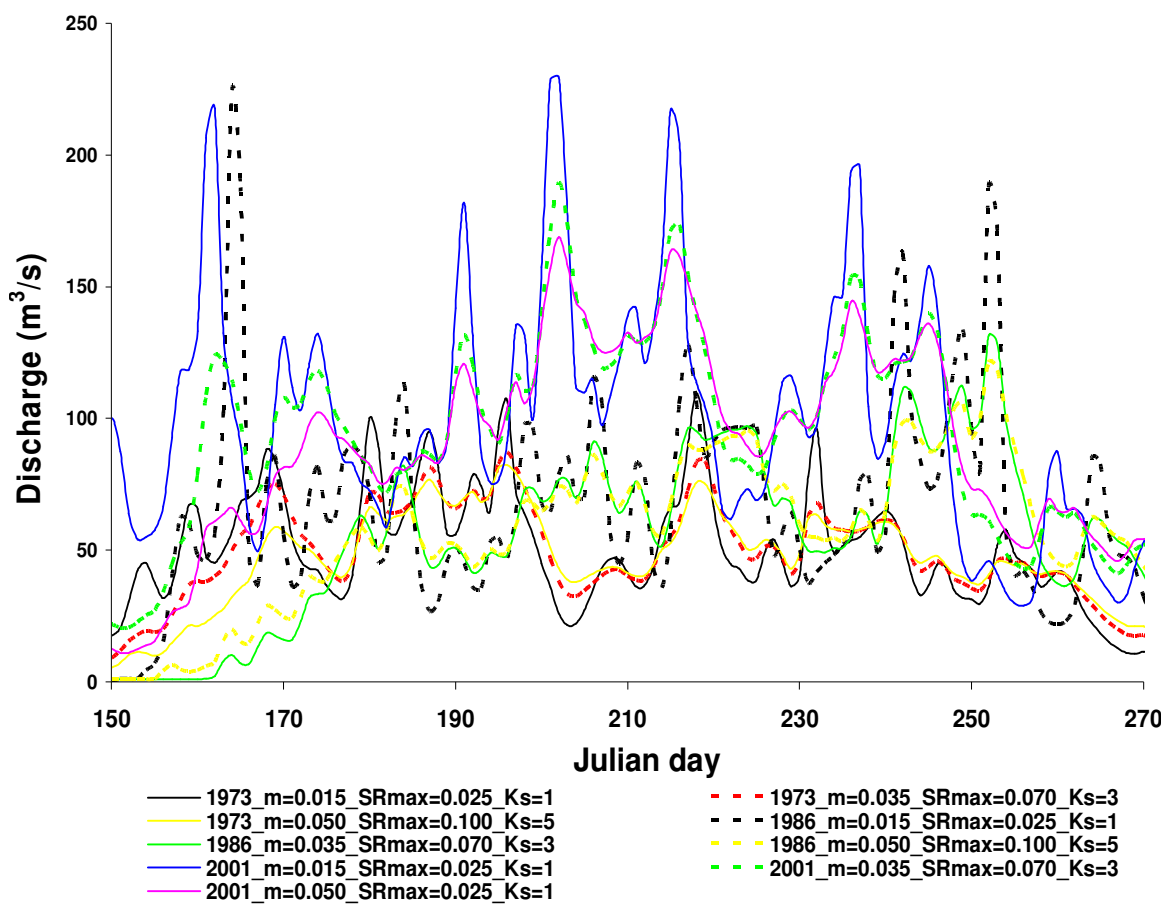

Figure 5-16: Sensitivity analysis on agricultural land.

6. CONCLUSIONS AND RECOMMENDATIONS

6.1. Conclusions

- TOPMODEL was applied to simulate streamflow for the Upper Gilgel Abay River basin with satisfactory results. This study demonstrated that the rainfall-runoff model can be extended beyond its original design of using the topographic index for predicting local variations in water table (Kirkby, 1975) to simulate impacts of land use change in a catchment with chosen important parameters for any time period.

- The first research question was to assess whether land surface parameterization of TOPMODEL can be achieved by the use of remote sensing. Land surface parameterization was done in two parts, i.e. topographic indices and vegetation indices. In relation to topographic indices, this study showed that it is important to integrate the various quantification abilities of remote sensing together with the spatial data handling capabilities of GIS to process data for hydrological modelling. Remote sensing was used for acquiring a fine resolution DEM which is critical for the prediction of hillslope flow paths for distributed hydrological modeling. Therefore in this study an ASTER 30m DEM was used for proper specification of flow pathways that are important for computation of the topographic index > The results show that the topographic index plays a dominant role in simulating streamflow in the Gilgel Abay River basin. The second research question was on how well TOPMODEL can simulate streamflow in the catchment. Results of calibration process showed a good Nash-Sutcliffe model efficiency (NS) of 0.805 and a Relative Volume Error (RV_E) of 6.1%. This suggests that TOPMODEL simulates streamflow with good performance. The model was validated using a 2003 dataset and a satisfactory model performance of NS=0.75, RV_E= -4.0 % was also obtained.

- Landuse change is a major factor that alters the hydrological processes over a range of temporal and spatial scales. Land surface parameterization was again successfully achieved through derivation of vegetation parameters from remote sensing. Spectral vegetation indices such as the Soil-Adjusted Vegetation Index (SAVI) and Leaf Area Index (LAI) were determined from remote sensing imagery. Interception of precipitation from different landcover types was calculated as a function of LAI. The rainfall runoff model has been further enhanced by the aggregation of evapotranspiration according to specific vegetation cover using the crop

coefficient approach. Furthermore there was an addition of infiltration excess flow module of the Green and Ampt model.

- The above helped to answer the research question on how the TOPMODEL structure could be modified so that it can account for hydrologic impacts of landuse change. The most approximate way of implementation of land-use in TOPMODEL was done by treatment of each vegetation/landuse type as a 'subcatchment' through a GIS overlay of landuse types thus creating a topographic index distribution for each landuse type. These were run separately with specific landuse parameters. The areally weighted results were summed to get a total output imitating having multiple subcatchments with different topographic index distributions.

- TOPMODEL was then applied to analyse streamflow contributions from different landuse types, *viz* agriculture, grassland and forest and shrubs and water and marshy areas in the Upper Gilgel Abay basin. Furthermore the model was used to assess how landuse change affects the peakflow, baseflow and volume of runoff in the basin. Results have shown that there are significant increases in maximum peakflow and annual runoff volume from agricultural land over the period 1973-1986 and 1986-2001 which corresponds to increases in agricultural land between the years 1973, 1986 and 2001 shown in figure 4-10. Over the same period of time, forest and shrubland decreased in maximum peakflow and annual runoff volume which could also be attributed to decreases in forest and shrubland land in the same period of time. For grassland, increases in grassland resulted in significant increases in peakflow and volume runoff between 1973 and 1986 but decreases in grassland resulted in decrease in maximum peakflow and volume of runoff between 1986 and 2001. Annual runoff volume also increased by 136 % between 1973 and 1986 but decreased by 26% between 1986 and 2001. The water and marshy area stream flow contribution in 1986 has been found to be higher than in 2001 even though there has been a slight increase in area occupied by water and marshy from between this period of time. This demonstrated the significant local effects of landuse change on the hydrology of a catchment. Furthermore this study has demonstrated that different landuse classes contribute to significantly different streamflow. This confirmed the work by Chan *et al*. (2009) who also observed that each land use type affect the runoff generation and concentration by altering hydrological factors such as interception, infiltration and evaporation.

- It was however difficult to assess whether the streamflow contributions from each landuse are accurate because the model is run separately for each landuse. Furthermore, on the actual ground, a landuse class is not a hydrological subcatchment. The most approximate way was

through summing the simulated streamflow from the different land uses and by comparing with the observed outflow for the whole catchment. This answer the research question on how the combined discharge from different landuse classes compare to the observed discharge. The following satisfactory model efficiencies were obtained on the comparison between the sum of all landuse simulated discharge and the observed discharge at the outlet: 1973 (NS=0.81, RV_E=5.82); 1986 (NS=0.72, RV_E=29.72) and 2001 (NS=0.73, RV_E= 18.50). This demonstrated that TOPMODEL performs with varying degrees of success in terms of matching the observed surface runoff, peakflow and time to peak for all landuse classes.

6.2. Recommendations

- In order to improve the prediction of the spatial and temporal patterns of hydrological response units in the Upper Gilgel Abay basin, more advanced coupling of TOPMODEL with remote sensing data can further be done. In this study parameterization of TOPMODEL through remote sensing has only been done for the land surface parameters. For further research, complete parameterization of this rainfall runoff model can be achieved through remote sensing to allow TOPMODEL to be applied in a fully distributed fashion. Thus satellite rainfall blending techniques could provide effective means for calculating areal rainfall estimates. Furthermore satellite based actual evapotranspiration estimation techniques could as well provide effective means of estimating spatial and hyper-temporal evapotranspiration as inputs to TOPMODEL.

- Manual calibration of the parameters in this study has been found to be both time consuming and often erroneous. Automatic calibration using GLUE (Generalized Likelihood Uncertainty Estimation) could improve simulation (Fisher J and Beven K.J, 1996). In GLUE, the parameter sets are sampled randomly from physically reasonable ranges, often using uniform sampling where there is no strong information about prior expectations of parameter values (Blazkova and Beven, 2009). This can be a better approach for obtaining the values of parameters that have been identified for sensitivity analysis in this study: m, T_o and SR_{max}. When applied to landuse simulation this can be done also on additional parameters such as K_s.

- Another way of analysing the impacts of landuse change could be by creating land use scenarios. Three hypothetical scenario targets can be prepared, namely agriculture, deforestation and afforestation. Different scenarios can then be established by giving different percentages of landcover and TOPMODEL run to simulate the impact responses.

- Future fieldwork campaigns also should measure hydraulic properties of soils since they play an important role in movement of soil moisture from the land surface to the water table through the unsaturated zone and, hence, affect the runoff and groundwater recharge processes. In this regard, data generated through these field work investigations are expected to be useful for modelling of unsaturated flow and to develop catchment based rainfall runoff relationships for similar type of catchments.

- To allow for landuse change impact assessments using TOPMODEL, a number of additional parameter values have been used to simulate infiltration by the Green and Ampt model. These parameters are fixed at each run (*a priori*). However, the challenge that can be tackled in future studies is that the effective root zone storage from tree types can change dramatically depending on soil depths. This is the case mainly in forests and shrub land and future studies could focus on how this could be implemented.

REFERENCES

Allen, R.G., Pereira, L.S., Raes, D. and Smith, M., 1998. Crop evapotranspiration- Guidelines for computing crop water requirements, FAO Irrigation and Drainage Paper 56, FAO, ISBN 92-5-104219-5. , Rome, Italy.

Ambroise, B., Beven, K. and Freer, J., 1996. Toward a generalization of the TOPMODEL concepts: Topographic indices of hydrological similarity. Water Resources Research, 32(7): 2135-2145.

Ashenafi, S., 2007. Catchment modelling an preliminary application of isotopes for model validation in Upper Blue Nile basin, Lake Tana, Ethiopia, MSc Thesis, UNESCO-IHE, Delft, The Netherlands.

Band, L.E. et al., 1991. Forest ecosystem processes at the watershed scale: basis for distributed simulation. Ecol. Modelling, 56: 171-196.

BCEOM, 1998. Abbay River Basin Integrated Development Master Plan Project, Environment, Part-3 Limnology Addis Ababa, Ethiopia.

Beven, K., 1984. Infiltration into a class of vertically non-uniform soils. Hydrol. Sci, 29(4): 425-434.

Beven, K., 1991. Spatially Distributed Modelling: Conceptual Approach to Runoff Prediction. In: D.S. Bowles and P.E. O'Connell, Editors, Recent Advances in the Modelling of Hydrologic Systems, Kluwer, Dordrecht (1991), pp. 373–387.

Beven, K., 1997a. "TOPMODEL: A CRITIQUE". Hydrological Processes, 11: 1069-1085.

Beven, K. and Freer, J., 2000. A dynamic TOPMODEL. Hydrological Processes, 15(10): 1993-2011.

Beven, K., Lamb, R., Quinn, P., Romanowicz, R. and Freer, J., 1995. TOPMODEL. In: Sing VP (Ed), Computer Models of Watershed Hydrology. Water Resources Publications: 627-668, Colorado, USA.

Beven, K.J., 1997b. Distributed hydrological modelling: Applications of the TOPMODEL concept. . John Wiley and Sons Ltd, Chichester, U.K

Beven, K.J., 2001. Rainfall-Runoff Modelling The Primer. John Wiley & Sons, Lancaster.

Beven, K.J. and Kirkby, M.J., 1979. A physically based, variable contributing area model of basin hydrology. Hydrological Sciences-Bulletin-des Sciences Hydrologiques, 24(1): 43-69.

Beven, K.J. and Wood, E.F., 1983. Catchment geomorphology and the dynamics of runoff contributing areas. J. Hydrol., 65: 139±158.

Blazkova, S. and Beven, K.J., 2009. Uncertainty in flood estimation. Structure and Infrastructure Engineering Maintenance, Management, Life-Cycle Design and Performance, 5 (4). pp. 325-332.

Braden, H., 1985. Ein Energiehaushalts- uind verdunstungsmodell fur wasser- und Stoffhaushaltsuntersuchungen landwirttschaftlich geutzter Einzugsgebiete. Mitteilungen Deutsche Bodenkundliche Gesellschaft, 22: 294-299.

Champerlin, T.W., 1972. Interflow in the mountaneous forest soils of coastal British Columbia. In: D. Slaymaker and H.J. McPherson (Editors), Mountain Geomorphology. Tantalus Research, Vancouver, pp. 121-127.

Chen, Y., Xu, Y. and Yin, Y., 2009. Impacts of land use change scenarios on storm-runoff generation in Xitiaoxi basin, China. Quaternary International, 208(1-2): 121-128.

Childs, E.C. and Bybordi, M., 1969. The vertical movement of water in. IUGG 282. stratified porous material Water Resources Research.

Choudhury, B.J., Ahmed, N.U., Idso, S.B., Reginato, R.J. and Daughtry, C.S.T., 1994. Relations between evaporation coefficients and vegetation indices studied by model simulations. Remote Sensing of Environment, 50: 1-17.

Chrysoulakis, N., Abrams, M., Feidas, H. and Velianitis. D, 2004. Analysis of ASTER multispectral stereo imagery to produce DEM and land cover databases for Greek Islands: the REALDEMS project, EU-LAT Workshop on e-Environment, Brussels, Belgium 13-17 December.

D'Urso, G. and Santini, A., 1996. Advanced Procedures for the Management of Irrigation Systems. Proceed. Intern. Workshop on Evapotranspiration and Irrig. Scheduling, ASAE, USA.

Daughtry, C.S.T., Gallo, K.P., Goward, S.N., Prince, S.D. and Kustas, W.P., 1992. Spectral estimates of absorbed radiation and phytomass production in corn and soybean canopies Remote Sensing of Environment, 39: 141-152.

Deginet, M.D., 2008. Land surface representation for regional rainfall - modelling, Upper Blue Nile basin, Ethiopia, MSc Thesis, ITC, Enschede, 64 pp.

Dunne, T., 1978. Field studies of hillslope flow processes. In: M.J. Kikby (Editor), Hillslope Hydrology. Wiley, London, pp. 227-294.

Famiglietti, J.S. and Wood, E.F., 1995. Multiscale modeling of spatially variable water and energy balance processes. Water Resour. Res., 30(11): 3061–3078.

Fedak, R., 1999. Effect of Spatial Scale on Hydrologic Modeling in a Headwater Catchment, MSc Thesis, Virginia Polytechnic Institute and State University, Virginia, USA.

Fisher J and Beven K.J, 1996. Modelling of stream flow at Slapton Wood using TOPMODEL within an uncertainty estimation framework. Field Studies 8: 577-584.

Garbrecht, J. and Martz, L.W., 1999. Digital elevation model issues in water resources modeling. In: Proceedings from invited water resources sessions, ESRI international user conference, pp. 1-17.

Gash, J.H.C., 1979. An analytical model of rainfall interception by forests. Q. J. R. Meteor. Soc, 105: 43-55.

Gash, J.H.C., Lloyd, C.R. and Lachaud, G., 1995. Estimating sparse forest rainfall interception with an analytical model Journal of Hydrology, 170: 79-86.

Green, W.H. and Ampt, G., 1911. Studies of soil physics, part I - The flow of air and water through soils J. Ag. Sci., 4: 1-24.

Gunter, A., Uhlenbrook. S, Sibert, J. and C, L., 1999. Multi-criterial validation of TOPMODEL in a mountaneous catchment. Hydrological Processes, 13: 1603-1620.

Hengl, T., Maathuis, B.H.P. and Wang, L., 2007. Terrain parameterization in ILWIS. Chapter 3 (pp. 29-48). In: Hengel, Hannes and Reuter (Editors), 'Geomorphometry' the textbook. European Commission, DG Joint Research Centre, Institute for Environment and Sustainability, Land Management and Natural Hazards Unit, Ispra, Italy.

Huang, B. and Jiang, B., 2002. AVTOP: a full integration of TOPMODEL into GIS. Environmental Modelling & Software, 17(3): 261-268.

Huete, A.R., 1988. A soil-adjusted vegetation index (SAVI). Remote Sensing of Environment, 25(3): 295-309.

Huete, A.R., Jackson, R.D. and Post, D.F., 1985. Spectral response of a plant canopy with different soil backgrounds. Remote Sensing of Environment, 17: 37-53.

Hutjes, R.W.A., 1990. Rainfall interception in the Tai forest, Ivory Coast, Application of two simulation models to a humid tropical system Journal of hydrology, 114: 259-274.

Janssen, P.H.M. and Heuberger, P.S.C., 1995. Calibration of process-oriented models. Ecological Modelling, 83(1-2): 55-66.

Kebede, E.W., 2009. Hydrological Responses to Land Cover Changes in Gilgel Abbay Catchment, Ethiopia. MSc Thesis Work, ITC, Enschede.

Kim, S. and Delleur, J.W., 1997. Sensitivity analysis of extended TOPMODEL for agricultural watersheds equipped with tile drains. Hydrological Processes, 11(9): 1243-1261.

Kincaid, D.R., Osborn, H.B. and Gardner, J.R., 1966. Use of unit-source watersheds for hydrologic investigations in the semi-arid Southwest. Water Resources Research, 2(3): 381-392.

Kirkby, M.J., 1975. Hydrograph Modelling Strategies In: R. Peel, M. Chisholm and P. Haggett (Editors), Processes in Physical and Human Geography John Wiley, Heinemann, London, pp. 69-90.

Kozak, J.A., Ahuja, L.R., Green, T.R. and Ma, L., 2007. Modelling crop canopy and residue rainfall interception effects on soil hydrological components for semi-arid agriculture. Hydrological Processes, 21(2): 229-241.

Kroes, J.G. and van Dam, J.C., 2003. Reference Manual SWAP version 3.0.3. Wageningen, Alterra, Green World Research. Alterra-report 773. Reference Manual SWAP version 3.0.3, Wageningen, The Netherlands.

Lamb, R., 1996. Distributed hydrological prediction using generalised TOPMODEL concepts, PhD Thesis, Lancaster University, Lancaster, UK.

Lane, S.N., Brookes, C.J., Kirkby, M.J. and Holden, J., 2004. A network-index-based version of TOPMODEL for use with high-resolution digital topographic data. Hydrol. Process., 18: 191-201.

Li, X., 1996. A review of the international researches on land use/land cover changes. Acta Geographica Sinica, 51(5): 553-558.

Liang, X., Lettenmaier, D.P., Wood, E. and Burges, S., 1994. A simple hydrological based model of land surface water and energy fluxes for general circulation models Journal of Geophysical Research, 99(D7): 14 415-14 428.

Lucas, L., Janssen, F., Gerrit, C. and Hurneman., 2002. Principles of Remote Sensing, ITC Educational Textbooks Series; 2, Second Edition.

Lusby, G.C., Turner, G.F., Thompson, J.R. and Reid, V.H., 1963. Hydrologic and biotic characteristics of grazed and ungrazed watershed of the badger Wash Basin in western Colarado, 1953-58 1953-66. Geological Survey Water-Supply Paper 1532-D. US Geological Survey, Washington, DC, USA.

Minshall, N.W. and Jamison, V.C., 1965. Interflow in claypan soils. Water Resources Management, 1: 381-390.

Molicová, H., Grimaldi, M., Bonell, M. and Hubert, P., 1997. Using TOPMODEL towards identifying and modelling the hydrological patterns within a headwater, humid, tropical catchment. Hydrological Processes, 11(9): 1169-1196.

Musgrave, G.W. and Holtan, H.N., 1964. Infiltration. In: V.T. Chow (Editor), Handbook of Applied Hydrology. McGraw-Hill, New York, pp. 12.1-12.30.

Nash, J.E. and Sutcliffe, J.V., 1970. River flow forecasting through conceptual models. Part I: a discussion of principles. J. Hydrol., 10: 282-290.

Neitsch, S.L., Arnold, J.G., Kiniry, J.R., Williams, J.R. and King, K.W., 2002. Soil Water Assessment Tool User's manual, version 2000, TWRI Report TR-192, Texas Water Resources Institute, College Station, Texas, USA

Niehoff, D., Fritsch, U. and Bronstert, A., 2002. Land-use impacts on storm-runoff generation: scenarios of land-use change and simulation of hydrological response in a meso-scale catchment in SW-Germany. Journal of Hydrology, 267 80-93.

Niu, G., Yang, Z., Dickson, R.E. and Gulden, L.E., 2005. A simple TOPMODEL-based runoff parameterization (SIMTOP) for use in global climate models. Journal of Geophysical Research, 110(D21106).

Panigrahy, N., Jain, S.K., Kumar, V. and Bhunya, P.K., 2009. Algorithms for Computerized Estimation of Thiessen Weights. Journal of Computing in Civil Engineering, 23(4): 239-247.

Parodi, G.N., 2002. AHVRR Hydrological Analysis System Algorithms and theory - Version 1.3, WRES-ITC 2000, Enschede, The Netherlands.

Peters-Lidard, C.D., Zion, M.S. and Wood, E.F., 1997. A soil-vegetation-atmosphere transfer scheme for modeling spatially variable water and energy balance processes. J. Geophys. Res., 102(D4): 4303-4324.

Peters, N.E., Freer, J. and Beven, K., 2003. Modelling hydrologic responses in a small forested catchment (Panola Mountain, Georgia, USA): a comparison of the original and a new dynamic TOPMODEL. Hydrol. Process. , 17: 345-362.

Pilot, A.M., 2002. Modelling of the initial soil moisture distribution for the rainfall-runoff model FlowSim. Application of the TOPMODEL-concept, MSc Thesis, Delft University of Technology, Delft, The Netherlands.

Qin, C. et al., 2007. An adaptive approach to selecting a flow-partition exponent for a multiple-flow-direction algorithm. International Journal of Geographical Information Science, 21(4): 443 - 458.

Quinn, P., Beven, K., Chevallier, P. and Planchon, O., 1991. The prediction of hillslope flow paths for Distributed Hydrological Modelling using Digital Terrain Models. Hydrological Processes, 5: 59-79.

Quinn, P.F. and Beven, K.J., 1993. Spatial and temporal predictions of soil moisture dynamics, runoff, variable source areas and evapotranspiration for Plynlimon, Mid-Wales. Hydrological Processes, 7(4): 425-448.

Quinn, P.F., Beven, K.J. and Lamb, R., 1995. The Ln(a/TanB) Index: How to calculate it and how to use it within the Topmodel framework. Hydrological Processes, 9: 161-182.

Refsgaard, J.C. and Storm, B., 1995. MIKE SHE, in Computer Models of Watershed Hydrology, Vijay P. Singh, ed., Water Resources Publications, Highlands Ranch, Colorado., USA.

Rientjes, T.H.M., 2007. Modeling in Hydrology. Lecture Notes. ITC, Enschede, Netherlands.

Salas, J.D., 1993. Analysis and modelling of hydrologic time series. In: D.R. Maidment (Editor), Handbook of hydrology. McGraw-Hill, inc, Texas, pp. 19.1-19.72.

Saulnier, G.-M., Beven, K. and Obled, C., 1997. Including spatially variable effective soil depths in TOPMODEL. Journal of Hydrology, 202(1-4): 158-172.

Seibert, J., Bishop, K.H. and Nyberg, L., 1997. A test of TOPMODEL's ability to predict spatially distributed groundwater levels. Hydrological Processes, 11(9): 1131-1144.

SMEC, I.P., 2007. "Hydrological Study of The Tana-Beles Sub-Basins." part 1. Sub-basins Groundwater Investigation Report.

Sorooshian, S. and Gupta, V., 1995. Model calibration. In Computer Models of Watershed Hydrology, Singh VP (ed.) Water Resources Management Publications, Highlands Ranch, CO, pp. 23-67.

Tessema, S.M., 2006 Assessment Of Temporal Hydrological Variations Due To Land Use Changes Using Remote Sensing/GIS: A Case Study Of Lake Tana Basin. MSc Thesis, TRITA-LWR

van Dam, J.C., 2000. Field-scale water flow and solute transport: SWAP model concepts, parameter estimation and case studies. PhD Thesis, Wageningen, Netherlands.

van Leeuwen, W.J.D. et al., 1997. Deconvolution of remotely sensed spectral mixtures for retrieval of LAI, fAPAR and soil brightness. Journal of Hydrology, 188-189: 697-724.

Veldkamp, A. and Fresco, L., 1997. Exploring land use scenarios, an alternative approach based on actual land use. Agriculture Systems, 55: 1-17.

Wale, A., Rientjes, T.H.M., Gieske, A.S.M. and Getachew, H.A., 2009. Ungauged catchment contributions to Lake Tana's water balance. Hydrological Processes, 23: 3682-3693.

Watson, F.G.R., 1999. Large scale, long term, physically based modelling of the effects of land cover change on forest water yield, University of Melbourne, Melbourne.

Whipkey, R.Z., 1969. Storm runoff from forested catchments by subsurface routes, Symbosium of Leningrad. Internat. Assoc. Sci. Hydrology, pp. 773-779.

Whipkey, R.Z. and Kirkby, M.J., 1978. Flow within the soil. In: M.J. Kikby (Editor), Hillslope hydrology. Wiley, London, pp. 121-144.

Wolock, D.M. and McCabe, G.J., Jr., 1995. Comparison of Single and Multiple Flow Direction Algorithms for Computing Topographic Parameters in TOPMODEL. Water Resour. Res., 31.

APPENDICES

Appendix 1: acronyms and abbreviations

ASTER	Advanced Space born Thermal Emission Radiometer
DEM	Digital Elevation Model
DTM	Digital Terrain Model
GIS	Geographic Information System
GPS	Global Positioning System
IDL	Interactive Data Language
LAI	Leaf Area Index
NASA	National Aeronautics and Space Administration
RMSE	Root Mean Square Error
RV_E	Relative Volume Error
SAVI	Soil Adjusted Vegetation Index
UTM	Universal Transverse Mercator

Appendix 2: Correlations between station rainfall (2001-2003)

		Dangila	Adet	Kidamaja	Sekela	Wotet Abay	Enjibara
	Missing	0	42	2	58	11	365
Dangila	Pearson Correlation	1	0.400	0.398	0.418	0.529	0.5
	Sig. (2-tailed)		0.000	0.000	0.000	0.000	0.000
	N	1095	1053	1093	1037	1084	730
Adet	Pearson Correlation	0.400	1	0.321	0.35	0.460	.355
	Sig. (2-tailed)	0.000		0.000	0.000	0.000	0.000
	N	1053	1053	1051	999	1042	705
Kidamaja	Pearson Correlation	0.398	0.321	1	0.352	0.415	0.429
	Sig. (2-tailed)	0.000	0.000		0.000	0.000	0.000
	N	1093	1051	1093	1036	1082	729
Sekela	Pearson Correlation	0.418	0.350	0.352	1	0.388	0.452
	Sig. (2-tailed)	0.000	0.000	0.000		0.000	0.000
	N	1037	999	1036	1037	1026	716
Wotet Abay	Pearson Correlation	0.529	0.460	0.415	0.388	1	0.463
	Sig. (2-tailed)	0.000	0.000	0.000	0.000		0.000
	N	1084	1042	1082	1026	1084	719
Enjibara	Pearson Correlation	0.5	0.355	0.429	0.452	0.463	1
	Sig. (2-tailed)	0.000	0.000	0.000	0.000	0.000	
	N	730	705	729	716	719	730

Appendix 3: The LAI maps for the wet and dry seasons (1986, 2001)

Wet season (Oct 1973)

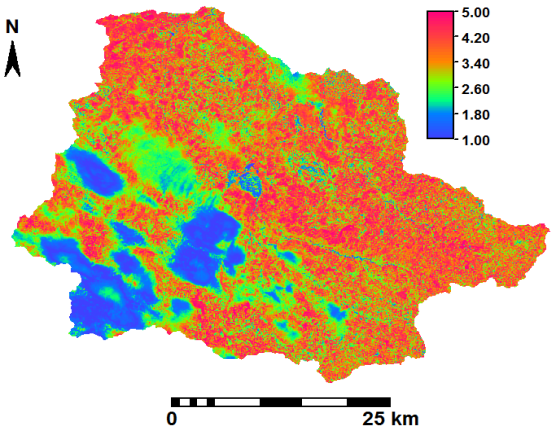

Dry season (Feb 1986)

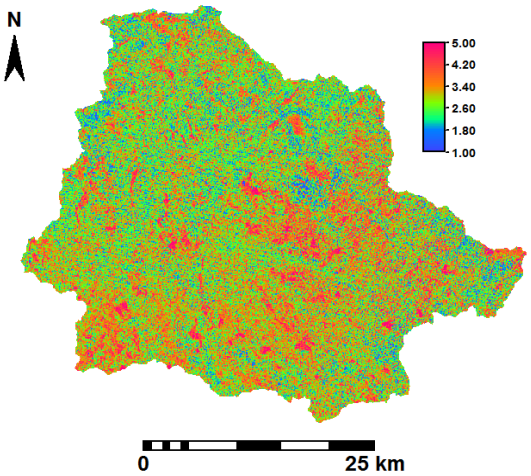

Wet season (August 1986)

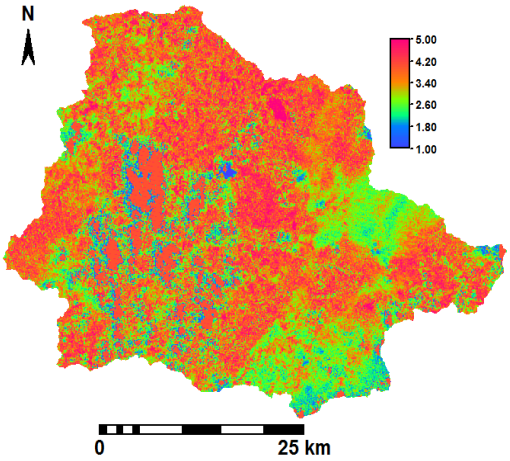

Dry season (Feb 2001)

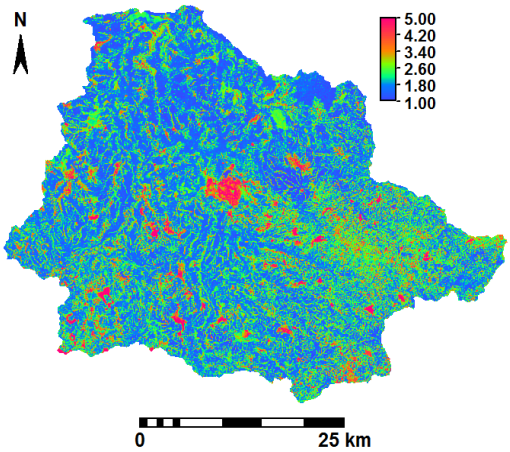

Wet season (Sept 2001)

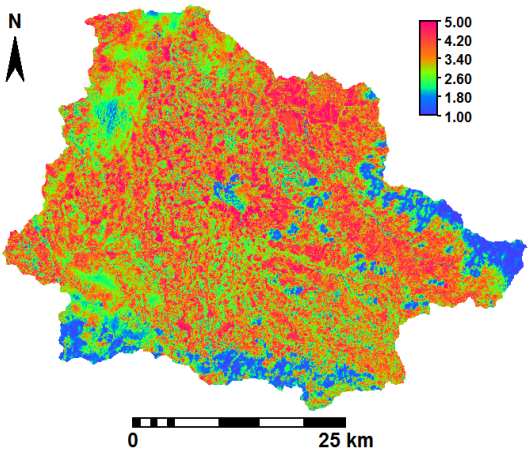

Appendix 4: The amount of daily interception storages from the different landuse classes